

1977

Dielectric Relaxation in the UHF and RF Regions

Theodore Bryant Kingsbury

College of William & Mary - Arts & Sciences

Follow this and additional works at: <https://scholarworks.wm.edu/etd>

 Part of the [Physical Chemistry Commons](#)

Recommended Citation

Kingsbury, Theodore Bryant, "Dielectric Relaxation in the UHF and RF Regions" (1977). *Dissertations, Theses, and Masters Projects*. Paper 1539624976.

<https://dx.doi.org/doi:10.21220/s2-0c8z-vv88>

This Thesis is brought to you for free and open access by the Theses, Dissertations, & Master Projects at W&M ScholarWorks. It has been accepted for inclusion in Dissertations, Theses, and Masters Projects by an authorized administrator of W&M ScholarWorks. For more information, please contact scholarworks@wm.edu.

DIELECTRIC RELAXATION IN THE
UHF AND RF REGIONS

A Thesis
Presented to
The Faculty of the Department of Chemistry
The College of William and Mary in Virginia

In Partial Fulfillment
Of the Requirements for the Degree of
Master of Arts

by
Theodore Bryant Kingsbury IV
1977

APPROVAL SHEET

This thesis is submitted in partial fulfillment of
the requirements for the degree of

Master of Arts

Theodore B. Kingsbury II
Author

Approved June 1977

David E. Kranbuehl
David E. Kranbuehl

Robert A. Orwoll
Robert A. Orwoll

Kyle E. Dolbow
Kyle E. Dolbow

DEDICATION

To my family and friends, whose unceasing encouragement, support, assistance, and understanding made this possible.

TABLE OF CONTENTS

	Page
ACKNOWLEDGMENTS.	vi
LIST OF FIGURES.	vii
LIST OF PLATES	viii
ABSTRACT	ix
CHAPTER I. STATIC PERMITTIVITY.	2
CHAPTER II. DIELECTRIC RELAXATION	17
CHAPTER III. THEORY OF UHF MEASUREMENTS	31
CHAPTER IV. UHF EXPERIMENTAL EQUIPMENT AND PROCEDURE. .	43
CHAPTER V. UHF EXPERIMENTAL RESULTS	55
CHAPTER VI. SUPERCOOLED LIQUIDS AND THE GLASSY STATE. .	61
CHAPTER VII. RF AND Q-METER THEORY.	66
CHAPTER VIII. RF EXPERIMENTAL EQUIPMENT AND PROCEDURE .	78
CHAPTER IX. RF Q-METER EXPERIMENTAL RESULTS	87
APPENDIX I. COMPUTER PROGRAM TO CALCULATE C_n , $b^2 - a^2$, $2ab$, AND TAN	93
APPENDIX II. TABLE OF C_n , $b^2 - a^2$, $2ab$, AND $TAN \delta$	97
APPENDIX III. COMPONENTS OF UHF MEASUREMENT SYSTEM. . .	109
APPENDIX IV. COMPUTER PROGRAM TO FIT UHF DATA	111
APPENDIX V. PLOTS OF ϵ' AND ϵ'' VERSUS CONCENTRATION . .	114
APPENDIX VI. RELAXATION TIMES AND SMYTH PARAMETERS FOR UHF DATA	148

	Page
APPENDIX VII. UNCERTAINTY IN ϵ'' FOR Q FROM 130 TO 1000.	158
APPENDIX VIII. COMPUTER PROGRAMS FOR RF MEASUREMENTS. .	162
APPENDIX IX. TABLES AND GRAPHS OF RF Q-METER RESULTS. .	167
BIBLIOGRAPHY	181

ACKNOWLEDGMENTS

The writer wishes to express his appreciation for the invaluable assistance and continual encouragement given him by the faculty members of both the chemistry and physics departments; especially Professor David E. Kranbuehl, under whose guidance this research was conducted, and Professors Robert A. Orwoll and Kyle Dolbow for their careful reading and criticism of this thesis. Not least of all, Mr. Stan Hummel of the physics shop deserves special thanks for his help in designing and building much of the experimental apparatus.

LIST OF FIGURES

Figure	Page
1-1 Parallel plate capacitor in vacuo	3
1-2a Parallel plate capacitor with isotropic, non-polar dielectric	4
1-2b Charge distribution with and without an applied field	4
1-3 Diagram for the calculation of local field contributions	9
2-1 Polarization versus t/T for a suddenly applied field18
2-2 Polarization versus t/T for a suddenly removed field19
2-3 Debye plot of ϵ' and ϵ'' versus $\log(\omega T)$20
2-4 Complex plane representation of ϵ' and ϵ''22
2-5a Cole-Cole plot of ϵ' and ϵ'' versus $\log(\omega T)$. .	.22
2-5b Cole-Cole plot of ϵ' versus ϵ''23
2-6 Cole-Davidson plot of ϵ' versus ϵ'' for various values of α23
4-1 Admittance meter and auxillary equipment44
4-2 UHF dielectric cell48
4-3 Block diagram of UHF component interconnection .	.49
7-1a Q-meter circuit with empty cell attached67
7-1b Q-meter circuit with filled cell attached68
8-1 RF measurement apparatus - interconnection79
8-2 Capacitance versus $1/t$ for 2-terminal cell80
8-3 RF 2-terminal dielectric cell82

LIST OF PLATES

- Plate 1 1602-B Admittance Meter - Front
- Plate 2 Admittance Meter - Rear
- Plate 3 UHF Dielectric Cell - Assembled
- Plate 4 UHF Dielectric Cell - Disassembled
- Plate 5 Interconnection of UHF Components -
Dielectric Cell and Admittance Meter
- Plate 6 UHF Components - Oscillators and IF
Amplifier
- Plate 7 RF Measurement Equipment
- Plate 8 Detail of Q-Meter with Dielectric Cell
Attached
- Plate 9 Two-terminal Dielectric Cell for RF
Measurements - Assembled
- Plate 10. . . . Two-terminal Cell - Disassembled

ABSTRACT

The purpose of this investigation was to gain information on the relaxation processes of certain small polar molecules, both in the liquid state, and also in the supercooled liquid and glassy states.

The first part of this study was carried out on dilute solutions of nitroaromatic compounds in benzene at 25 and 60°C, using UHF transmission line techniques to measure the complex dielectric constants.

Relaxation times were found for the various compounds studied. In conjunction with data previously obtained in the microwave frequency range, the data indicated a dependence of the relaxation time on the volume swept out by the molecule during relaxation, rather than on the molecular volume.

The second part of this investigation was the development of an experimental technique to measure the complex dielectric constants of supercooled dilute solutions of small polar molecules in the weakly polar solvent, orthoterphenyl.

The presence of a low frequency, cooperative relaxation process in the supercooled state has been well established by previous experimental work. Johari and Goldstein, among others, have proposed the existence of a second relaxation process, due to hindered reorientation of solute molecules "encaged" by relatively immobile solvent molecules. This β -process should require a much lower activation energy than the α , or cooperative process, and thus occur at lower temperatures and/or higher frequencies.

As a result of Q-meter measurements in the RF region, this β -process appears to occur in the temperature-frequency region below -70°C and above 5MHz for the compounds studied. As expected, its magnitude is much lower than that of the α peak, previous studies having indicated that the α -process accounts for the majority of the total loss.

DIELECTRIC RELAXATION IN THE
UHF AND RF REGIONS

CHAPTER I

STATIC PERMITTIVITY

All atoms can be thought of as having a particular spatial distribution of electric charge. That distribution is characteristic of the electronic configuration of the atom under consideration, and is also affected by neighboring charge distributions. This inherent charge distribution of the atom (or molecule) under study can be affected by an external electric field, and that effect can be measured. The study of such interaction between matter and electromagnetic fields constitutes the field of dielectric phenomena.

Since molecules are combinations of atoms, the charge distribution of a molecule depends on the types of atoms involved and their structural arrangement. In an electrically neutral molecule, although there are equal amounts of positive and negative charge, that charge may be distributed in such a way that the positive and negative centers of charge are physically separated, thus giving rise to an electric dipole. Another way to express this is to say that if a molecule belongs to the point group C_i , then it does not have a permanent dipole moment. It may, however, possess quadrupole or higher moments which, in most cases, probably make negligible contributions to the electric

moment.¹

In this paper we will be concerned with the permittivity (dielectric constant) of certain materials which, in most cases, are polar; i.e., they have permanent dipole moments.

In regard to the derivation of the mathematical relations necessary to analysis of dielectric properties, we will first consider a parallel plate condenser. The plate area is large compared to the separation between the plates, and there is vacuum around the whole apparatus. A potential, V , is applied across the plates and they acquire charges $+Q$ and $-Q$ per unit area.¹ The capacitance is defined as

$$/ 1.1 / \quad C_0 = Q / V$$

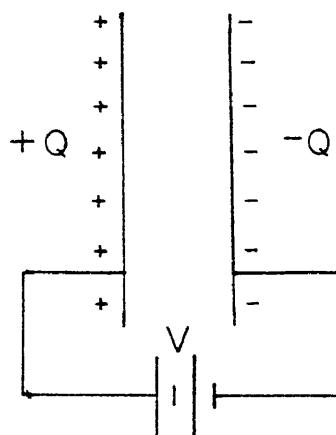


Figure 1-1

When an isotropic, non-polar dielectric is placed between the plates, (Figure 1-2a)¹ the electric field due to the charges on the plates will polarize the molecules of the dielectric; i.e., it will cause a distortion of the

normally symmetrical charge distributions of the molecules.

(Figure 1-2b)²

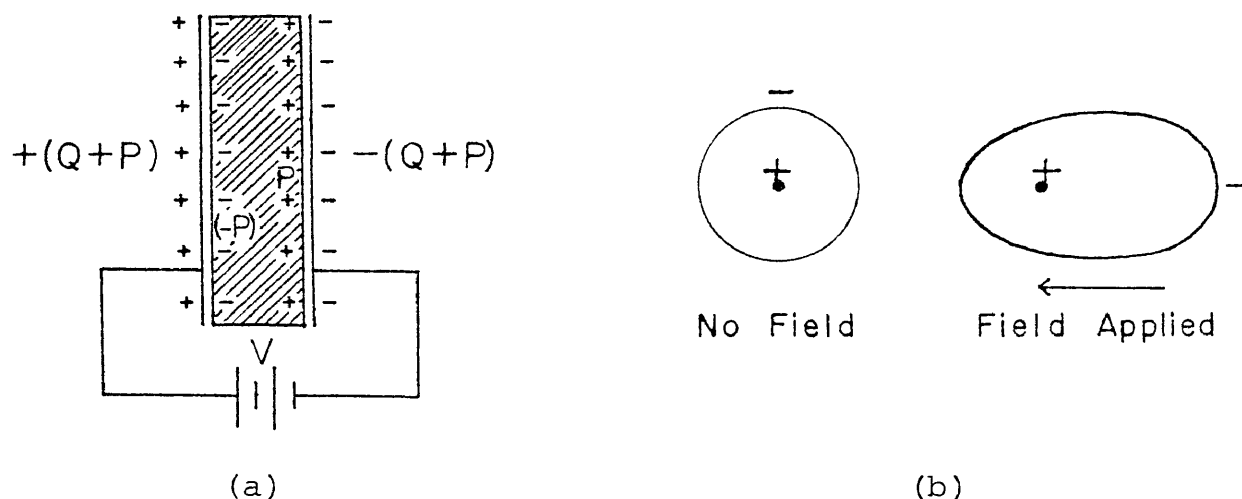


Figure 1-2

The capacitor can now hold a charge $(Q+P)$ at potential V , and the capacitance is now

$$/ 1.2 / \quad C = (Q + P) / V.$$

The (static) relative permittivity is defined as¹

$$/ 1.3 / \quad \epsilon_0 = C/C_0 = (Q + P)/Q$$

The permittivity is thus dependent on the polarizability of the material. For a non-polar molecule, polarizability arises from two sources, displacement of the electrons relative to the nucleus (electronic polarization), and displacement of the atomic nuclei relative to one another (atomic polarization), with electronic polarization usually being predominant. If a polar molecule is used instead of a non-polar one, a third effect contributes to the total

polarization of the molecule. The permanent dipole of a molecule will attempt to align itself parallel to the incident electric field, in opposition to the randomizing effect of thermal agitation.¹

Obviously, then, the total polarization of polar molecules will be temperature dependent; whereas the only effect of temperature on non-polar molecules is to change the density, giving a small effect on the polarization. The total polarizability of the molecule is designated α_T , and is the sum of the electronic, atomic, and orientation polarizations mentioned above; i.e.,

$$/ 1.4 / \quad \alpha_T = \alpha_a + \alpha_e + \alpha_o$$

When a dielectric material is subjected to an electric field of intensity and direction E , displacement of the charge distribution occurs such that a bound surface charge P is induced. These two vector quantities are related by the equation,¹

$$/ 1.5 / \quad \epsilon_o = 1 + 4\pi P/\epsilon_o E$$

Assuming that the individual dipole moments within such a volume are additive,¹

$$/ 1.6 / \quad P = N_1 \langle \mu \rangle$$

where N_1 is the number of dipoles per unit volume. Also assuming $\langle \mu \rangle$ is proportional to the local field strength, F , (not the same as E),¹

$$/ 1.7 / \quad \langle \mu \rangle = \alpha_T F$$

where α_T is the polarizability, then,

$$/ 1.8 / \quad P_T = N_1 \alpha_T F .$$

This can be divided into two parts:

$$/ 1.8a / \quad P_D = N_1 F (\alpha_d + \alpha_e) , \text{ and}$$

$$/ 1.8b / \quad P_O = N_1 F \alpha_o , \text{ with } P_T = P_D + P_O .$$

The problem of determining the static permittivity of a dielectric is best considered as a two part problem. First, α_o , the contribution of the permanent dipoles of the molecules to the polarizability, must be calculated; and second, the local field, F , i.e., the actual effective field at the molecule, must be calculated in terms of the applied field, E .

The first theory proposed, and the first which we shall consider, is that of Debye.³ He assumed that the structure of the material exerted a negligible effect of the orientation of the permanent dipoles of the molecules. The distribution of permanent dipoles about an applied field is in accordance with Boltzmann's law; thus, a dipole of moment μ and with angle θ to the applied field has a potential energy,

$$/ 1.9 / \quad U = -\mu F \cos \theta \quad (F \neq E)$$

and the probability that the dipole axis will lie within

the solid angle dw , centered around θ is,

$$\text{/ 1.10 /} \quad \frac{\exp\left[(\mu F \cos \theta)/kT\right] dw}{\int \exp\left[(\mu F \cos \theta)/kT\right] dw}$$

If dw is the solid angle between θ and $\theta + d\theta$, then $dw = 2\pi \sin \theta d\theta$, and the average value of the dipole component parallel to the field is

$$\text{/ 1.11 /} \quad \mu \langle \cos \theta \rangle = \frac{\int_0^\pi \mu \cos \theta e^{\mu F \cos \theta / kT} \sin \theta d\theta}{\int_0^\pi e^{\mu F \cos \theta / kT} \sin \theta d\theta}.$$

Substituting $x = \cos \theta$, and integrating the numerator by parts, we get

$$\begin{aligned} \text{/ 1.12 /} \quad \langle \cos \theta \rangle &= \coth(\mu F / kT) - (kT / \mu F) \\ \langle \cos \theta \rangle &= L(\mu F / kT). \end{aligned}$$

A function of the general form $L(y) = \coth y - (1/y)$ is called Langevin's function, and for field strengths that are normal in permittivity measurements, $\mu F / kT \ll 1$, so that $L(y)$ can be approximated satisfactorily by $y/3$. Thus the polarization due to the dipoles is

$$\text{/ 1.13 /} \quad P_o = N_1 \mu \langle \cos \theta \rangle = N_1 \mu^2 F / 3kT$$

where N_1 is the number of dipoles per unit volume. The polarization due to distortion has been found previously in equation 1.8, and on adding these two contributions, the total polarization is found to be³

$$/ 1.14 / \quad P_T = N_l(\alpha_d + \mu^2/3kT)F ; \quad \alpha_d = \alpha_e + \alpha_a .$$

The first part of the problem has been solved, and it remains now to calculate the local field F in terms of the applied field E .

In order to determine the local field, certain assumptions must be made. First, the following model is postulated: A sphere, large in relation to molecular dimensions but small on a macroscopic scale, is envisioned with the point at which the local field, F , is to be determined, at the center of the sphere. The interior of the sphere is considered to be composed of individual molecules and the surrounding dielectric is a continuum.¹

The local field, F , can be thought of as composed of three components; F_1 which is the contribution from the free charges on the capacitor plates; F_2 , from the free ends of the dipoles on the surface of the imaginary cavity; and F_3 , which constitutes the contribution from the other molecules which are, in reality, within the cavity and thus close enough to affect the field at the center.¹ By definition:

$$/ 1.15 / \quad F_1 = E = 4\pi Q/\epsilon_0 .$$

The contribution from the free ends of the dipoles lining the surface of the cavity can be calculated by referring to figure 1-3.¹

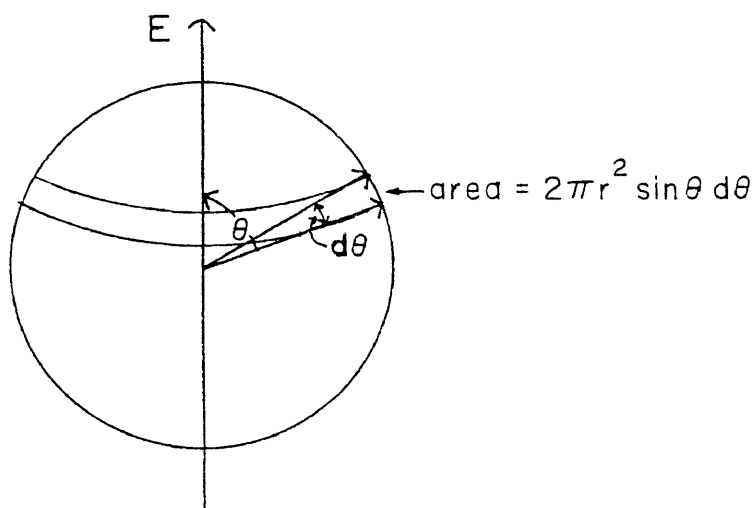


Figure 1-3

The charge density of the cavity walls is caused by bound charges, and is thus determined by the normal component of the polarization, P . Since the cavity was assumed to be spherically symmetric, the horizontal components of P cancel out and only the vertical components need be evaluated. These give a surface charge density of $P \cos \theta$ normal to the surface, and a component parallel to E of $P \cos^2 \theta$. Using Coulomb's law, $P \cos^2 \theta$ for the parallel component, dividing the cavity walls into rings of area $2\pi r^2 \sin \theta d\theta$, and integrating over all θ , the field contribution of the cavity wall is¹

$$/ 1.16 / \quad F_2 = \int_0^\pi \frac{2\pi P \cos^2 \theta r^2 \sin \theta d\theta}{\epsilon_0 r^2} = \frac{4\pi P}{3\epsilon_0}$$

Since F_3 can only be determined if information on the geometry and polarizability of the molecules within the sphere

is available, and then only after extremely difficult mathematical treatment, the assumption is made that these contributions cancel each other so that

$$/ 1.17 / \quad F_3 = 0,$$

an assumption first made by Mossotti in 1850.⁴ Thus, we can now write:

$$/ 1.18 / \quad F = F_1 + F_2 = E + 4\pi P/3\epsilon_0 ;$$

and from equation 1.5,

$$/ 1.5' / \quad 4\pi P = (\epsilon_0 - 1)\epsilon_0 E ,$$

which, upon combination with equation 1.14 give

$$/ 1.19 / \quad P = N_1 (\alpha + \mu^2/3kT)(\epsilon_0 + 2)E/3 ,$$

which can be rearranged to

$$/ 1.20 / \quad \frac{\epsilon_0 - 1}{\epsilon_0 + 2} = 4\pi N_1 (\alpha + \mu^2/3kT) 3\epsilon_0$$

We would like to remove the dependence of the polarization on the density of the substance; and as long as the molecules themselves are the dipoles, then this can be done by utilizing the relation,

$$/ 1.21 / \quad N_0 = \frac{N_1 M}{\rho} = 6.023 \times 10^{23} ,$$

where N_0 is Avogadro's number, M is the molecular weight in kilograms, and ρ is the density in kilograms per cubic

meter.¹ Substituting N_0 into equation 1.20, we get the Clausius-Mossotti relation,

$$\text{/ 1.22 /} \quad \frac{\epsilon_0 - 1}{\epsilon_0 + 2} \frac{M}{\rho} = \frac{4\pi N_0}{3\epsilon_0} (\alpha_0 + \mu^2/3kT) ,$$

the left hand side being called the molar polarization. The analogous equation for energy in the optical region is the Lorentz-Lorenz equation

$$\text{/ 1.23 /} \quad \frac{n^2 - 1}{n^2 + 2} \frac{M}{\rho} = \frac{4\pi N_0}{3\epsilon_0} (\alpha_0 + \mu^2/3kT) .$$

For the Clausius-Mossotti equation, ϵ_0 is to be a real quantity. The equation can be generalized merely by substituting ϵ^* for ϵ_0 .¹ It must be kept in mind that these equations are valid only so far as the assumption that $F_3 = 0$ is a reasonable approximation of the real situation.

Debye's two main assumptions were, (1) The molecules will be distributed according to Langevin's law, and (2) The Lorentz field applies; i.e., $F_3 = 0$. The first assumption is probably only reasonable for the case of liquids in which the dipoles experience no strong local interactions due to neighboring molecules. The assumption that $F_3 = 0$ will not apply to crystalline solids and will probably only approximate the true situation for gases at low to moderate pressures, and for dilute solutions of polar molecules in non-polar solvents.¹

From equation 1.23, it can be seen that, for a non-

polar material, the molar polarizability should be a constant, and the permittivity should be directly proportional to density.¹

For a polar dielectric, the molar polarizability should be linearly related to $1/T$, and μ can be found from the slope of a plot of molar polarization versus $1/T$. Further analysis of this equation shows that there should be a temperature,

$$/ 1.24 / \quad T = \frac{4\pi N_0 \rho \mu^2}{9 M k \epsilon_0} ,$$

below which spontaneous polarization occurs and the material becomes ferroelectric.¹ Although a few crystalline ferroelectric materials are known, this phenomenon is not common. As an example, water should, according to this equation, be ferroelectric below 1100°K thus making life on Earth impossible. This is an obvious instance of the non-validity of the assumption that $F_3 = 0$.¹ One attempt to improve this situation was made by Onsager.⁵

Onsager's calculation of the local field is based on the following model: "The molecule is treated as a polarizable point dipole at the center of a spherical cavity of molecular dimensions in a continuous medium of (static) permittivity n^2 ."¹ The cavity size is defined by the equation:

$$/ 1.25 / \quad 4\pi N_1 a^3 / 3 = 1 ,$$

which merely says that the sum of the volumes of the spherical cavities equals the total volume of the material. As in Debye's theory,³ the assumptions of a spherical cavity and homogeneity outside the cavity, limit applicability to dielectrics with no strong local forces.¹

The detailed derivation of Onsager's equation can be found in any book on the theory of permittivity. The result is:

$$\text{/ 1.26 /} \quad \frac{(\epsilon_0 - n^2)(2\epsilon_0 + n^2)}{\epsilon_0 (n^2 + 2)^2} = \frac{4\pi N_1 \mu^2}{9kT\epsilon_0},$$

where an "internal refractive index", n^2 , is defined as

$$\text{/ 1.27 /} \quad (n^2 - 1)/(n^2 + 2) = \alpha/\epsilon_0 d^3 = 4\pi N_1 \alpha / 3\epsilon_0 ;$$

and where

$$\text{/ 1.28 /} \quad 1 - r\alpha/d^3 = 3(2\epsilon_0 + n^2)/(2\epsilon_0 + 1)(n^2 + 2)$$

$$\text{/ 1.29 /} \quad 4\pi N_1 \alpha / \epsilon_0 = 3(n^2 - 1)/(n^2 + 2) ; \left\{ r = 2(\epsilon_0 - 1)/(2\epsilon_0 + 1)\epsilon_0 \right\}.$$

Comparison of the two theories shows that while Debye's theory predicts the occurrence of ferroelectricity (incorrectly in most cases), Onsager's theory predicts that ferroelectricity will not occur. Both Debye and Onsager use "semi-statistical" methods, in that the calculation of the dipolar polarizability uses statistical arguments, whereas the calculation of the local field are based on macroscopic treatments of specific models.¹

Two theories which attempt to carry out a complete

statistical treatment of the problem are those of Kirkwood⁶ and Fröhlich.⁷ Differences arise only on the inclusion of distortion polarization; if non-polarizable dipoles are assumed, the two theories give the same result.¹ In Kirkwood's theory, distortion polarization is treated by assuming that the dipole has a polarizability α , and that the local field which that dipole feels is Onsager's cavity field -- $G = 3\epsilon_0 E / (2\epsilon_0 + 1)$. Kirkwood's equation (including distortion polarization) is then:

$$/ 1.30 / \quad \frac{(\epsilon_0 - 1)(2\epsilon_0 + 1)}{3\epsilon_0} = \frac{4\pi N}{V\epsilon_0} \left(\alpha + \frac{g\mu^2}{3kT} \right),$$

where $N/V = N_1$, and $g = \bar{\mu}/\mu$. The correlation parameter, g , measures the degree of interaction of the dipoles with their neighbors; $\bar{\mu}$ is the average moment of a finite spherical region around one molecule which is fixed, and μ is the moment of that fixed molecule. In other words, if fixing one dipole has no effect on others, then $g = 0$; if fixing one tends to align others parallel to that one, $g > 1$; and if in an anti-parallel direction, $g < 1$.¹

Fröhlich,⁷ in including distortion polarization, maintains the non-polarizability of the dipole in the cavity and assumes that instead, the surrounding continuum has a permittivity n^2 . This has the effect of changing the cavity field to

$$/ 1.31 / \quad G = 3\epsilon_0 E / (2\epsilon_0 + n^2),$$

which leads to Frohlich's equation for the static permittivity:

$$/ 1.32 / \quad \frac{(\epsilon_0 - n^2)(2\epsilon_0 + n^2)}{\epsilon_0(n^2 + 2)^2} = \frac{4\pi N g \mu_g^2}{9kTV\epsilon_0} .$$

(μ_g = moment of gas molecule.)

This is the same as Onsager's equation except for g , the correlation parameter described above.

The differences between the Kirkwood's and Fröhlich's theories disappear if the total local field, rather than Onsager's cavity field, is used in Kirkwood's calculations.¹ That is, instead of $G = 3\epsilon_0 E / (2\epsilon_0 + 1)$, one uses $F = 3\epsilon_0 (n^2 + 2)E_0 / [(2\epsilon_0 + n^2)(\epsilon_0 + 2)]$.

These, then, are the major theories which relate permittivity to dipole moment. They all have been based on an applied field which is constant and are thus theories of static permittivity. In chapter II the effects of a time dependent external field will be discussed.

NOTES FOR CHAPTER I

1. Nora E. Hill, et. al., "Dielectric Properties and Molecular Behavior," Van Nostrand Reinhold Co., New York, N.Y., 1969.
2. Arthur R. Von Hippel, "Dielectrics and Waves," The M.I.T. Press, Cambridge, Massachusetts, 1966.
3. Peter Debye, "Polar Molecules," The Chemical Catalogue Company, Inc., New York, N.Y., 1929.
4. O.F. Mosotti, Mem. Soc. Ital., 14, 49 (1850).
5. L. Onsager, J. Am. Chem. Soc., 58, 1486 (1939).
6. J.G. Kirkwood, J. Chem. Phys., 7, 911 (1939).
7. H. Frohlich, "Theory of Dielectrics," Oxford University Press, London, 1949.

CHAPTER II

DIELECTRIC RELAXATION

Dielectric relaxation occurs when a dielectric material is subjected to an external field of varying intensity. The permittivity of the dielectric falls off with increasing frequency, due to the fact that the dipolar (orientation) part of the polarization cannot change fast enough to reach equilibrium with the applied field. To treat this phenomenon on a macroscopic basis, we first divide the polarization into two parts; the distortion polarization, P_1 , which consists of the atomic and electronic polarizations and can reach its maximum value effectively instantaneously; and the orientation polarization, P_2 , which requires a significant time to reach its equilibrium value. We then make the assumption that P_2 increases at a rate proportional to its departure from equilibrium value:¹

$$\text{/ 2.1 /} \quad \frac{dP_2}{dt} = \frac{P - P_1 - P_2}{T}$$

(P = total polarization at equilibrium.)

The macroscopic relaxation time, T , is defined as the time required for the experimentally observed dielectric polarization to decrease from P_{\max} to $1/e$ times P_{\max} . The microscopic, or molecular relaxation time, τ , is not the

same as T ; and as will be shown, depends on the form chosen for the local field.

Equation 2.1 can be rearranged to give;

$$/ 2.2 / \quad \frac{d(P - P_1 - P_2)}{P - P_1 - P_2} = \frac{-dt}{T},$$

for which the solution is,

$$/ 2.3 / \quad \ln(P - P_1 - P_2) = -t/T + C ; C = \text{constant}.$$

Now if a field, E , is suddenly applied at $t = 0$, then $P_2 = 0$ and $C = \ln(P - P_1)$. Substituting this solution back into equation 2.3 gives

$$/ 2.4 / \quad P_2 = (P - P_1)(1 - e^{-t/T}) ;$$

that is to say, P_2 approaches equilibrium at an exponential rate as shown in Figure 2-1.¹

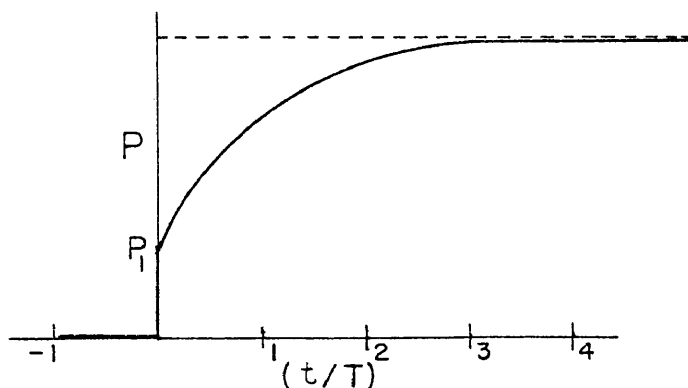


Figure 2-1

Similarly, if a constant field is present and is suddenly removed, $P_1 = 0$, and

$$/ 2.5 / \quad \frac{dP_2}{dt} = - \frac{P_2}{T} \quad ; \quad \ln P_2 = C - t/T .$$

At $t = 0$; $P_2 = P - P_1$, $C = \ln(P - P_1)$ and $P_2 = (P - P_1)e^{-t/T}$ as shown in Figure 2-2.¹

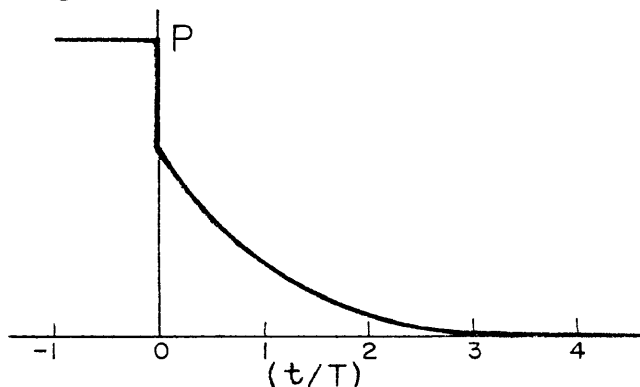


Figure 2-2

An alternating field of frequency $2\pi f = \omega$, can be represented by the equation,

$$/ 2.6 / \quad E = E_0 e^{i\omega t}$$

The static permittivity and the refractive index are given in terms of P and P_1 by¹

$$/ 2.7 / \quad 4\pi P = \epsilon_0(\epsilon_0 - 1)E, \quad \omega \rightarrow 0$$

$$/ 2.8 / \quad 4\pi P_1 = \epsilon_0(n^2 - 1)E .$$

Plugging these values for P and P_1 into equation 2.2 we get

$$/ 2.9 / \quad \frac{dP_2}{dt} = \frac{\epsilon_0}{4\pi T} (\epsilon_0 - n^2) E_0 e^{i\omega t} - \frac{P_2}{T} .$$

For the steady state, the solution to this equation should have the form $P_2 = Ae^{i\omega t}$, where A is found by plugging this solution back into equation 2.9.¹

$$/ 2.10 / \quad A = \epsilon_0(\epsilon_0 - n^2)E_0 / 4\pi(1 + i\omega T) \quad ;$$

$$/ 2.11 / \quad P_2 = \epsilon_0(\epsilon_0 - n^2)E / 4\pi(1 + i\omega T) \quad .$$

From this it is seen that the orientation part of the polarization is out of phase with the applied field. Thus we can write the polarization as a complex quantity,

$$/ 2.12 / \quad P_1 + P_2 = P' + iP'' = \frac{\epsilon_0}{4\pi} (n^2 - 1)E + \frac{\epsilon_0(\epsilon_0 - n^2)}{4\pi(1 + i\omega T)}E ,$$

where P' and P'' are both real.¹ It follows that if the polarization is complex, so is the permittivity; and it can be expressed as,¹

$$/ 2.13 / \quad \epsilon^* = \epsilon' - i\epsilon'' = 1 + 4\pi(P' - iP'')/\epsilon_0 E \\ = n^2 + (\epsilon_0 - n^2)/(1 + i\omega T) \quad ,$$

where both ϵ' and ϵ'' are real and have the values:

$$/ 2.14 / \quad \epsilon' = n^2 + \frac{\epsilon_0 - n^2}{1 + \omega^2 T^2} \quad ; \quad \epsilon'' = \frac{(\epsilon_0 - n^2)\omega T}{1 + \omega^2 T^2} .$$

When these are plotted versus $\log(\omega T)$, the graph shown in Figure 2-3¹ results.

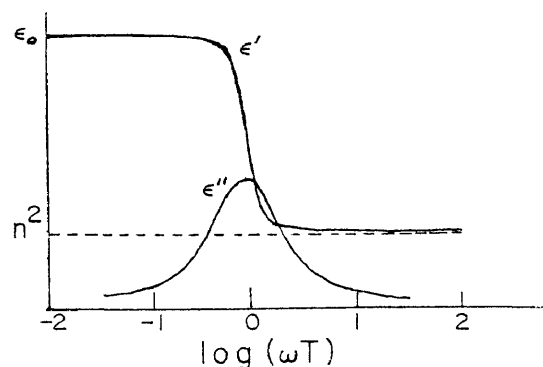


Figure 2-3

The fact that there is a phase difference between the applied field and the orientation polarization causes energy absorption by the dielectric material. When the polarization of the dielectric changes, a displacement current of density \underline{i} is generated such that,

$$/ 2.15 / \quad i = \frac{dP}{dt} ,$$

and Joule heating, H , occurs where

$$/ 2.16 / \quad H = Ei = E \frac{dP}{dt} \text{ per unit volume.}$$

When the average value of H for one complete cycle of the electric field is determined, this equation is found:¹

$$/ 2.17 / \quad H_{av} = E_o^2 \epsilon_o \epsilon'' \omega / 8 \pi$$

That is, ϵ'' is directly proportional to the average rate of Joule heating created by absorption of electrical energy by the dielectric. Because of this, ϵ'' is often called the dielectric loss factor, and the quantity ϵ''/ϵ' is called the loss tangent.¹

The permittivity can be represented graphically by utilizing the fact that the equations for ϵ' and ϵ'' can be reduced and combined into,

$$/ 2.18 / \quad (\epsilon' - \frac{\epsilon_o + n^2}{2})^2 + \epsilon''^2 = (\frac{\epsilon_o - n^2}{2})^2 ,$$

which is the equation of a circle with center $[(\epsilon_o + n^2)/2, 0]$, and radius $(\epsilon_o - n^2)/2$.¹ Only the semicircle for $\epsilon'' > 0$ is

meaningful, and the usual representation is shown in Figure 2-4.¹

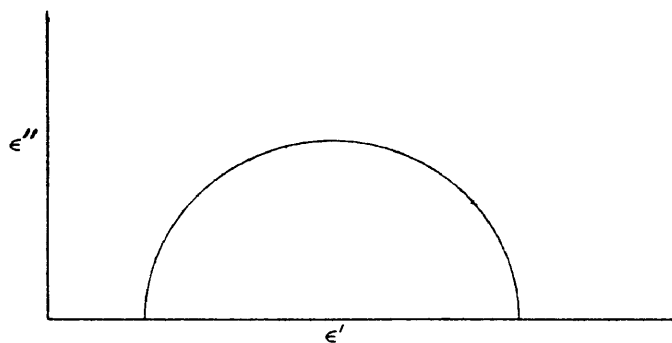


Figure 2-4

This curve does fit the data for many simple liquids, but many other materials do not fit. Cole and Cole² have proposed an empirical equation of the form,

$$\text{ / 2.19 / } \quad \epsilon^* - n^2 = \frac{\epsilon_0 - n^2}{1 + (i\omega\tau)^{(1-h)}}$$

(h is a constant; $0 < h < 1$.)

This seems to fit much data for polymers and long chain molecules whose plots of experimental data resemble the plots shown in Figure 2-5a and b.¹

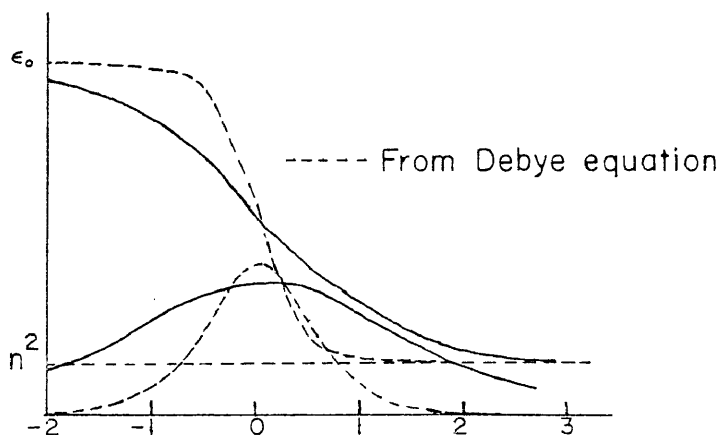


Figure 2-5a

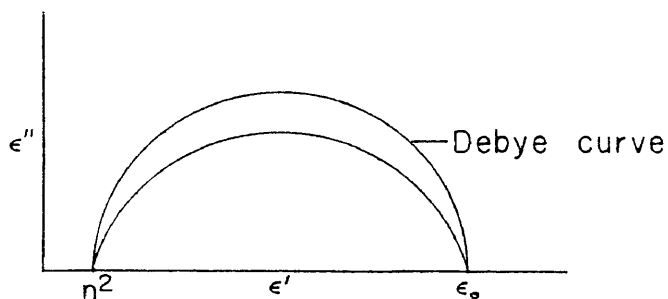


Figure 2-5b

The plot of ϵ' versus ϵ'' is symmetrical about a line through the center and parallel to the ϵ'' axis. Cole and Davidson³ found certain materials best fitted a skewed arc, and suggested the equation:

$$\text{ / 2.20 / } \quad \frac{\epsilon^* - n^2}{\epsilon_0 - n^2} = \frac{1}{(1 + i\omega\tau)^\alpha} ; 0 < \alpha \leq 1 .$$

Shapes of this equation for various values of α are shown in Figure 2-6.¹ Experimental data acquired at low temperatures seems to fit this equation well with α approaching 1 as the temperature increases.⁴

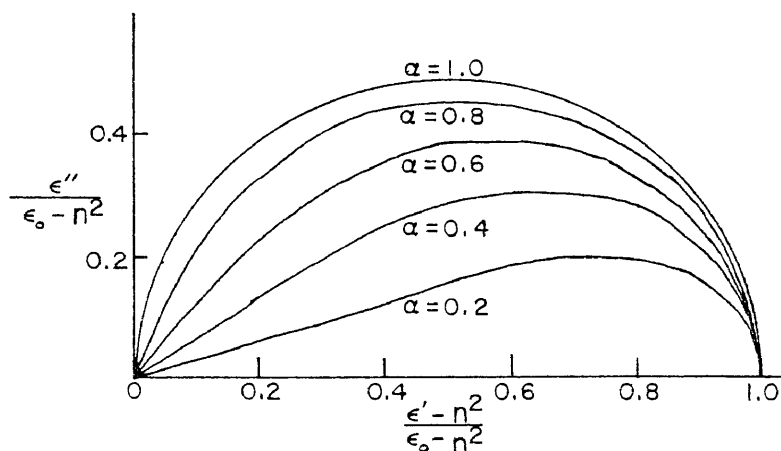


Figure 2-6

Thus far we have been considering macroscopic theories of dielectric relaxation. Now we will look at this phenomenon from a microscopic or molecular viewpoint.

Since the phenomenon of dielectric dispersion is directly related to the physical rotation of the molecules under the influence of an external field, it is necessary to examine the mechanism or mechanisms whereby these molecules rotate. It is to be expected that this mechanism will depend on a number of factors, including the state of the dielectric material.

Debye⁵ assumed that rotation of a molecule due to an external field was interrupted by collisions with neighboring molecules. This assumption is reasonable in the case of liquids but less justifiable in the case of solids, or gases of low to medium pressure. Using the theory of Brownian motion as developed by Einstein, and assuming the Lorentz field, Debye derives the following relation:

$$/ 2.21 / \quad \frac{\epsilon^* - n^2}{\epsilon_0 - n^2} = \frac{1}{1 + i\omega\tau} ; \tau = \frac{\epsilon_0 + 2}{n^2 + 2} \tau ,$$

where τ is the molecular relaxation time as defined previously.

Extension of Onsager's theory of static permittivity to the high frequency region⁶ leads to the expression,

$$/ 2.22 / \quad \epsilon^* - n^2 = \frac{A}{1 + i\omega\tau} \frac{\epsilon^*}{\epsilon^* + \frac{1}{2}} ,$$

where A is frequency independent and is given by,

/ 2.23 /

$$A = \frac{(n^2 + 2)(2\epsilon_0 + 1) 8\pi N_1 \mu^2}{(2\epsilon_0 + n^2) 9kT\epsilon_0}$$

Debye's assumption that the applied field rotates molecules at their terminal velocity is seen to hold reasonably well up to frequencies near 1 to 2 gigahertz. At higher frequencies, inertial corrections, which Debye neglects, cause the actual angular velocity to deviate more and more from the terminal velocity.^{6,1}

A number of other theories of microscopic relaxation have been proposed. Eyring^{7,1} draws an analogy between dipole rotation and chemical rate processes. Bauer's theory^{8,1} is similar to Eyring's and both theories make the assumption of a potential barrier of some type which affects free rotation. Cole^{9,1} presents a theory which produces a result of the same form as Debye:

$$\text{/ 2.24 /} \quad \frac{\epsilon^* - n^2}{\epsilon_0 - n^2} = \frac{1}{1 + \left[\frac{\epsilon_0 + 2}{n^2 + 2} \right] i\omega T_s},$$

except that here T_s is the macroscopic relaxation time for a sphere as opposed to the microscopic time which appears in Debye's theory (equation 2.21). The term in brackets is a result of the choice of a spherical model. Changing the assumed shape (for instance, to ellipsoidal) will change the ratio of the two relaxation times (microscopic to macroscopic).¹

A relation is also derived based on a model of a small

sphere within the overall spherical specimen.^{9,10} This result is:

$$/ 2.25 / \quad T_s = (1 - A) T_m ,$$

where T_s is the relaxation time of the spherical specimen and T_m is the time for the small internal sphere. Also if the correlation function of a dipole at the center of the small internal sphere is defined by

$$/ 2.26 / \quad \gamma(t) = \langle \mu(0) \cdot \mu(t) \rangle / \langle \mu(0) \cdot \mu(0) \rangle ,$$

the surrounding material is treated as a continuum, and $\gamma(t)$ is assumed to be a simple exponential ($\gamma(t) = \exp(-t/\tau)$) ; it is found that^{1,9}

$$/ 2.27 / \quad T_s = \frac{3\epsilon_o (n^2 + 2)}{(2\epsilon_o + n^2)(\epsilon_o + 2)} \tau ;$$

$$/ 2.28 / \quad T = \frac{3\epsilon_o}{2\epsilon_o + n^2} \tau$$

Fatuzzo and Mason^{11,1} have questioned one of the assumptions used in the above derivation, and Klug, Kranbuehl and Vaughan^{12,1} have derived the following equation based on this modified assumption:

$$/ 2.29 / \quad \frac{(\epsilon^* - n^2)(2\epsilon^* + n^2)}{\epsilon^*} = \frac{(\epsilon_o - n^2)(2\epsilon_o + n^2)}{\epsilon_o} = \frac{1}{1 + i\omega\tau} .$$

Glarum¹³ has proposed a model which can account for the experimentally observed "skewed arc" behavior found by Davidson and Cole^{3,4}; although, as Mopsik¹⁴ points out, this

model "admittedly has many defects."

In the normal case, all molecules feel the same average hindrance to reorientation and thus exhibit a single relaxation time. This hindrance is a result of the environment of each molecule, and these environments are assumed to be the same for all molecules. In Glarum's model, "defects" are present in the solid or liquid, and are distributed throughout the sample according to a diffusive law. The presence of a "defect" in the environment of a molecule greatly decreases the hindrance to reorientation, thus allowing the dipole to relax essentially spontaneously. This process is assumed to be independent of the normal relaxation process. Although the expression for the general case is complicated, three specific cases yield interesting results. If the rate of arrival of defects is small compared to the normal relaxation time, then a result corresponding to Debye type relaxation is obtained. If the rate of arrival is equal to the normal relaxation time, then a skewed arc with $\alpha = 0.5$ (eq. 2.20) is obtained; and if the rate of arrival is much greater than the normal relaxation time, then a semicircle with $h = 0.5$ (eq. 2.19) is predicted.¹

A number of authors^{15,16} have proposed theories based on the concept of "free volume", defined differently by different authors, but basically the local room which each molecule has available. These theories are related to Glarum's in that all assume more than one time dependent

process which affects reorientation.

Thus far we have considered dielectric relaxation only in general microscopic terms. We would like to relate the relaxation to some macroscopic property or properties of the specimen. Debye⁵ suggested making the assumption that the molecule could be represented by a sphere rotating in a homogenous medium of viscosity η equal to the viscosity of the bulk sample according to Stokes law. This assumption, when applied to Debye's theory gives:

$$/ 2.30 / \quad \tau = 4\pi\eta a^3 / kT ,$$

where a is the radius of the molecular "sphere". This gives results which are 5 to 10 times too high, and numerous attempts at improvement have been made.¹⁷⁻²⁰

A basic problem with Debye's assumption is that unless the polar molecule is large compared to the surrounding non-polar solvent, the solvent cannot really be treated as a continuous medium of viscosity η .

Wirtz and his co-workers²⁰ have attempted to take into account the discontinuous nature of the surrounding medium. Their results indicate that when the polar molecules are large compared to the surrounding molecules

$$/ 2.31 / \quad \tau = 4\pi\eta a^3 / kT ,$$

the same result obtained by Debye. When the molecules are all the same size (e.g., a pure polar liquid),

$$\tau = 2\pi\eta a^3 / 3kT ,$$

a relaxation time six times smaller than that predicted by Debye, and in much better agreement with experiment.

NOTES FOR CHAPTER II

1. Nora E. Hill, et.al., "Dielectric Properties and Molecular Behavior," Van Nostrand Reinhold Co., N.Y., N.Y., 1969.
2. K.S. Cole and R.H. Cole, J. Chem. Phys., 9, 341(1949).
3. D.W. Davidson, R.H. Cole, J. Chem. Phys., 18, 1417(1951).
4. D.W. Davidson, R.H. Cole, J. Chem. Phys., 19, 1484(1951).
5. Peter Debye, "Polar Molecules," The Chemical Catalogue Company, Inc., New York, N.Y., 1929.
6. M.Y. Rocard, J. Phys. Radium, Paris, 4, 247(1933).
7. S. Glasstone, K.I. Laidler, H. Eyring, "The Theory of Rate Processes," McGraw-Hill, New York, N.Y., 1941.
8. E. Bauer, Cah. Phys., 20, 1(1944).
9. R.H. Cole, J. Chem. Phys., 42, 637(1965).
10. S.H. Glarum, J. Chem. Phys., 33, 1371(1960).
11. E. Fatuzzo, P. Mason, Proc. Phys. Soc., 90, 741(1967).
12. Dennis D. Klug, David E. Kranbuehl, and Worth E. Vaughan, J. Chem. Phys., 50(9), 3904(1969).
13. S.H. Glarum, J. Chem. Phys., 33, 369(1960).
14. F.I. Mopsik, Doctoral Thesis, Brown University, 1964; University Microfilms, 65-2229, Ann Arbor, MI, 1975.
15. J. Anderson, R. Ullman, J. Chem. Phys., 47, 2178(1967).
16. M. Cohen, D. Turnbull, J. Chem. Phys., 31, 1164(1959).
17. F. Perrin, J. Phys. Radium, Paris, 5, 497(1934).
18. E. Fischer, Phys. Z., 60, 645(1939).
19. A. Budo, E. Fischer, S. Miyanoto, Phys. Z., 40, 337(1939).
20. A. Gierer and K. Wirtz, Z. Naturf., 8a, 532(1953).

CHAPTER III
THEORETICAL CONSIDERATIONS OF UHF DIELECTRIC MEASUREMENTS
Transmission Line Theory

The theoretical approach used for a given experiment depends upon the frequency range under consideration. At lower frequencies the sample is small enough compared to the wavelength, that bridge or resonant methods may be used in conjunction with either lumped or distributed circuit analysis. Above approximately 200Mhz, the sample is no longer small compared to the wavelength of the applied field, and transmission line techniques must be used. An upper limit of approximately 75GHz is imposed on this technique by the difficulty of fabricating components with the required precision in their physical dimensions. Free space methods can be used in this frequency range.¹

In the frequency ranges which require transmission line methods it is necessary to investigate the electric and magnetic fields which are present. This is best done by starting from Maxwell's equations: From any general text on electromagnetics, the following pertinent equations can be found.

$$/ 3.1 / \quad \text{div } D = \nabla \cdot D = 4\pi\rho \quad ,$$

where ρ is the free charge density and D is the dielectric

displacement.

$$/ 3.2 / \quad \text{div } B = \nabla \cdot B = 0 ,$$

where B is the magnetic induction or magnetic flux density.

$$/ 3.3 / \quad \text{curl } H = \nabla \times H = \frac{1}{c} \left[\dot{D} + 4\pi J \right] ,$$

where H is the magnetic field intensity; J is the current density; and c is the speed of light in vacuo.

$$/ 3.4 / \quad \text{curl } E = \nabla \times E = - \frac{1}{c} \dot{B} ,$$

where E is the electric field intensity. The following three relations also hold.

$$/ 3.5 / \quad D = \epsilon' E ;$$

$$/ 3.6 / \quad J = \sigma_c E ;$$

$$/ 3.7 / \quad H = B/\mu_o ; \quad B/H = \mu_o ,$$

where ϵ' is the real part of the permittivity and σ_c is the ohmic conductivity of the medium. μ_o is the permeability.

The following derivation is based on that of Glarum.² We assume that the materials of interest are non-magnetic so that $\mu_o = 1$. We can now write for a conducting medium:

$$/ 3.8 / \quad \nabla \cdot D = \nabla \cdot (\epsilon' E) ;$$

$$/ 3.9 / \quad \nabla \cdot B = \nabla \cdot H = 0 ;$$

$$/ 3.10 / \quad \nabla \times E = - \frac{1}{c} \dot{H} .$$

Substituting into equation 3.3 gives

$$/ 3.11 / \quad \nabla \times H = \frac{1}{c} [\epsilon' \dot{E} + 4\pi\sigma_c E]$$

If we assume that the applied field is alternating sinusoidally, then,

$$/ 3.12 / \quad E(t) = E_0 e^{i\omega t},$$

from which it can be shown that

$$/ 3.13 / \quad E = - \frac{i \dot{E}}{\omega},$$

which, when substituted into equation 3.11, gives

$$/ 3.14 / \quad \nabla \times H = \frac{1}{c} \left[\epsilon' \dot{E} - \frac{i 4\pi\sigma_c \dot{E}}{\omega} \right] = \frac{\dot{E}}{c} \left[\epsilon' - \frac{i 4\pi\sigma_c}{\omega} \right].$$

A normal dielectric has zero free charge density so that $\nabla \cdot D = \nabla \cdot (\epsilon' E) = 4\pi\rho = 0$. If we now assume that the dielectric constant is complex and of the form

$$/ 3.15 / \quad \epsilon^* = \epsilon' - i\epsilon'',$$

then

$$/ 3.16 / \quad \nabla \times H = \frac{\epsilon^* \dot{E}}{c}$$

We see that equation 3.14 is of the same form as that for a non-conducting dielectric.

Consequently, to a solution of the field equations involving a nonconducting dielectric, there exists a formally similar solution in which a complex dielectric constant appears in place of the real dielectric constant provided, of course, that the electric fields involved are of the form given by Equation 3.12.²

If the complex dielectric constants given in equations 3.15 and 2.13 are equivalent, ϵ'' is related to σ_c as shown in equations 2.11 through 2.17.

To generate the pertinent field equations we take the curl of both sides of equation 3.10:

$$/ 3.17 / \quad \nabla \times (\nabla \times E) = - \frac{1}{c} \left[\nabla \times \left(\frac{\partial H}{\partial t} \right) \right]$$

Due to the interchangeability of space and time derivatives³ we can rewrite 3.17 as

$$/ 3.18 / \quad \nabla \times (\nabla \times E) = - \frac{1}{c} \left[\frac{\partial (\nabla \times H)}{\partial t} \right] ;$$

and substituting from equation 3.16, we get

$$/ 3.19 / \quad \nabla \times (\nabla \times E) = - \frac{\epsilon^*}{c^2} \left[\frac{\partial (\partial E / \partial t)}{\partial t} \right] = - \frac{\epsilon^*}{c^2} \ddot{E} .$$

From standard vector relationships, we obtain the identity

$$/ 3.20 / \quad \nabla \times (\nabla \times E) = \nabla (\nabla \cdot E) - (\nabla \cdot \nabla) E ;$$

and since $\nabla \cdot E = 0$, we can combine 3.19 and 3.20 to give the desired wave equation:

$$/ 3.21 / \quad \nabla^2 E = - \frac{\epsilon^*}{c^2} \ddot{E}$$

In exactly the same manner, we find that

$$/ 3.22 / \quad \nabla^2 H = - \frac{\epsilon^*}{c^2} \ddot{H}$$

For a fixed frequency, plane waves travelling in a waveguide in the z direction will reasonably give

$$/ 3.23 / \quad E = E_o(x,y) e^{i\omega t - \gamma z} \quad , \text{and}$$

$$/ 3.24 / \quad H = H_o(x,y) e^{i\omega t - \gamma z} \quad .$$

The variable γ in the above equations is known as the propagation constant. It is complex and can be written in general as

$$/ 3.25 / \quad \gamma = \alpha + i\beta \quad ,$$

where α is an attenuation factor and β is a measure of the phase velocity of the wave.²

It can be shown that if propagation is to occur in a hollow waveguide, either E_o or H_o must have a non-zero z component. Modes of propagation with z components of the E and H fields equal to zero are designated TE and TM respectively. If a center conductor is present, as in coaxial line, neither E nor H need have a z component, and the resulting mode is designated TEM.²

Substitution of equations 3.23 and 3.24 into the wave equations 3.21 and 3.22 results in a solution for γ ,²

$$/ 3.26 / \quad \gamma^2 = k_c^2 - \frac{\omega^2 \epsilon^*}{c^2} \quad ,$$

where k_c is a geometric parameter which depends on the mode of propagation and the dimensions of the waveguide. There is a cut-off frequency ω_c such that

$$/ 3.27 / \quad \omega_c = ck_c ;$$

and therefore, if ω_c is less than ω , and the wave guide is in vacuum, so that $\epsilon^* = 1$,

$$/ 3.28 / \quad \gamma^2 = \frac{\omega_c^2 - \omega^2}{c^2} ; \quad \gamma = \frac{\sqrt{\omega_c^2 - \omega^2}}{c} .$$

This indicates that above the cut-off frequency, propagation with no attenuation occurs; and below the cut-off frequency, attenuation occurs without propagation. For a waveguide of given dimensions, there are an infinite number of modes (designated TE_{mn} and TM_{mn} , with m and n 0,1,2,etc.) each having a certain cut-off frequency. Below a certain frequency none of the modes will propagate and above some other frequency, more than one mode can propagate.² Since one normally wishes to study only the lowest mode possible for a given waveguide, the bandwidth for each waveguide is limited.

For the TEM mode for coaxial line, k_c is zero. Due to the possibility of higher modes, an upper frequency limit exists which is given by²

$$/ 3.29 / \quad \omega = 2.136c/(a + b),$$

where a is the outside radius of the inner conductor and b is the inside radius of the outer conductor. At this frequency another, higher mode will begin to propagate; and since we only want the TEM mode, we must operate between

zero and ω_c .

If λ_o is the free space wavelength corresponding to ω and λ_c corresponds to ω_c , then the complex dielectric constant can be written from equation 3.26 as

$$/ 3.30 / \quad \epsilon^* = (\lambda_o / \lambda_c)^2 - (\lambda_o / 2\pi)^2 \gamma^2 .$$

Thus ϵ^* may be found by experimental determination of the propagation constant. This determination may, in practice, involve a number of problems.

In our work we will use another method which necessitates the development of the concept of wave impedance. This is defined as the ratio of the transverse component of the electric field to that of the magnetic field.² For a traveling wave in a coaxial line (TEM mode), it can be shown that the characteristic wave impedance η_o , is constant and given by

$$/ 3.31 / \quad \eta_o = \pm \sqrt{\mu_o / \epsilon^*} ,$$

where the plus and minus signs refer to the direction of travel of the waves.² For an air filled coaxial line such as we used, both μ_o and ϵ^* are essentially equal to 1 so that $\eta_o = \pm 1$. This is not to be confused with the surge impedance, Z_o , which is defined as the ratio of voltage to current and given by

$$/ 3.32 / \quad Z_o = \frac{1}{2\pi} \left(\frac{\mu}{\epsilon^*} \right)^{1/2} \ln(b/a) .$$

A dielectric filled section of coaxial line will have

a wave impedance η_{02} and a propagation constant γ_2 . Suppose that this section has a termination with a complex reflection coefficient, ρ_2 , which is defined as the ratio of the reflected field to the incident field: $\rho_2 \equiv E_{\uparrow}^{-} / E_{\uparrow}^{+}$. It can be shown that $\rho_2 = -H_{\uparrow}^{-} / H_{\uparrow}^{+}$, and we can write the following equations which apply at the termination.²

$$/ 3.33 / \quad E_{\uparrow}^{-} = \rho_2 E_{\uparrow}^{+} \quad ;$$

$$/ 3.34 / \quad H_{\uparrow}^{-} = -E_{\uparrow}^{-} / \eta_{02} = -\rho_2 E_{\uparrow}^{+} / \eta_{02} = -\rho_2 H_{\uparrow}^{+} \quad .$$

Assuming that both the incident and reflected waves travel in a positive direction along the z axis, and that the termination is at $z = 0$; then, at some distance d in front of the termination, the z coordinate will be d and $-d$ for the reflected and incident waves respectively. For sinusoidal waves this gives

$$/ 3.35 / \quad E_{\uparrow}^{+} = E_0 e^{i\omega t - \gamma_2 z} = E_0 e^{i\omega t + \gamma_2 d} \quad ; \quad z = -d$$

$$/ 3.36 / \quad E_{\uparrow}^{-} = E_0 e^{i\omega t - \gamma_2 z} = E_0 e^{i\omega t - \gamma_2 d} \quad ; \quad z = d$$

$$/ 3.37 / \quad H_{\uparrow}^{+} = E_{\uparrow}^{+} / \eta_{02} = E_0 e^{i\omega t + \gamma_2 d} / \eta_{02} \quad ; \quad z = -d$$

$$/ 3.38 / \quad H_{\uparrow}^{-} = -E_{\uparrow}^{-} / \eta_{02} = -\rho_2 E_0 e^{i\omega t - \gamma_2 d} / \eta_{02} \quad ; \quad z = d$$

From the definition of wave impedance

$$/ 3.39 / \quad \eta_d = \frac{E_{\uparrow}^{+} + E_{\uparrow}^{-}}{H_{\uparrow}^{+} + H_{\uparrow}^{-}} \quad ,$$

and substituting from 3.35-3.38 we obtain

$$/ 3.40 / \quad \eta_d = \frac{E_o e^{i\omega t + \gamma_2 d} + \rho_2 E_o e^{i\omega t - \gamma_2 d}}{(E_o e^{i\omega t + \gamma_2 d} - \rho_2 E_o e^{i\omega t - \gamma_2 d}) \eta_{02}} ,$$

$$/ 3.41 / \quad \eta_d = \frac{\eta_{02} (e^{\gamma_2 d} + \rho_2 e^{-\gamma_2 d})}{(e^{\gamma_2 d} - \rho_2 e^{-\gamma_2 d})}$$

For the important case when the termination is a short, $\rho_2 = -1$, and equation 3.41 becomes²

$$/ 3.42 / \quad \eta_d = \eta_{02} \left[\frac{e^{\gamma_2 d} - e^{-\gamma_2 d}}{e^{\gamma_2 d} + e^{-\gamma_2 d}} \right] = \eta_{02} \tanh \gamma_2 d .$$

The usefulness of this experimental procedure lies in the fact that it allows the use of real rather than complex values. Most other methods using transmission line techniques require complicated mathematical procedures to obtain the desired results from the experimentally determined parameters.^{2,4}

These complex values are eliminated by using a variable length section of dielectric filled coaxial line, terminated in a short circuit. The distance can be adjusted so that, at one or more positions of the short, the input impedance η is entirely resistive, i.e., real. These distances are functions of the real and imaginary parts of the propagation constant. If we know a distance for which the impedance is real, and the corresponding impedance, we can find the propagation constant.^{2,4}

For a dielectric filled line with propagation constant γ , and where η_o is the characteristic wave impedance,

equations 3.25, 3.30 and 3.31 can be combined to give

$$/ 3.43 / \quad 1/\eta_o = (\lambda_o/2\pi)(\beta - i\alpha) \quad .$$

The wave admittance Y is defined as $1/\eta$, so that equation 3.42 now gives

$$/ 3.44 / \quad Y = 1/\eta_o \coth \gamma d \quad ,$$

which on substituting from equation 3.43, gives

$$/ 3.45 / \quad Y = (\lambda_o/2\pi)(\beta - i\alpha) \left[\frac{b \sinh 2\alpha d - i \sin 2\beta d}{\cosh 2\alpha d - \cos 2\beta d} \right]$$

Setting $2\alpha d = a$, and $2\beta d = b$, the above equation becomes

$$/ 3.46 / \quad Y = (\lambda_o/4\pi d) \left[\frac{(b \sinh a - a \sin b) - i(a \sinh a + b \sin b)}{\cosh a - \cos b} \right] .$$

When we experimentally adjust the distance so that Y is real, the second term in the bracketed numerator is zero; i.e., $(a \sinh a + b \sin b) = 0$, and

$$/ 3.47 / \quad Y = (\lambda_o/4\pi d) \left[\frac{b \sinh a - a \sin b}{\cosh a - \cos b} \right] = (\lambda_o/4\pi d) C_n(a, b) \quad .$$

For any value of $Y/(\lambda_o/4\pi d)$, there are multiple solutions of $C_n(a, b)$. Using equations 3.25 and 3.30 and remembering $a = 2\alpha d$, $b = 2\beta d$, and that $\omega_c = 0$ for the TEM mode, the complex dielectric constant can be separated and expressed as

$$/ \text{ 3.48 } / \quad \epsilon' = (\lambda_o/4\pi d)^2 (b^2 - a^2) \quad ,$$

$$/ \text{ 3.49 } / \quad \epsilon'' = (\lambda_o/4\pi d)^2 2ab \quad ,$$

and $\tan \delta = 2ab/(b^2 - a^2)$. A computer program and the resultant tables of values for $C_n(a,b)$, $b^2 - a^2$, $2ab$, and $\tan \delta$, are presented in Appendices I and II.

NOTES FOR CHAPTER III

1. Worth E. Vaughan, Chapter II: Experimental Methods, in "Dielectric Properties and Molecular Behavior," Nora E. Hill, Ed., Van Nostrand Reinhold, Co., New York, N.Y., 1969.
2. S.H. Glarum, Doctoral Thesis, Brown University, 1960; University Microfilms, 62-5745, Ann Arbor, Michigan, 1975.
3. W.T. Scott, "The Physics of Electricity and Magnetism," John Wiley & Sons, Inc., New York, N.Y., 1966.
4. F.I. Mopsik, Doctoral Thesis, Brown University, 1964; University Microfilms, 65-2229, Ann Arbor, Michigan, 1975.

CHAPTER IV

UHF EXPERIMENTAL

The equipment and procedure are based on previous work done by Mopsik¹ and Glarum².

All electronic equipment was purchased from General Radio Company, West Concord, Massachusetts. A complete list of all components is given in Appendix III.

The central component of the measurement apparatus was a General Radio type 1602-B admittance meter which is a direct reading instrument and covers the frequency range from 40 to 1500 megahertz (to 20MHz with the appropriate correction). Its stated accuracy is $\pm(3\% + 0.2\text{mmhos})$ from 0 to 20 millimhos below 1000MHz, and with the 1607-P10 multiplier plate provided, the accuracy is improved to $\pm(3\% \pm 0.04\text{mmhos})$ from 0 to 2.0mmhos.³ A schematic diagram is shown in Figure 4-1, and includes the auxillary equipment -- (generator, detector, standards, and the unknown).

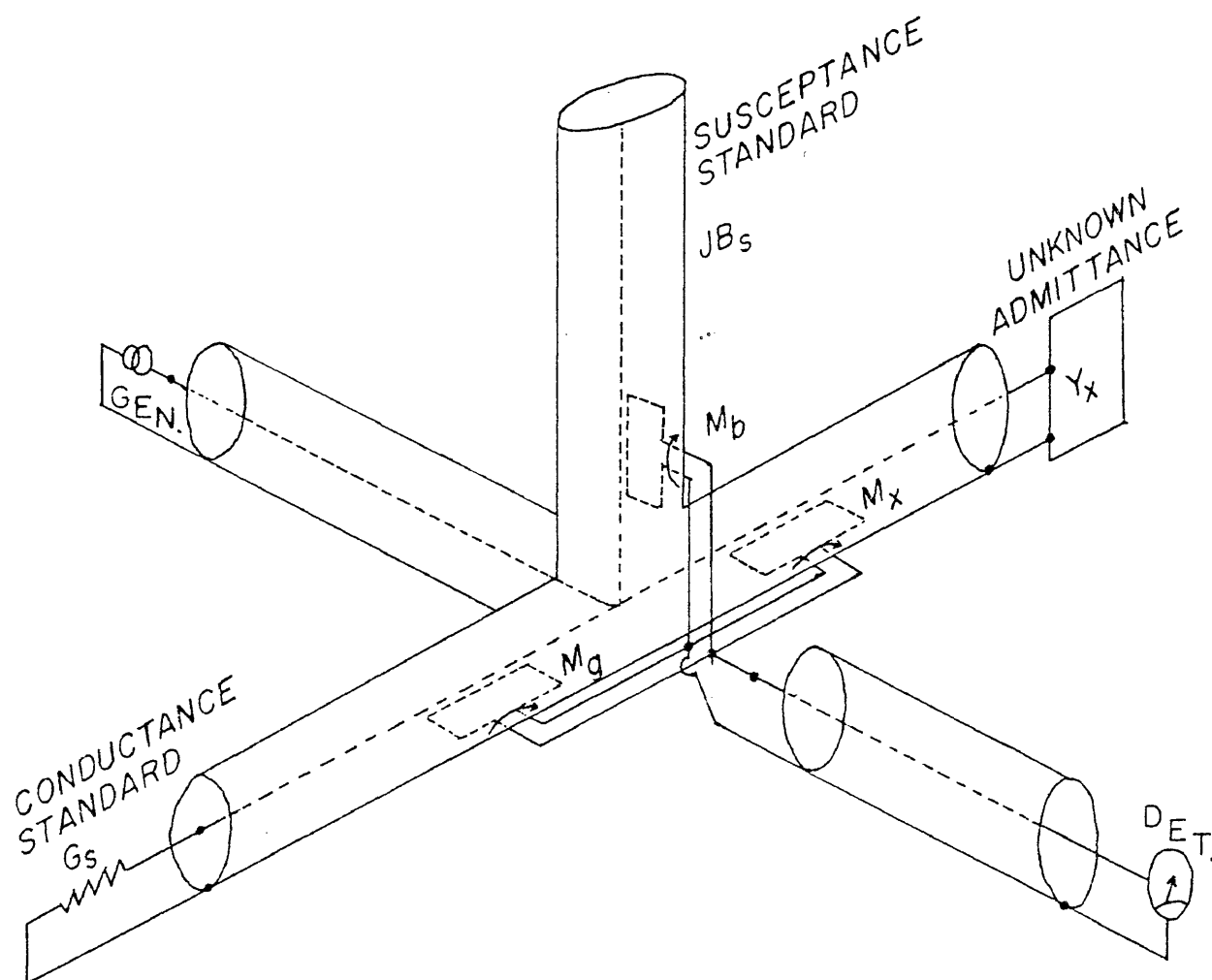


Figure 4-1

The admittance meter is also shown in Plates 1 and 2. Although it is a null reading device, the admittance meter is not a true bridge. It has three coaxial lines which are fed from a common junction, and the current flowing in these lines is measured by three rotatable coupling loops which sample the magnetic component of the field in each of three arms (unknown, conductive, and susceptive). The susceptance loop is rotatable through 180° and the conductance and unknown loops can be rotated through 90° . The voltages induced in the loops are proportional to the

cosines of the angles which the loops make with the coaxial line. These three loops are connected in parallel to a coaxial line which feeds the crystal mixer and heterodyne detector. When the loops are properly oriented, the combined output is zero and a null is read on the detector. In this sense, the admittance meter balances as does a bridge.³

The conductance standard is a pure resistance equal to 50 ohms, the characteristic surge impedance of the coaxial line; and the susceptance standard is a short circuited length of coaxial line. In actual practice, the susceptance standard was replaced with a type 874-WOL open circuit, since our procedure is based on the premise that the imaginary (susceptive) part of the admittance is zero.

The admittance meter actually measures the admittance at a point directly under the center of the unknown coupling loop. Thus, if the admittance is desired at some other point on the coaxial line, correction for the effect of the length of the transmission line must be made. If the electrical length of the line between the center of the coupling loop and the point at which the admittance is desired is exactly an integral number of half-wavelengths, then the measured and unknown admittances will be equal. Also, if the distance is an odd number of quarter-wavelengths, the admittance meter will read the resistive and reactive (rather than conductive and susceptive) components of the unknown.³ For example, in our procedure, a short circuit is placed $\frac{1}{4}$ wavelength from the interface of the cell and

the constant impedance adjustable line; and the adjustable line is set to give a null reading, which occurs when the overall electrical length is $\frac{3}{4}$ wavelength. Therefore, the cell window is then $\frac{1}{2}$ wavelength from a point above the center of the coupling loop, and the meter will measure the input admittance of the cell.

If we are to use the equations previously presented, we need to know the relationship between the admittance measured by the meter and the input wave admittance, Y , which appears in equations 3.44 - 3.47.

$$/ 4.1 / \quad Y = \frac{1}{\eta_o} \coth \gamma d \quad ; \quad (\rho = -1) \quad ; \quad (\text{eq. 3.44})$$

If we treat the dielectric filled section as a termination with complex reflection coefficient, ρ , equation 4.1 can be rewritten as

$$/ 4.2 / \quad Y = \frac{1}{\eta_{o1}} \frac{e^{\gamma d} - \rho e^{-\gamma d}}{e^{\gamma d} + \rho e^{-\gamma d}}$$

where η_{o1} is the characteristic wave impedance of the section in front of the interface. Since $d=0$ at the interface, 4.2 becomes

$$/ 4.3 / \quad Y = Y_{o1} \frac{1 - \rho}{1 + \rho}$$

From the definition of ρ , it can be shown that

$$/ 4.4 / \quad \rho = \frac{Y_o - Y_x}{Y_o + Y_x}$$

where Y_0 is the characteristic surge admittance of the transmission line (20mmhos), and Y_x is the characteristic wave admittance of the unknown. Therefore,

$$/ 4.5 / \quad Y = Y_x/Y_0 = \frac{\text{measured admittance}}{20\text{mmhos}}$$

Thus the measured admittance must be divided by 20mmhos before being used in equation 3.48 and 3.49.

The cell was constructed by the William and Mary Physics Department shop using the 50cm stub and BNC adapter, following the description given by Mopsik.¹

It (the cell) consists of a modified General Radio type 874-D50 adjustable stub. The outer conductor was cut to the desired length and surrounded with a jacket through which thermostating fluid could be pumped. Also entry was provided for the insertion of a thermocouple for the measurement of temperature. The bottom end of the outer conductor butted against a small land in the jacket for alignment purposes and was made the same inner diameter as the outer conductor so that electrically it would be continuous. A Kel-F window sealed off the bottom which was made the same physical size as the polystyrene window in a General Radio type 874 connector so that when the entire cell was assembled, any discontinuities would be no worse than that due to a similar connector. Around the outer edge, and the inner one, small rings of Teflon were placed to provide a liquid-tight seal. Below the window is the outer part of a type 874-QBPA adapter with the 874 connector removed. A nut threaded into the bottom of the outer jacket tightened down on this piece by means of a small ring inserted in a groove in the adapter. By this means, sufficient pressure could be applied for the Teflon seal to be liquid tight. When the entire assemble was put together, it should be electrically as smooth as the top half of a General Radio connector and therefore, adequate for the purposes of measurement.

The inner conductor of the stub on top of the window was joined to the inner conductor of the adaptor below the window by a short section of threaded brass rod which also allowed

sufficient tightening to be applied to the Teflon seal. The shorting piston assembly was made from the contact fingers and a small length of solid continuation in the original stub. These could be separated into inner and outer finger pieces which were reassembled around a brass ring of the proper dimensions to fill the space between the pieces up to where the fingers began. Then a thin brass tube was affixed to the brass ring, concentric to the center conductor, of sufficient length to reach above the cell when the plunger was at the bottom of the cell. The entire plunger assembly was made so that the fingers were on top and the brass ring was flush with the bottom in order to present a smooth, flat surface to the electrical circuit.

The finished cell is shown in Figure 4-2 and in Plates 3 and 4. The only major differences between our cell and that described by Mopsik are the lack of a third outlet in the thermo jacket, use of a finely scribed line on the plunger as a measuring reference since measurement was by optical rather than physical means; and the use of stainless steel for the plunger tube.

Figure 4-3 and Plates 5 and 6 show the interconnection of the components.

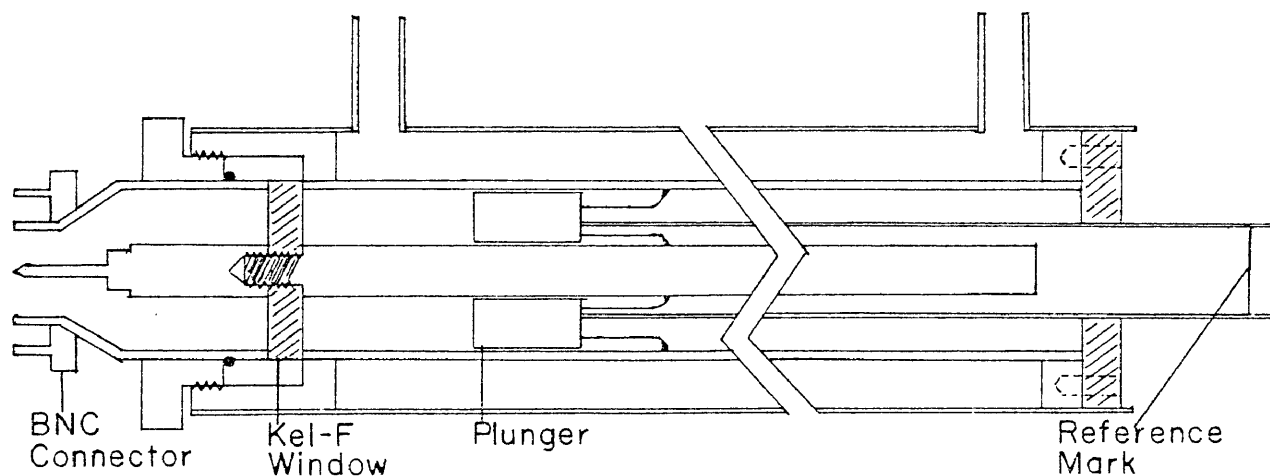


Figure 4-2

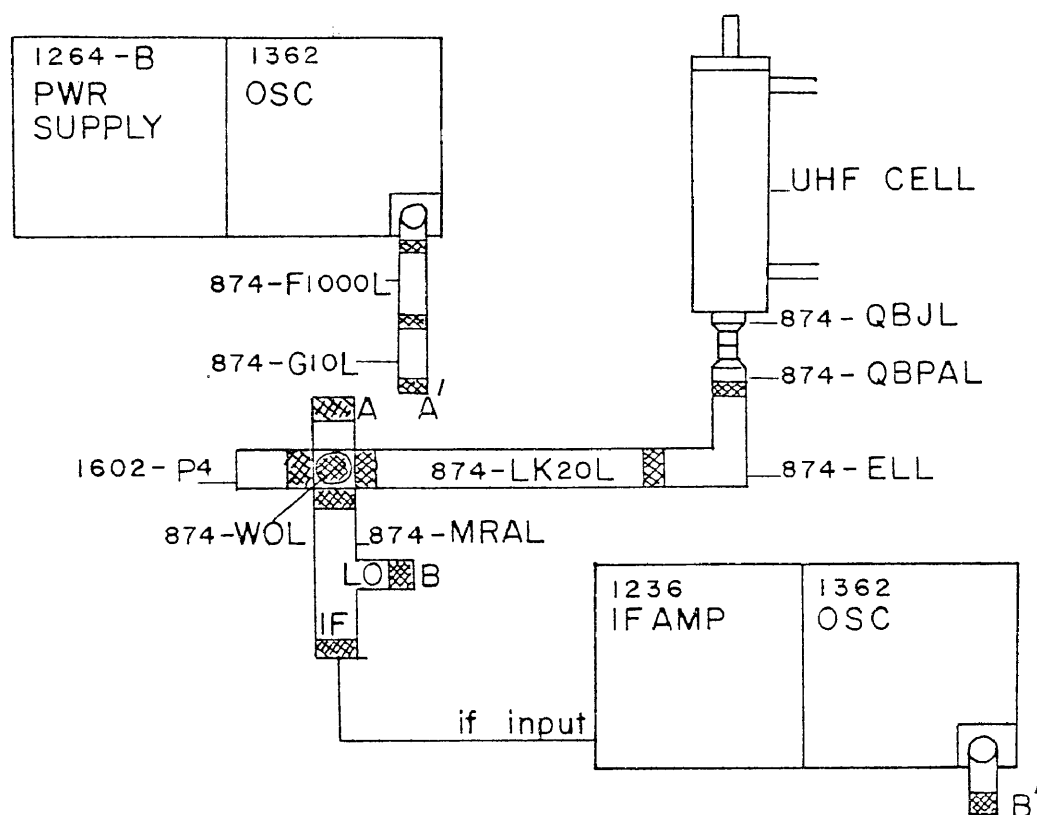


Figure 4-3

In addition to the interconnection as shown, the cell was mounted vertically and rigidly on a vacuum rack, but in such a way that it could be easily removed for solution changes, cleaning and maintenance. The cathetometer, which was used to measure the extension of the plunger, was placed on a low table close to the cell so that there was an unobstructed view of the plunger tube.

Operation of the equipment was relatively simple. The signal generator was turned on, and the oscillator was set to the desired frequency. According to the instruction manual, drift should be less than 0.1% after fifteen minutes and negligible after one hour. In practice the signal generator and the detector were allowed to warm up for at

least two hours; and if continual use over a several day period was anticipated, they were left on, although turned down as low as possible in between measurement periods.

Once sufficient warm up time had passed, the modulation level was set to an arbitrarily chosen level (seven on the scale of ten). The IF oscillator was tuned to a frequency 30 Megahertz lower (or higher) than the signal generator, as indicated by a peak reading on the detector meter. The IF amplifier was used in the normal switch position and the calibrated attenuation adjusted as necessary. Once the detector had been tuned, the mixer current was checked by placing the switch on the IF amplifier in the appropriate position. The current should read between 50 and 100 on the scale and was adjusted with the sliding attenuator on the oscillator section of the IF amplifier. A setting of 85 was used throughout the measurements.

The multiplier plate type 1607-P10 was installed in the admittance meter so that the conductance scale would read times 0.1. The multiplier arm was set to zero as was the susceptance arm. With the connections and settings made as described, and the cell hooked up; calibration of the equipment using carbon tetrachloride and benzene was performed.

To calibrate the cell, the plunger was pushed all the way to the bottom of the cell; and then, using the cathetometer, the plunger was extended one quarter wave-length (calculated from the nominal generator frequency with the speed of light equal to $299,792.4562^4$ kilometers per second).

With the cell length thus fixed, the constant impedance line was adjusted for a null on the meter. Then the conductance arm of the meter was adjusted for a further null. A very slight adjustment of the susceptance arm may be necessary to achieve a perfect null. The value of the conductance was found to be approximately 0.1 millimhos when the frequency was 500 megahertz. The constant impedance line was locked in place and not moved unless the frequency was changed; in which case, the procedure in this paragraph was repeated.

The solution to be measured was introduced into the cell, and the plunger and the conductance arm were reset for a null. The plunger height was measured with the cathetometer to give the value of d , and the admittance, Y , was calculated by subtracting the zero offset determined above from the new measurement and dividing that difference by 20, the value in millimhos of the standard 50 ohm termination.

The complex dielectric constant could then be calculated from equations 3.48 and 3.49:

$$/ 3.48 / \quad \epsilon' = \left(\frac{\lambda_0}{4\pi d} \right)^2 \cdot (b^2 - a^2)$$

$$/ 3.49 / \quad \epsilon'' = \left(\frac{\lambda_0}{4\pi d} \right)^2 \cdot 2ab$$

The values of $b^2 - a^2$ and $2ab$ for the experimentally determined value of $C_n(a,b)$ were found from the table in Appendix II. Glarum² has shown that simple interpolation is

sufficient to determine these values accurately.

If this calculated value of the dielectric constant did not agree with the accepted value for the reference liquid, the above procedure was repeated using a certain amount of offset in the physical setting of the plunger. The actual amount of offset was dependent on the physical configuration of the plunger since that configuration directly affects the electrical properties of the plunger. The offset was found to be on the order of 0.5 cm. The actual value was determined by choosing a certain arbitrary amount and setting the plunger that much shorter than a quarter wave length. For example, with a $\frac{1}{4}$ wavelength of 10.0 cm and a trial offset of 0.5 cm, the plunger would be set to a physical distance of 9.5 cm. The constant impedance line and the conductance arm were reset for a null with the cell empty, liquid introduced again into the cell, and the plunger moved and the conductance adjusted until a new null is achieved. However, this time, the trial offset was added to the actual measured plunger distance to give d . This procedure was repeated with various trial offsets until the calculated dielectric constant was in agreement with the accepted value. The offset should be frequency independent as pointed out by Mopsik¹, but our findings seem to indicate a small variation on the order of 0.05 cm per 100 megahertz. Therefore, a determination of the offset for each different frequency is recommended.

Once this calibration has been carried out, the cell

can be used to measure the complex dielectric constants of unknown solutions.

NOTES FOR CHAPTER IV

1. F.I. Mopsik, Doctoral Thesis, Brown University, 1964; University Microfilms, 65-2229, Ann Arbor, Michigan, 1975.
2. S.H. Glarum, Doctoral Thesis, Brown University 1960; University Microfilms, 62-5745, Ann Arbor, Michigan, 1975.
3. General Radio Company, Instruction Manual, Type 1602-B Admittance Meter, General Radio Company, West Concord, Massachusetts, 1968.
4. Robert C. Weast, Ed., "Handbook of Chemistry and Physics, 54th Edition" CRC Press, Cleveland, Ohio, 1973.

CHAPTER V

EXPERIMENTAL RESULTS

Measurements on a number of solutions at two frequencies (500 and 700 MHz) and at two temperatures (25° and 60°C.) have been carried out. The following mixtures were measured:

nitrobenzene in benzene,
ortho-nitrobiphenyl in benzene,
para-nitrobiphenyl in benzene, and
2,2'-dinitrobiphenyl in benzene.

For each combination, either three or four solutions with a linear change in concentration were made; the most concentrated solution being on the order of 1.5 mole per cent for the first two compounds above; and, due to limited solubility, about 0.4 mole per cent for the second two.

A typical measurement on one solution was made as follows: The frequency generator had been previously turned on and allowed to warm up for at least two hours. The desired frequency was selected and the IF oscillator was tuned to thirty megahertz below the generator frequency. The mixer current was set to 85. The multiplier arm and the susceptance arm were set to zero. By means of difference measurements, the cell plunger was extended so that the physical distance was one quarter wavelength, less the

offset for the particular frequency. Since this setting did not usually correspond exactly to an electrical quarter wavelength, the constant impedance line was adjusted to give a null. Also, because there are slight conductances present in the system, the conductance scale may not null at exactly zero. This conductance offset, as well as the plunger offset, must be noted and taken into account in the calculations. Once this null had been found with the cell empty, the unknown liquid was poured into the cell and allowed to reach temperature equilibrium. The plunger and the conductance arm were then adjusted to give the new null point. Again by difference measurements, the distance, d , was measured. Before this value could be used, the plunger offset had to be added. Likewise, the conductance offset must be subtracted from the value of Y as read from the scale. This difference must then be divided by 20 millimhos, the value of the standard termination, to give the value of Y to be used in equations 3.48 and 3.49.

Typical values for a nominal 1.0 mole per cent solution of nitrobenzene in benzene at 25°C. and 700MHz are:

distance offset = 0.47 cm.,

conductance offset = 0.15 mmhos,

$Y = (\text{measured } Y - \text{offset})/20 = (.42 - .15)/20 = 0.0135,$

$d = \text{measured } d + \text{offset} = 6.317 + .47 = 6.787 \text{ cm.}$

From these values, the value of $C_n(a,b)$ can be found as

$$/ 5.1 / \quad C_n(a,b) = \frac{4\pi d Y}{\lambda_0} = 2.6884 \times 10^{-2}$$

Appendix II then gives values for $b^2 - a^2$ and $2ab$ of 9.8699 and 0.1075 respectively. These, in turn, yield values for ϵ' and ϵ'' of 2.489 and 0.0271.

The solution data is analysed by the method of C. P. Smyth and co-workers. This "provides the 'best' values for the solute, whilst also checking for the presence of inter-molecular interaction (solute-solute) over the concentration range studied. . ."¹

The values for ϵ' and ϵ'' for each solution - frequency - temperature combination are plotted versus the concentration of the solute (in mole per cent) and the best straight lines are found by a computer least squares analysis. These slopes, a' and a'' , and the similarly obtained slopes, a_o and a_∞ , are the Smyth parameters per unit concentration of the solute. The macroscopic relaxation time was then calculated for each slope from the equations,

$$\begin{array}{l} / \text{ 5.2 } / \\ \text{and} \quad a' = \frac{a_o - a_\infty}{1 + \omega^2 T^2} + a_\infty \end{array}$$

$$/ \text{ 5.3 } / \quad a'' = \frac{(a_o - a_\infty)\omega T}{1 + \omega^2 T^2}$$

The data which were collected for the four benzene solutions were combined with data which Howe had gathered at higher frequencies² and a computer program was written to find the best fit of all data. This program, and plots of ϵ' and ϵ'' versus concentration, appear in Appendices IV and V.

The macroscopic relaxation time is calculated from equations 5.2 and 5.3. These equations were solved by computer for a' and a'' as functions of T . The relaxation time is then determined by finding the minimum in the sum of the residuals between the calculated and experimental values of a' and a'' .

Howe estimates the error in this determination to be about $\pm 15\%$ due to a combination of experimental error and the use of the Debye model.²

The Debye model applies to rigid, spherical molecules whose total dipole moment is in one direction. The molecules studied are, however, non-spherical, non-rigid, and some have multidirectional components of their dipole moments.

The Debye equation for the microscopic relaxation time (eq. 2.30) (for dilute solutions, macroscopic and microscopic times are essentially equal) has three parameters which can affect the theoretical relaxation time. These are temperature, molecular radius (or volume, if the Van der Waals volume is used), and the bulk viscosity of the solution. Howe analyzes the effects of each parameter and concludes that the Debye model predicts the temperature dependence fairly well.² The consistent overestimation of the relaxation time by equation 2.30 is usually attributed to the use of the macroscopic (bulk) viscosity rather than the internal molecular viscosity. One of the attempts to improve theoretical and experimental agreement by modifying

the viscosity parameter can be found in reference 20 of Chapter II. A more complete discussion can be found in Hill.¹

Since the ortho and para-nitrobiphenyls have the same molecular volume, equation 2.30 predicts that the relaxation times will be the same, whereas the experimental values differ by approximately a factor of 2. Likewise, the ratio of molecular volumes for nitrobenzene and p-nitrobiphenyl is 1:1.7, whereas the experimental relaxation times have a ratio of 1:5.²

Howe explains these discrepancies by showing that the "effective" molecular volume is essentially the volume swept out by the molecule during relaxation. An analysis of the geometry of the molecules studied, the components of their dipole moments, and the possible modes of relaxation, leads to logical explanations for the experimentally observed relationships among the relaxation times.

For example, p-nitrobiphenyl sweeps out a volume 4.9 times larger than that swept out by nitrobenzene, and its relaxation time is 5 times larger. The ratio of molecular volumes is only 1.7:1.²

The conclusion can then be drawn that it is the volume swept out during relaxation, rather than the molecular volume, which is important in determining the relaxation time.²

NOTES FOR CHAPTER V

1. Nora E. Hill, et. al., "Dielectric Properties and Molecular Behavior," Van Nostrand Reinhold Co., New York, N.Y., 1969.
2. Allen K. Howe, Jr., Honors Thesis in Chemistry, The College of William and Mary in Virginia, 1974.

CHAPTER VI

SUPERCOOLED LIQUIDS AND THE GLASSY STATE

A liquid can be simply defined as "a fluid which if placed in a closed vessel at once conforms to the shape of the vessel without necessarily filling the whole of its volume."¹ A liquid is thus distinguished from a solid by its indefinite shape, and from a gas by the fact that it may not completely fill its container. While this definition is usually adequate, some materials (for example some polymers) do not fit. These materials appear as solids at room temperature, but on heating, begin to flow, usually with high viscosity, and without exhibiting a sharp melting point. These last two properties are characteristic of a supercooled liquid; when the viscosity becomes infinite (or when the flow is imperceptible) the material is termed a glass. A glass, then, has the external appearance of a solid and the internal characteristics of a liquid.¹

Most liquids can be made to solidify in the glassy state if they are cooled through the crystallization temperature range faster than the time needed for crystal nuclei to form.² This is fairly easy to do for liquids of a low order of symmetry, or if the rate of rotational isomerization from the normal liquid configuration to that required for crystallization is slow at temperatures below the

melting point.²

The temperature at which the transition to a glass occurs is characterized by a second order thermodynamic transition; and in the vicinity of the glass transition temperature, T_g , the viscosity may change by several orders of magnitude within 10°K .^{2,3,4} This transition is not thermodynamic in nature since the temperature at which a thermodynamic transition due to a structure change occurs is independent of the thermal history of the material.^{3,4} The faster the rate of cooling, the higher the glass transition temperature will be.^{2,3,4} In a supercooled liquid, the volume decrease which occurs in normal liquids on cooling is delayed, so that the density decreases as the rate of cooling increases.²

Above and adjacent to T_g in the supercooled liquid region there seem to be two regions of dielectric dispersion, indicative of two independent relaxation processes. One theory proposes that the low frequency or α process is due to cooperative relaxation of a group of molecules, and the β , or higher frequency process is caused by hindered reorientation of individual molecules which are surrounded by other molecules which are unable to reorient cooperatively.^{3,5}

Studies by Williams and Hains⁶ of dilute solutions of small molecules in supercooled ortho-terphenyl, support the theory that cooperative motion is the mechanism by which the α process occurs. Comparison of data from some

polymers and copolymers suggests that a similar process may be present in these materials.⁷

The α process has rather strict requirements due to the necessity of simultaneous interaction among a number of molecules. Johari⁵ has found that intermolecular potential barriers are significant in producing β relaxation. He and Goldstein have proposed that the potential barriers necessary for the β process arise when a molecule is "encaged" by other molecules in such a way that the requirements for cooperative motion are not met.^{5,8}

Other studies by Johari indicate that the strength of the β process is related to the thermal history of the liquid. As mentioned previously, the faster the rate of cooling, the lower the density; thus, the more sites available in which the potential barriers are low enough to allow the "encaged" molecules to reorient.^{3,5}

Since each "encaged" molecule, depending on its orientation, can be presented with a number of different potential barriers, and since the potential barriers may vary from one site to another, the β process has a distribution of relaxation times.^{3,5}

Johari and Goldstein have found from studies of small rigid molecules that the β process is not due to internal hindered rotation of the molecules themselves, but due entirely to intermolecular forces.^{3,8}

Experimental results seem to indicate that the relative occurrence of the α and β processes is temperature

dependent. In normal liquids, both processes occur. As the supercooled liquid approaches T_g , the α process becomes less frequent, finally ceasing at T_g , while the β process continues to be present.³

NOTES FOR CHAPTER VI

1. Gilroy Harrison, "The Dynamic Properties of Supercooled Liquids," Academic Press, New York, N.Y., 1976.
2. Arnold A. Bondi, "Physical Properties of Molecular Crystals, Liquids, and Glasses," John Wiley & Sons, Inc., New York, N.Y., 1968.
3. Karen Rae Trimmer, Honors Thesis in Chemistry, The College of William and Mary in Virginia, 1975.
4. G.P. Johari, J. Chem. Ed., 51, 23(1974).
5. G.P. Johari, J. Chem. Phys., 4, 1766(1973).
6. G. Williams and P.J. Hains, Faraday Society of the Chemical Symposium, 6, 14(1972).
7. G. Williams, M. Cook, and P.J. Hains, Faraday Transactions II, 68, 1045(1972).
8. M. Goldstein, Am. Chem. Soc., 30, 117(1970).

CHAPTER VII

RF AND Q-METER THEORY

Bridge measurement methods have a practical upper frequency limit imposed by the increase in the admittance associated with stray capacitance. The use of substitution methods using simple resonant circuits can essentially eliminate this source of error.¹

A Q-meter is a commercially available instrument which uses a resonant circuit, and can be used to measure inductance, capacitance, resistance, and Q of a circuit or component. Our experiment makes use of a Hewlett-Packard type 4342A Q-meter to experimentally determine the complex dielectric constant of an unknown.

Before proceeding with the derivation of the pertinent equations for ϵ' and ϵ'' , a brief look at some basic AC circuit relations will be helpful.

In an AC circuit which contains inductance, capacitance, and resistance, the inductive reactance, $X_L = \omega L$, and the capacitive reactance, $X_C = 1/\omega C$, act as effective resistances in addition to the pure resistance present. The voltages due to the two reactances are 180° out of phase and each is 90° out of phase with the resistive voltage. The overall effective circuit resistance is called the impedance, and is the vector sum of resistance and

reactance.

$$/ 7.1 / \quad Z^2 = R^2 + X^2$$

where $X = X_L - X_C$ by convention. Since X_L is zero when $\omega = 0$, and increases with increasing frequency; and X_C is a maximum when $\omega = 0$ and decreases with increasing frequency, there is obviously some frequency at which the two are equal in magnitude. Since they are 180° out of phase, they cancel and only the pure resistance is effectively in the circuit. This condition when $X_L = X_C$ is known as resonance. We can write Ohm's law as²

$$/ 7.2 / \quad i = \mathcal{E} / \left[R^2 + \left(\omega L - \frac{1}{\omega C} \right)^2 \right]^{1/2}$$

and we see that current, and thus the voltage measured across the capacitors, will be a maximum when Z is a minimum; i.e., at resonance.

A generalized Q-meter circuit with an empty dielectric sample holder in place is shown in Figure 7-1a.

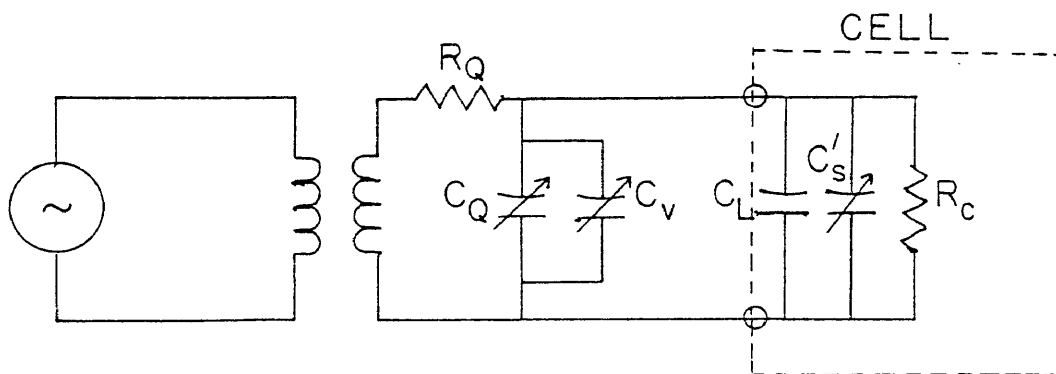


Figure 7-1 (a)

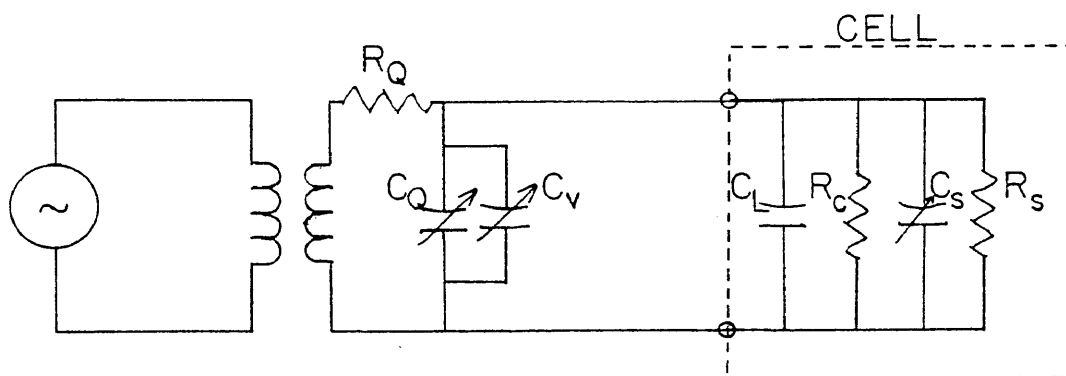


Figure 7-1 (b)

C_Q = Q-meter main tuning capacitor

C_V = Q-meter vernier tuning capacitor

C'_S = Capacitance of empty cell

C_S - Capacitance of sample

C_L = Capacitance of leads

R_Q = Series resistance of Q-meter circuit

R_C = Series resistance of the empty cell

R_S = Parallel resistance (loss) of the sample

Figure 7-1b shows the same circuit with the sample in place in the cell. With the sample out, the resistances are in series, and the total circuit resistance, R_0 , is equal to $R_Q + R_C$. Placing the sample in the cell has the effect of adding a resistance, R_S , in parallel with R_C so that the total circuit resistance is now $R_i = R_Q + (R_S R_C)/(R_S + R_C)$. The difference of the reciprocals can be written

$$\text{ / 7.3 / } \quad \frac{1}{R_i} - \frac{1}{R_0} = \frac{1}{R_Q + \frac{R_S R_C}{R_S + R_C}} - \frac{1}{R_Q + R_C}$$

and if we assume that $R_Q \ll R_s, R_c$ ($R_Q \approx 1.0$ milliohms for the 4342-A Q-meter), equation 7.3 reduces to

$$/ 7.4 / \quad \frac{1}{R_i} - \frac{1}{R_o} = \frac{R_s + R_c}{R_s R_c} - \frac{1}{R_c} = \frac{1}{R_s}$$

The measurement theory is quite simple and is based on the equation for the capacitance of a parallel plate capacitor:

$$/ 7.5 / \quad C = \frac{\epsilon' \epsilon_o A}{\uparrow t}$$

where ϵ' is the dielectric constant of the medium between the plates, ϵ_o is the permittivity of free space, A is the area between the plates in appropriate units, and t is the separation between the plates.

The measurement method is likewise simple and is basically a substitution procedure using reference liquids of accurately known dielectric constant. The technique is based on work done by several authors^{3,4}, but is primarily that of Kakimoto.⁵

Although the determination of ϵ' is basically an empirical procedure, the equations for ϵ'' require some derivation.

The actual procedure, which will be described in detail later, requires that C_s be set equal to C'_s , so that the total circuit capacitances, C_i and C_o respectively, are also equal. By definition, the dissipation factor of the sample is

$$/ 7.6 / \quad D_s \equiv \frac{1}{Q_s} = \frac{1}{\omega R_s C_s}$$

Substituting for $1/R_s$ gives

$$/ 7.7 / \quad D_s = \frac{1}{C_s} \left(\frac{1}{\omega R_i} - \frac{1}{\omega R_o} \right)$$

Multiplying the right hand side by C_o/C_i and rearranging the terms gives

$$/ 7.8 / \quad D_s = \frac{C_o}{C_s} \left[\frac{\omega R_o C_o - \omega R_i C_i}{(\omega R_o C_o)(\omega R_i C_i)} \right]$$

If the appropriate Q_n 's are substituted from equation 7.6, this becomes

$$/ 7.9 / \quad D_s = \frac{C_o}{C_s} \left(\frac{Q_o - Q_i}{Q_o Q_i} \right)$$

We would like to convert this to an equation in terms of parameters which are measurable by our particular experimental technique. To do this, we make use of the fact that our measurement procedure sets $C_o = C_i$. Remembering that we use a reference liquid for the sample out measurement, we can write from equation 7.5, and by referring to Figure 7-1b

$$/ 7.10 / \quad C_o = C_Q + C_v + C_L + \frac{\epsilon'_{ref} \epsilon_o A}{t_2}$$

where ϵ'_{ref} is the dielectric constant of the reference liquid at the experimental temperature and t_2 is the plate

separation (in mm.) at resonance. The capacitance of the sample is

$$/ 7.11 / \quad C_s = \frac{\epsilon'_{\text{ref}} \epsilon_o A}{t_2} = \frac{\epsilon' \epsilon_o A}{t_1}$$

where ϵ' is the dielectric constant of the unknown, and t_1 is the plate separation with the unknown in place, (nominally 3.0mm). Using the relations in 7.10 and 7.11, and letting $C'_Q = C_Q + C_V + C_L$, equation 7.8 becomes

$$/ 7.12 / \quad D_s = \frac{t_1}{\epsilon'} \left(\frac{C'_Q t_2 + \epsilon'_{\text{ref}} \epsilon_o A}{\epsilon_o A t_2} \right) \left(\frac{Q_o - Q_i}{Q_o Q_i} \right)$$

by definition, $D = \epsilon''/\epsilon'$, so that 7.12 can be rewritten as

$$/ 7.13 / \quad \epsilon'' = t_1 \left(\frac{C'_Q}{\epsilon_o A} + \frac{\epsilon'_{\text{ref}}}{t_2} \right) \left(\frac{Q_o - Q_i}{Q_o Q_i} \right)$$

This is the working equation which we use for all our Q-meter measurements.

We can derive the equation which is used by Tay and Walker⁴ by rewriting equation 7.9 as

$$/ 7.14 / \quad D_s = \frac{C_o}{C_s} \frac{1}{Q_o} \left(\frac{Q_o - Q_i}{Q_i} \right)$$

We now need to evaluate $1/Q_o$. The voltage measured across the circuit capacitance is the circuit current times the capacitive reactance. Using equation 7.2, we can write

$$/ 7.15 / \quad V = \frac{\mathcal{E}}{\left[R^2 + \left(\omega L - \frac{1}{\omega C} \right)^2 \right]^{1/2}} \cdot \frac{1}{\omega C},$$

where C is the total circuit capacitance. Squaring both sides, we obtain

$$/ 7.16 / \quad V^2 = \frac{\mathcal{E}^2}{\omega^2 R^2 C^2 + (\omega^2 LC - 1)^2}$$

which will have a maximum at

$$/ 7.17 / \quad C_0 = \frac{L}{R^2 + \omega^2 L^2}$$

C_0 is just the total circuit capacitance at resonance.

Substituting this result into equation 7.16 gives

$$/ 7.18 / \quad V_r^2 = \frac{\mathcal{E}^2 (R^2 + \omega^2 L^2)}{R^2}$$

where V_r is the measured voltage at resonance. If we choose V so that the ratio $V_r:V$ is $1:\sqrt{2}$, then we can divide equation 7.18 by equation 7.16 to obtain

$$/ 7.19 / \quad V_r^2 / V^2 = 2 = \frac{\left[R^2 \omega^2 C^2 + (\omega^2 LC - 1)^2 \right] \left[R^2 + \omega^2 L^2 \right]}{R^2}.$$

This can be rewritten as a quadratic equation in C:

$$/ 7.20 / \quad \omega^2 (R^2 + \omega^2 L^2) C^2 - 2\omega^2 LC - \frac{2R^2}{R^2 + \omega^2 L^2} + 1$$

Solving this equation for C gives two solutions:

$$/ 7.21 / \quad C = \frac{L}{R^2 + \omega^2 L^2} \pm \frac{R}{\omega(R^2 + \omega^2 L^2)} .$$

Multiplying the second term by L/L, and substituting from equation 7.17, this becomes

$$/ 7.22 / \quad C = C_o \pm \frac{RC_o}{\omega L}$$

By definition, $\omega L/R = Q$, so we can write the two equations for C as

$$/ 7.23 / \quad C_H = C_o + C_o/Q_o$$

$$/ 7.24 / \quad C_L = C_o - C_o/Q_o$$

where C_H and C_L are merely the capacitances which are higher and lower than the resonance capacitance, C_o . These equations indicate that the voltage resonance curve is symmetrical about C_o , unlike the current resonance curve which broadens slightly for $C > C_o$. If ΔC_o is defined as $C_H - C_L$, the expression for ΔC_o is obtained:

$$/ 7.25 / \quad \Delta C_o = C_o + \frac{C_o}{Q_o} - C_o + \frac{C_o}{Q_o} = \frac{2C_o}{Q_o}$$

Rearranging this gives the desired equation for $1/Q_o$.

$$/ 7.26 / \quad 1/Q_o = \frac{\Delta C_o}{2 C_o}$$

Substituting this result into equation 7.14 gives the desired equation for the dissipation factor, and since $D = \epsilon''/\epsilon'$ as mentioned, we obtain

$$/ 7.27 / \quad \epsilon'' = \frac{\Delta C_o}{2 C_s} \left(\frac{Q_o}{Q_i} \right)$$

the working equation of Tay and Walker.⁴

Broadhurst and Bur³ derive a similar equation:

$$/ 7.28 / \quad \epsilon'' = \left(\frac{C_T}{\epsilon_o A/t_s} \right) \Delta \left(\frac{1}{Q} \right) \left(\frac{C_{HO}}{C_T - C_s'} \right)^2 \left[1 - \frac{t_1 - t_s}{t_1} - \frac{C_{C2} - C_{C1}}{C_g} + \frac{C'}{C_g} \right]^{-2}$$

The term in brackets can be left out since this is an air gap correction, and applies only to solid samples. Likewise, the third term can be ignored since this accounts for lead inductance which is negligible below 30MHz.³ This then leaves us with

$$/ 7.29 / \quad \epsilon'' = \frac{t_s C_T}{\epsilon_o A} \Delta \left(\frac{1}{Q} \right) \quad ; \quad \Delta \left(\frac{1}{Q} \right) = \left(\frac{1}{Q_i} - \frac{1}{Q_o} \right)$$

Their t_s corresponds to our t_1 , and C_T is the total circuit capacitance which is the same whether the sample is in or out; i.e., $C_T = C_o = C_i$. Substituting from equation 7.10 and remembering that $C_Q' = C_Q + C_V + C_L$, we obtain

$$/ 7.30 / \quad \epsilon'' = t_1 \left(\frac{C_Q' + \epsilon_{ref}' \epsilon_o A/t_2}{\epsilon_o A} \right) \left(\frac{1}{Q_i} - \frac{1}{Q_o} \right)$$

which on rearrangement proves to be the same as our working equation, 7.13:

$$/ 7.31 / \quad \epsilon'' = t_1 \left(\frac{C'_Q}{\epsilon_o A} + \frac{\epsilon'_{ref}}{t_2} \right) \left(\frac{Q_o - Q_i}{Q_o Q_i} \right)$$

We can determine the effect of Q on the uncertainty in ϵ'' as given by equation 7.13. It is

$$/ 7.32 / \quad \frac{\Delta \epsilon''}{\epsilon''} = \left| \frac{\Delta t_1}{t_1} \right| + \left| \frac{\Delta t_2}{t_2} \right| + \left| \frac{\Delta A}{A} \right| + \left| \frac{\Delta (C'_Q t_2 + \epsilon'_{ref} \epsilon_o A)}{(C'_Q t_2 + \epsilon'_{ref} \epsilon_o A)} \right| +$$

$$\left| \frac{\Delta (Q_o - Q_i)}{Q_o - Q_i} \right| + \left| \frac{\Delta Q_o}{Q_o} \right| + \left| \frac{\Delta Q_i}{Q_i} \right|$$

If we arbitrarily assume the following values and uncertainties:

$$\begin{aligned} \epsilon'' &= 0.01 \\ A &= 1140 \text{mm}^2 \quad ; \quad \Delta A = \pm 1.5 \text{mm}^2 \\ C'_Q &= 200 \text{pf} \quad ; \quad \Delta C'_Q = \pm 0.1 \text{pf} \\ \epsilon'_{ref} &= 2.4718 \quad ; \quad \Delta \epsilon'_{ref} = \pm 0.01 \quad (T = 25^\circ \text{C}) \\ t_1 &= 2.0 \text{mm} \quad ; \quad \Delta t_1 = \pm 0.001 \text{mm} \\ t_2 &= 1.8345 \text{mm} \quad ; \quad \Delta t_2 = \pm 0.00141 \text{mm} \quad ; \end{aligned}$$

the first four terms become approximately 0.00293. The two ranges on the Q-meter which we use are 0-300 and 0-1000; and for both ranges, the Q-analog output is 0 to 1.000 volts. The digital voltmeter can be read to $\pm 0.0001 \text{V}$, so the uncertainties in Q for the two ranges are ± 0.03 and ± 0.1 at best. In practice ΔQ was probably closer to ± 0.06 or 0.2 (or even possibly as high as ± 1.0). If, in addition to

the above assumptions, we arbitrarily choose a value for Q_0 , we can back calculate Q_1 from equation 7.13. A computer program was written to calculate and plot the per cent uncertainty in ϵ'' for values of Q_0 between 130 and 1000. This program, along with the resultant graph and a table of values, is given in Appendix VI. For the 0-300 range, assuming a ΔQ of ± 0.06 , the uncertainty in ϵ'' (for $\epsilon'' = 0.01$) decreases from approximately 3% at $Q_0 = 130$, to 1.1% at $Q_0 = 300$. On the 0-1000 range, for $\Delta Q = \pm 0.2$, the uncertainty decreases from 2.2% at $Q_0 = 300$, to .86% at $Q_0 = 1000$.

NOTES FOR CHAPTER VII

1. Nora E. Hill, et. al., "Dielectric Properties and Molecular Behavior," Van Nostrand Reinhold Co., New York, N.Y., 1969.
2. W.T. Scott, "The Physics of Electricity and Magnetism," John Wiley & Sons, Inc., New York, N.Y., 1966.
3. Martin G. Broadhurst and Anthony J. Bur, J. Res. NBS 69C (Eng. and Instr.), No. 3, 165(1965).
4. S.P. Tay and S. Walker, J. Chem. Phys., 63, 1634(1975).
5. Akira Kakimoto, Rev. Sci. Instr., 43, 763(1972).

CHAPTER VIII

EXPERIMENTAL

The experimental equipment for measurement of the complex dielectric constant in the RF region consists of a Hewlett-Packard type 4342A Q-meter, a H-P type 5381A frequency counter, a Data Technology Model 40 digital voltmeter to measure the analog output of the Q-meter, the dielectric cell, and associated temperature control and measurement equipment.

The temperature control and measurement apparatus had been previously developed by Trimmer¹ and Wilkes². The cooling apparatus consists of a 25 liter dewar containing liquid nitrogen, into which a heating element consisting of a two foot length of resistance wire was placed. Two Variacs in series were used for coarse and fine control of the heating element which boiled off nitrogen, thus generating a variable flow of cold nitrogen gas. The gas, after cooling the cell, exhausted into the plastic bag containing the cell, thus giving a moisture free atmosphere. (Condensation on the cell can cause serious errors.) Temperature measurement was accomplished with a Yellow Springs Instruments type 44201 thermistor, and a voltage-resistance network, built by the William and Mary Physics Department electronics shop, which provided a linear output voltage

over the temperature range -50° to $+50^{\circ}\text{C}$.

The cooling apparatus, the Q-meter, cell, and associated equipment, were connected as shown in Figure 8-1 and in Plates 7 and 8.

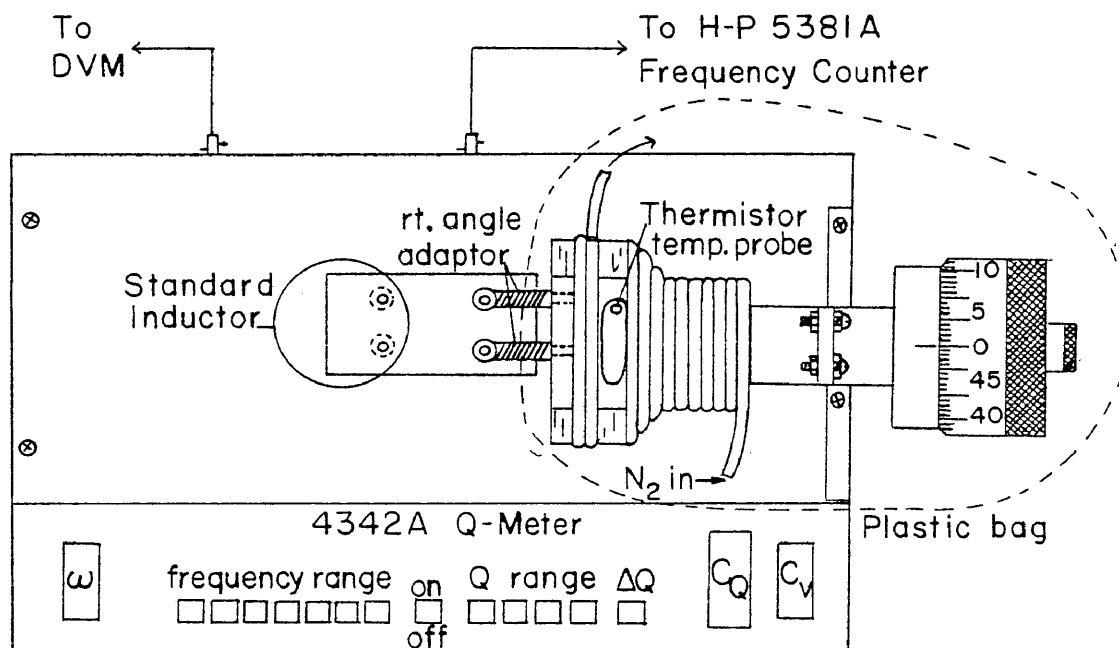


Figure 8-1

The samples were dilute solutions of the compound of interest, in the slightly polar solvent, o-terphenyl. The o-terphenyl, obtained from Eastman, was purified by recrystallization from methanol. After recrystallization, excess methanol was removed by treatment in a vacuum oven for six hours. The proper amounts of the solute and solvent were weighed and mixed together by heating to 60°C , giving a homogeneous solution which was then ready to be poured into the cell.

Prior to the actual measurements, a number of calibrations were performed.

In order to calculate the area of the cell plates, the capacitance was measured as a function of plate separation on a General Radio type 1615-A capacitance bridge. A plot of C versus $1/t$ (see equation 7.4) should have a slope, $\epsilon' \epsilon_0 A$. As can be seen from Figure 8-2, the function is not linear. Because of this, an area of 1140.1 mm^2 was used, calculated from the measured plate diameter of 1.5 inches. Inspection of the plot does seem to indicate that the slope approaches a limiting value corresponding to this calculated area.

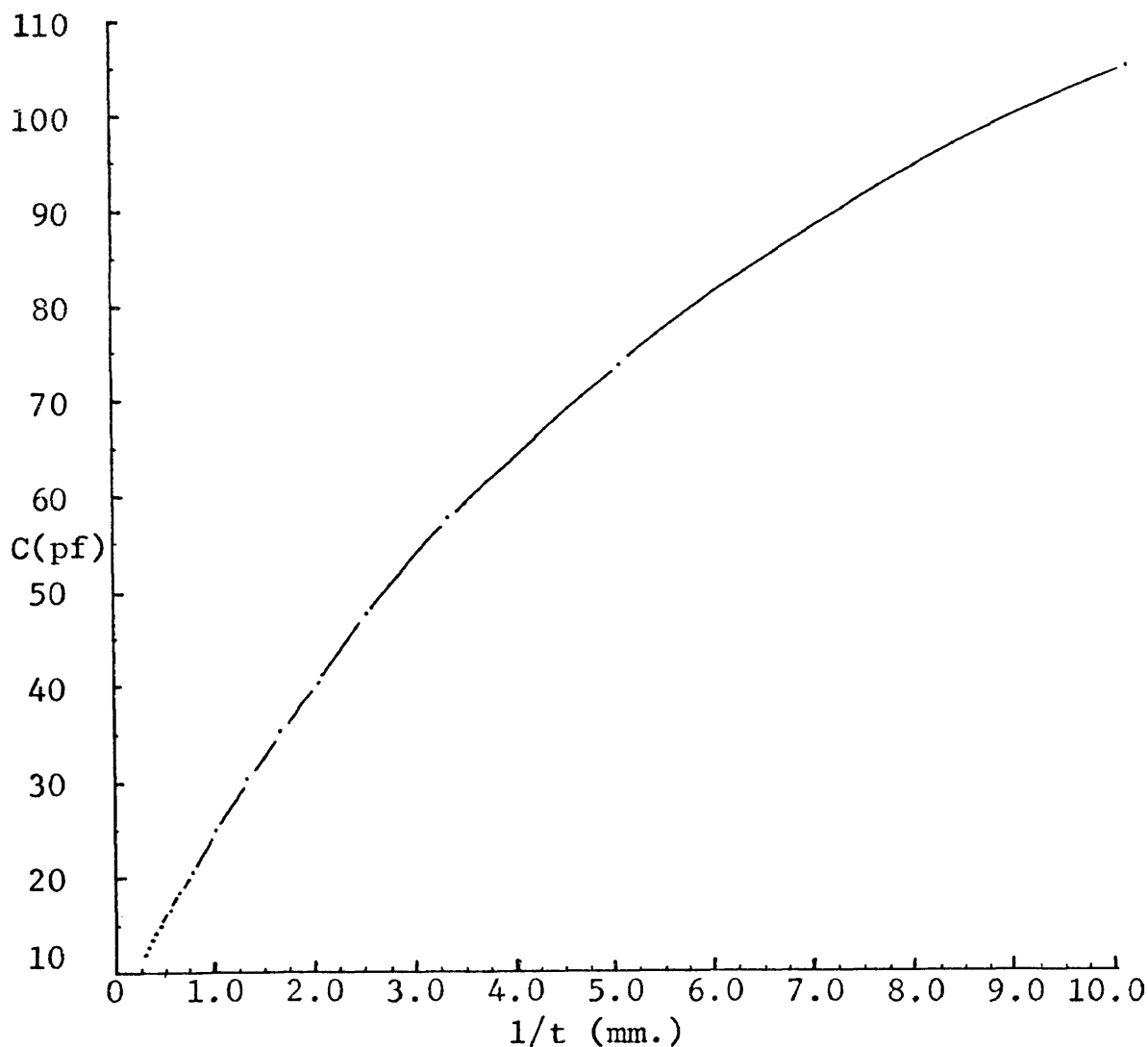


Figure 8-2

The true zero point for the micrometer is easily found by connecting an ohmmeter across the cell terminals and slowly decreasing the plate separation until a short is indicated. This was done prior to each actual measurement and provides a check on the dimensional stability of the cell.

The other correction which must be considered is the voltage offset and drift of the Q-meter analog output. This voltage should be $0.00 \pm 0.01\text{V}$ after three hours.³ This voltage was measured as a function of time with a chart recorder and was seen to decay exponentially with a fairly short time constant. Drift was negligible after a warm up time of three hours. In practice, the value of this voltage offset was checked before and after each series of measurements, and the measured values of Q adjusted accordingly.

The original dielectric cell was based on the design of Broadhurst and Bur⁴; but because of problems with leakage and non-linear response, no satisfactory data could be obtained. The cell did, however, allow the validity of the measurement technique to be verified.

A new cell was designed and built by Mr. Stan Hummel of the William and Mary Physics Department shop. The body was machined from solid brass with tubing for thermostatic control built directly into the body of the cell. The electrodes were also brass, and the stationary high potential electrode was insulated from the grounded case by

mounting it in a 3/4 inch thick piece of Teflon. The piston shaped movable electrode was made in two parts which were joined by a threaded stud on one and a tapped hole in the other. A tapered Teflon o-ring was placed in a circumferential groove at the junction of the two halves of the electrode. By tightening the two halves, the pressure on the o-ring could be adjusted to ensure a good seal. A L.S. Starrett type 1-461MP (25mm) micrometer head was mounted on the cell so that the electrode separation could be measured to the nearest 0.001mm. The cell is shown in Figure 8-3 and also in Plates 9 and 10.

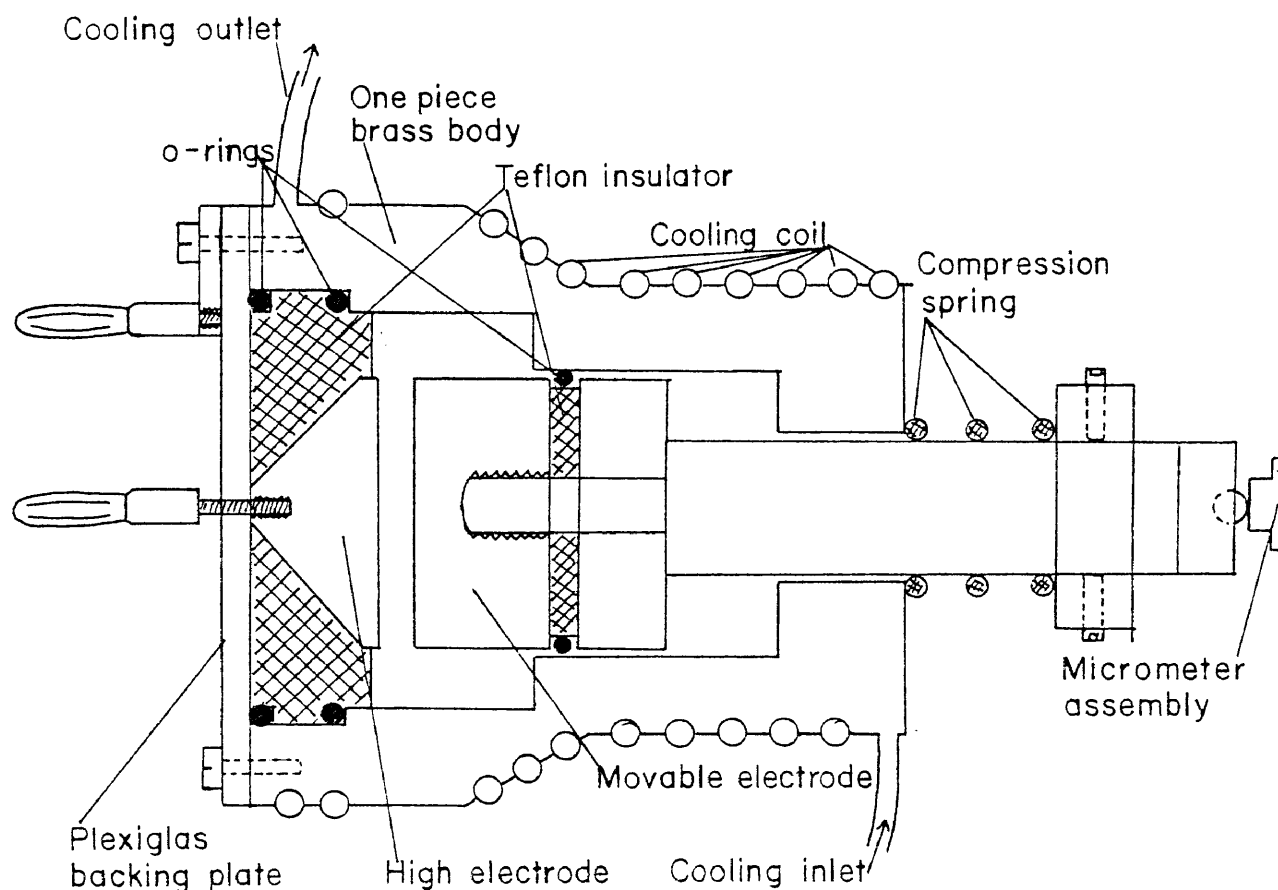


Figure 8-3

Measurement of ϵ'

Due to the fact that the high electrode cannot be moved with the supercooled o-terphenyl solution in the cell, a slight modification of Kakimoto's procedure⁵ was necessary.

The equipment is allowed to warm up for at least three hours. An appropriate reference inductor is plugged into the Q-meter and the capacitance is fixed at 200.0pf. This is an arbitrary value and is chosen so that, in combination with the reference inductor, resonance will occur in a convenient segment of one of the seven fixed frequency ranges. The reference inductors can be purchased separately from Hewlett-Packard. These are similar to inductors which were obtained from the National Bureau of Standards and which had Q values in the range from 150 to 250. In order to achieve better precision, the Q of the circuit should be as high as possible; (see Appendix VI) and, to this end, "Ultra High Q" inductors made by Rutherford Research were obtained. These inductors had Q values near 800 and would resonate with the 200pf capacitance of the Q-meter at frequencies ranging from approximately 150KHz to 1.5MHz.

The cell is connected, through the plastic bag, to the Q-meter terminals. Since these terminals are vertical banana jacks and the cell terminals are horizontal banana plugs, a right angle adaptor was fabricated from two banana plugs, two banana jacks, and short pieces of $\frac{1}{4}$ inch copper tubing. Another adaptor was made by embedding a small

piece of printed circuit board with banana plugs and jacks attached, in a block of epoxy. This proved to have too much loss and was not used.

Since the capacitance and Q of the circuit are extremely sensitive to the physical orientation of the cell and the adaptor, we constructed a framework in which to rigidly clamp the cell. This framework was fastened to the top of the Q -meter by removing two cover screws and one of the ground connection posts and replacing these with brass screws of sufficient length to go through the framework. The cell could thus be located reproducibly for each run.

With the cell in place, the micrometer was set to 3.000mm (taking into account the offset previously measured). This is an arbitrarily chosen distance and need only be wide enough to allow the hot *o*-terphenyl solution to be poured into the cell without trapping any bubbles between the plates. It must also be small enough so that when the calibration material with the highest dielectric constant is used, the plates can be opened wide enough to reestablish resonance. After placing the thermistor probe in the cell, the cooling apparatus is connected and turned on.

When the temperature reaches approximately -30°C , the hot *o*-terphenyl is poured into the cell and temperature equilibrium is established. With the temperature stable at the desired value, the frequency of the Q -meter oscillator is adjusted for resonance. The frequency and corresponding value of Q , (Q_i), are measured for each reference inductor

at each of the measurement temperatures.

For each temperature-solution combination, a calibration curve must be constructed. This is done by measuring a series of reference liquids whose dielectric constants range above and below 2.7, the nominal value for o-terphenyl.

Using the temperature-inductor-frequency combinations determined for each o-terphenyl solution, each reference liquid is placed in the cell and the circuit brought to resonance by adjusting the micrometer. The maximum value of Q , (Q_0), is noted, as well as the Q -analog output zero offset. Since this Q value is measured at the peak of the voltage versus spacing curve, accurate determination of the spacing may be difficult if the Q is low; and a better value may be obtained by averaging the spacings measured at the "half power points".

The values thus obtained (t_2 in the relevant equations) are plotted versus the corresponding dielectric constants (calculated from the measurement temperature, the known dielectric constant of the reference liquid, and its temperature coefficient). The resulting curves are fitted to a second order equation:

$$/ 8.1 / \quad at_2^2 + bt_2 + c = 0 \quad ,$$

and the o-terphenyl spacing can then be plugged into this equation to give ϵ' . Equation 7.13 is used to calculate ϵ'' .

NOTES FOR CHAPTER VIII

1. Karen Rae Trimmer, Honors Thesis in Chemistry, The College of William and Mary in Virginia, 1975.
2. Charles A. Wilkes, Honors Thesis in Chemistry, The College of William and Mary in Virginia, 1976.
3. Hewlett Packard, Operating and Service Manual - Model 4342A Q Meter, Yokogawa-Hewlett-Packard, Ltd., Tokyo, 1973.
4. Martin G. Broadhurst and Anthony J. Bus, J. Res. NBS 69C (Eng. and Instr.), No. 3, 165 (1965).
5. Akira Kakimoto, Rev. Sci. Instr., 43, 763 (1972).

CHAPTER IX

RESULTS OF Q-METER MEASUREMENTS

Measurements of the loss and dielectric constant for a number of nitroaromatic compounds in supercooled o-terphenyl were made in an attempt to observe the β -relaxation process discussed in Chapter VI.

Of the two processes proposed to be present, the α , or cooperative process is predominant. It has an activation energy on the order of 30 to 70 kcal mol⁻¹, and appears in the low frequency region (ca. 1KHz).¹⁻⁴ The β -process, due to hindered rotation of the small, polar solute molecules, has an activation energy on the order of 2 to 10 kcal mol⁻¹,³ and occurs at a much higher frequency. In addition, the α -process should cease to occur at or below T_g , since, at this temperature, the structure of the solvent becomes frozen in and cooperative motion is no longer possible. The β -process, however, should continue to occur.

Data gathered by Trimmer¹, Wilkes², and others^{3,4} indicates that the α -process accounts for 50 to 90% (or perhaps more) of the total loss in the supercooled region above T_g (ca. -10°C; $T_g \approx -30^\circ\text{C}$).

As mentioned, the β -process is thought to have an activation energy near 2 to 10 kcal mol⁻¹. This is

reasonable if one assumes that this relaxation process is similar to the process which occurs in the liquid phase. For example, Howe⁵ found an activation energy for nitrobenzene in benzene from 25 to 60°C of 1.8 kcal mol⁻¹. It would seem reasonable that the potential energy barriers which the encaged solute molecules would encounter would be greater in the supercooled state due to the decreased mobility and more ordered structure of the solvent molecules.

Based on the above range of activation energies, we would like to be able to predict the frequency range in which the β -process should occur. If we assume that the relaxation process follows first order kinetics, then the rate constant for the process will be proportional to the frequency of maximum loss. Applying the Arrhenius rate theory allows us to write

$$/ 9.1 / \quad f_{\max} \propto k = A e^{-\Delta E^\ddagger/RT}$$

where ΔE^\ddagger is the activation energy in kcal mol⁻¹, R is the gas constant equal to 1.987 x 10⁻³ kcal mol⁻¹ °K⁻¹, and T is the temperature in degrees Kelvin. We also assume that the activation energy is temperature independent, an assumption which seems to hold fairly well for normal liquids, but whose validity for the supercooled and glassy states is not certain.

Using equation 9.1, and a nominal relaxation time for nitrobenzene in benzene at 25°C of 10 picoseconds⁵, we can

construct the following table of frequency and temperature for various activation energies.

ΔE^\ddagger / T_{OK}	25 298	-25 248	-60 213	-85 188	-115 158
2	10^5	50,612	25,979	13,858	5,014
5		18,234	3,440	715	56
7		9,223	894	99	2.8
10		3,321	118	5	32KHz
15		605	4.1	37KHz	18Hz

(All frequencies in MHz unless otherwise noted)

Table 9-1

The highest frequency attainable with our experimental apparatus was approximately 13 MHz. Inspection of the above table indicates that for the β peak to be in the experimentally accessible range, the activation energy needs to be greater than approximately $7.5 \text{ kcal mol}^{-1}$. This is based on a lower temperature limit of -115°C , with the frequency of maximum loss occurring at -100°C .

Initially, the lowest temperature used was -85°C , and while the tail of the α peak was clearly discernible, the β peak was not obvious. The data seemed to show that the loss was beginning to increase, but that it had not yet peaked. We felt that perhaps the β peak was indeed being shifted into the observable range, but that at the same time, its magnitude was decreasing, thus making detection difficult.

One possible solution to this problem would be to

obtain reference inductors which would resonate at higher frequencies. However, since the maximum frequency at which the Q-meter operates is 70 MHz, this solution may not yield much improvement because Table 9-1 indicates that the activation energy still must be greater than approximately 6 kcal mol⁻¹.

If the magnitude of the β peak does decrease with decreasing temperature, measurement of compounds which have a large absolute magnitude of loss (i.e., a large dipole moment) which is attributable to the β -process, might allow detection of the β peak. To this end, measurements were made on 2,2'-dinitrobiphenyl and 2-bromo-2-methyl propane. While the percentage of the total loss due to the β -process for the former compound is approximately the same as for nitrobenzene (ca. 20%)^{1,2}, the magnitude of the total loss is greater. For the latter compound, the magnitude of the total loss is still relatively large, and the percentage due to the β -process is much greater (ca. 50+%)².

The step which proved to be decisive in allowing the definite observation of the β peak was the decrease of the experimental lower temperature limit to -115°C. (See the graphs in Appendix IX.)

In thus lowering the experimental temperature, it was found that the thermistor being used was extremely non-linear below -60°C. A calibration curve was constructed, allowing the thermistor to be used to measure temperatures with reasonable accuracy to -90°C. For the measurements at -115°C, a chromel-alumel thermocouple was used, the reference junction

at 0°C. While the accuracy of the thermocouple was not as good as that of the thermistor, the effect on the results was not appreciable.

Although the measurement technique does not allow the precise determination of exact values for the dielectric constant and loss, the relative values are readily measured. This is sufficient to allow observation of the β peak in the low temperature-high frequency region. The trends seen are as expected from theoretical predictions. At the lower frequencies (ca. 150 KHz), the peak occurs below -115°C; and as the frequency is increased to 13 MHz, the peak shifts up in temperature to near -85°C. The presence of the high frequency-low temperature tail of the α peak is also clearly evident. Although the peak cannot be located precisely from the available data, if we assume that it occurs at -85°C and 13 MHz, this is found to correspond to an activation energy of 9 kcal mol⁻¹. This is only a rough estimate, but it is obviously in the range of 2 to 10 kcal mol⁻¹ previously quoted for the β peak.

NOTES FOR CHAPTER IX

1. Karen Rae Trimmer, Honors Thesis in Chemistry, The College of William and Mary in Virginia, 1975.
2. Charles A. Wilkes, Honors Thesis in Chemistry, The College of William and Mary in Virginia, 1976.
3. G.P. Johari,
4. G. Williams and P.J. Hains, Faraday Society of the Chemical Symposium, 6, 14(1972).
5. Allen K. Howe, Jr., Honors Thesis in Chemistry, The College of William and Mary in Virginia, 1974.

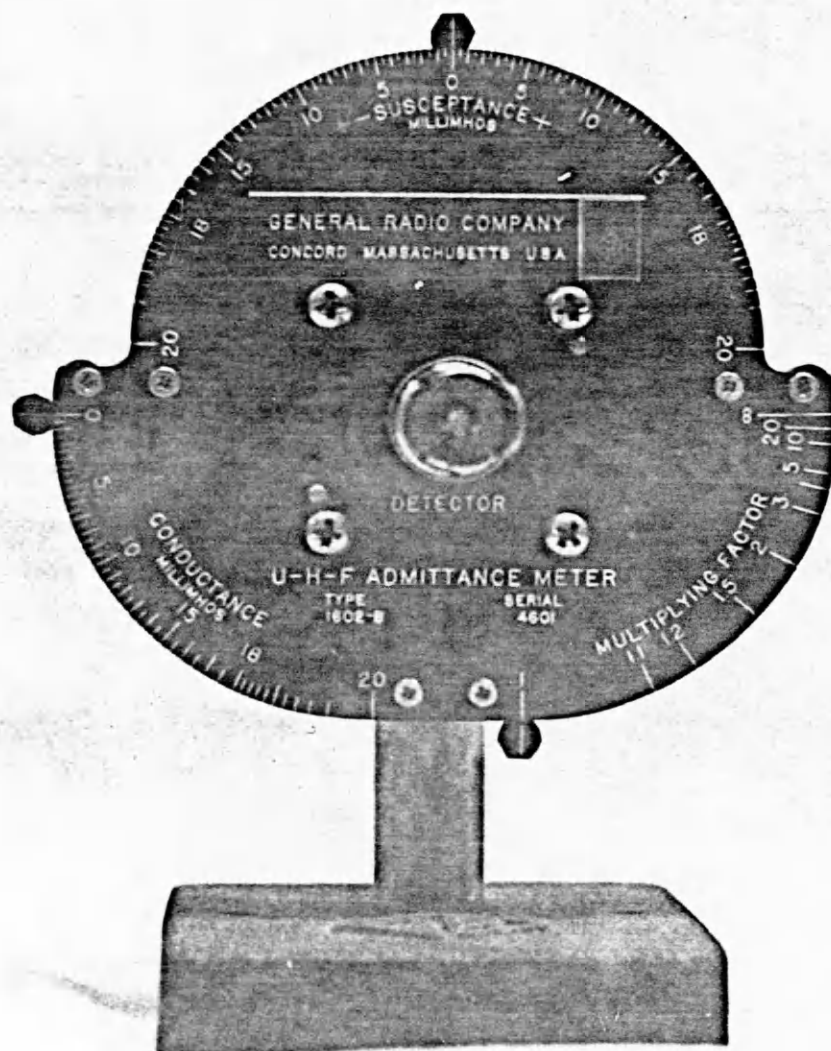


PLATE I
Admittance Meter - Front

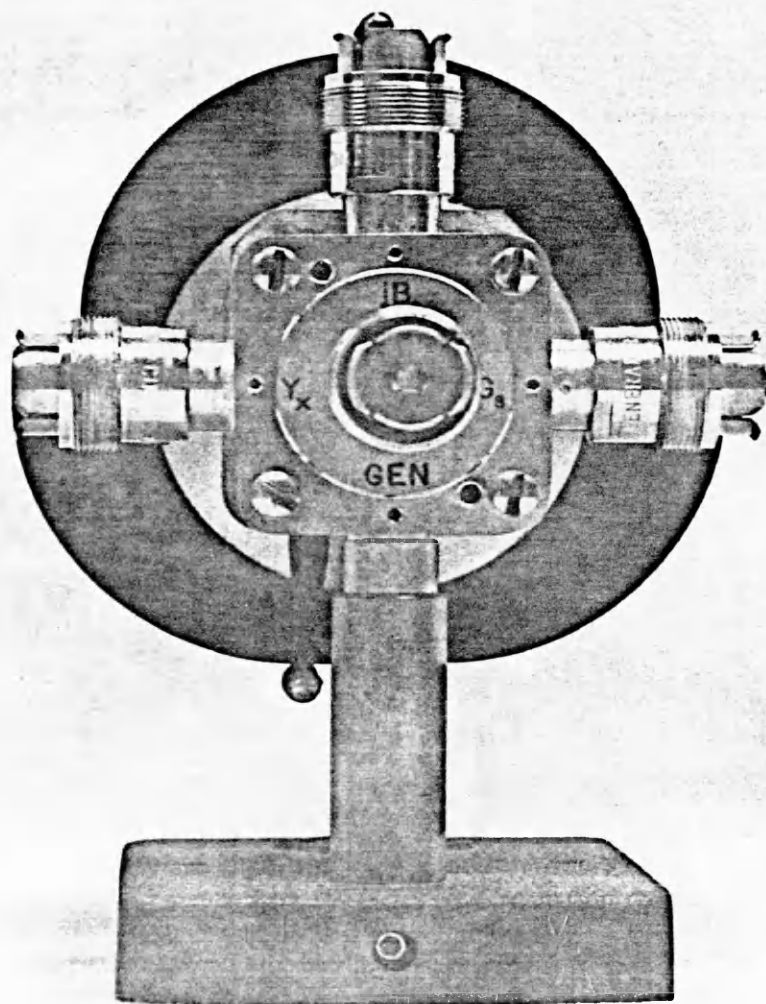


PLATE 2
Admittance Meter - Rear

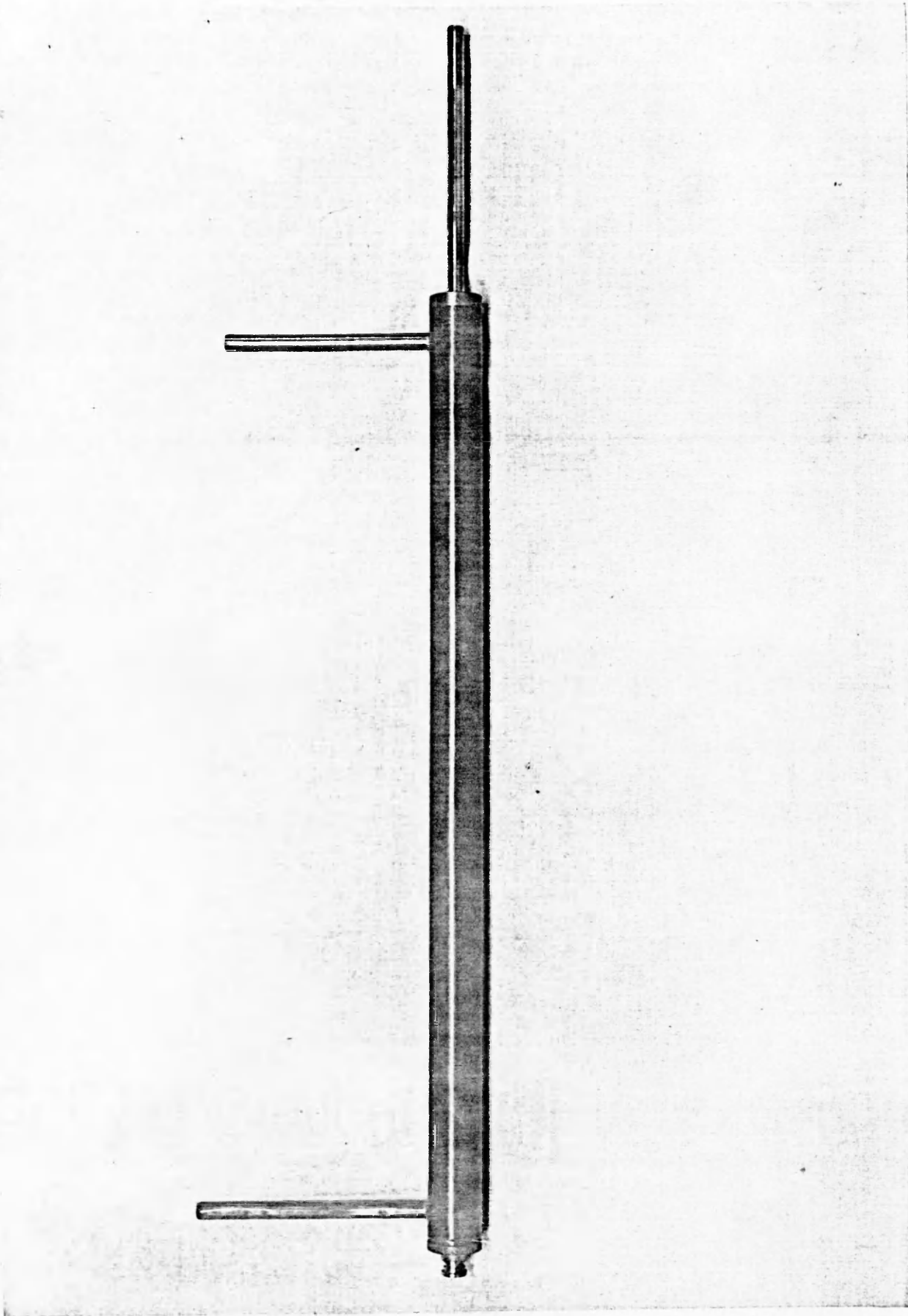


PLATE 3
UHF Cell - Assembled

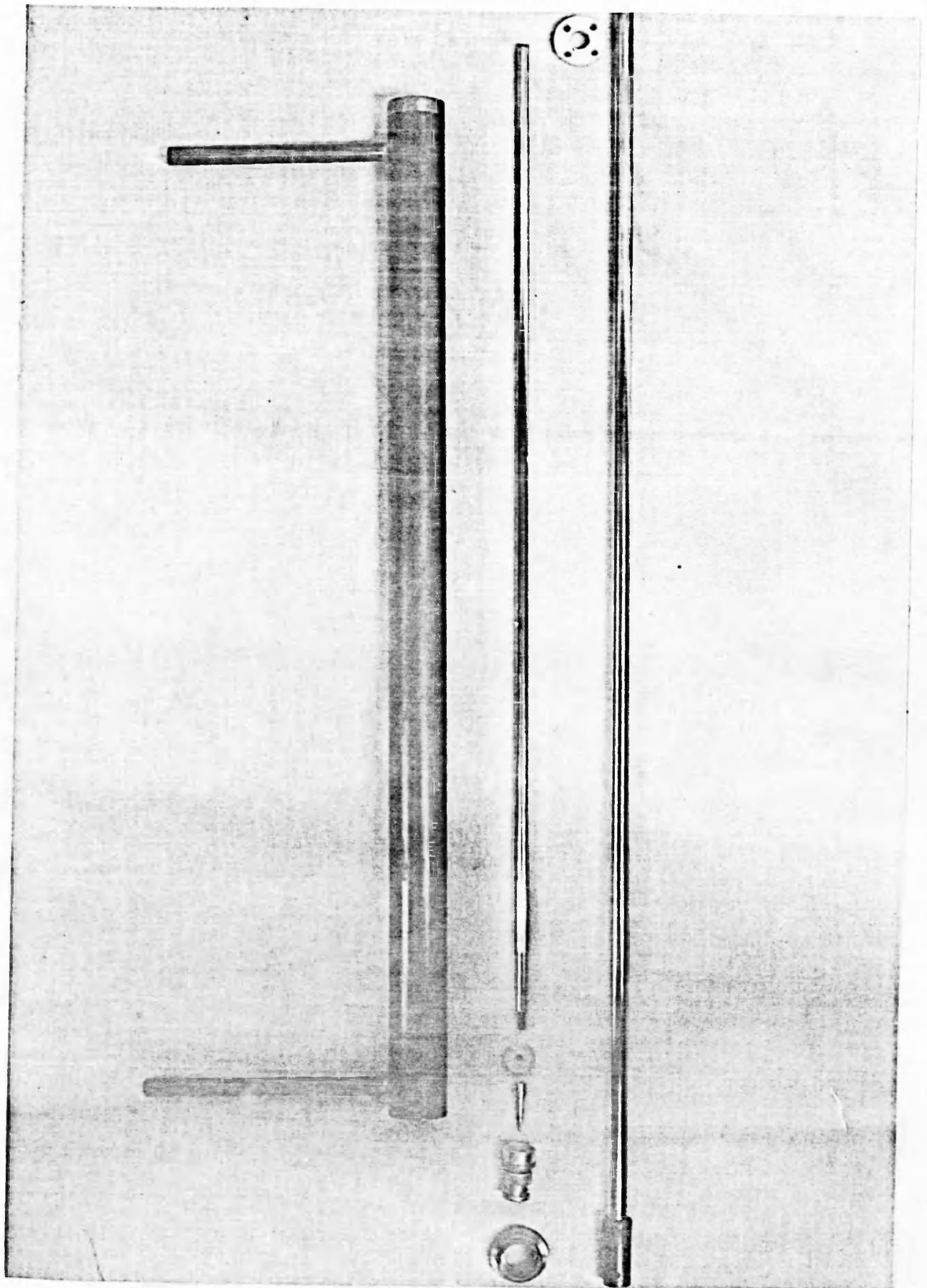


PLATE 4
UHF Cell - Disassembled

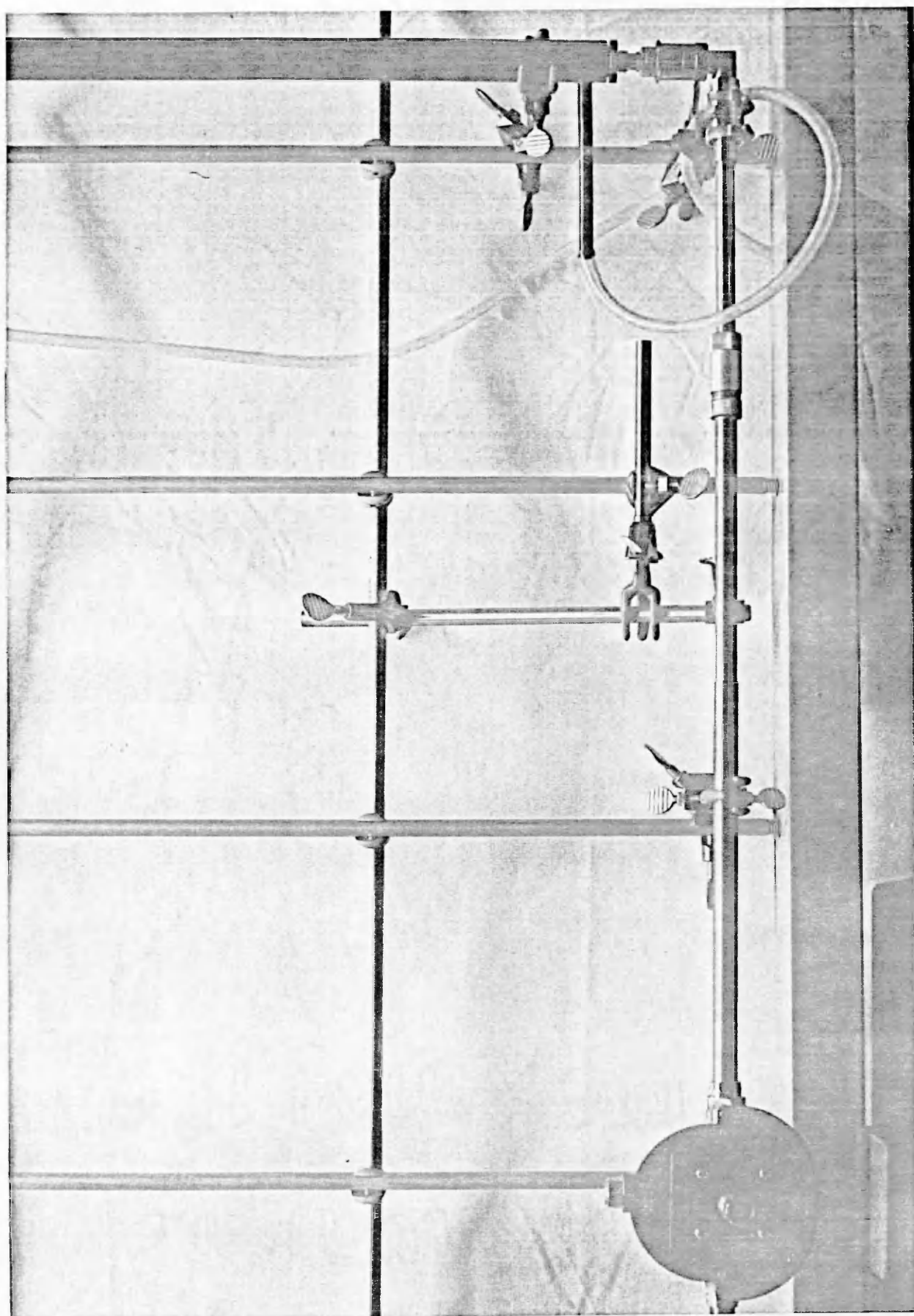


PLATE 5
Interconnection of UHF Components

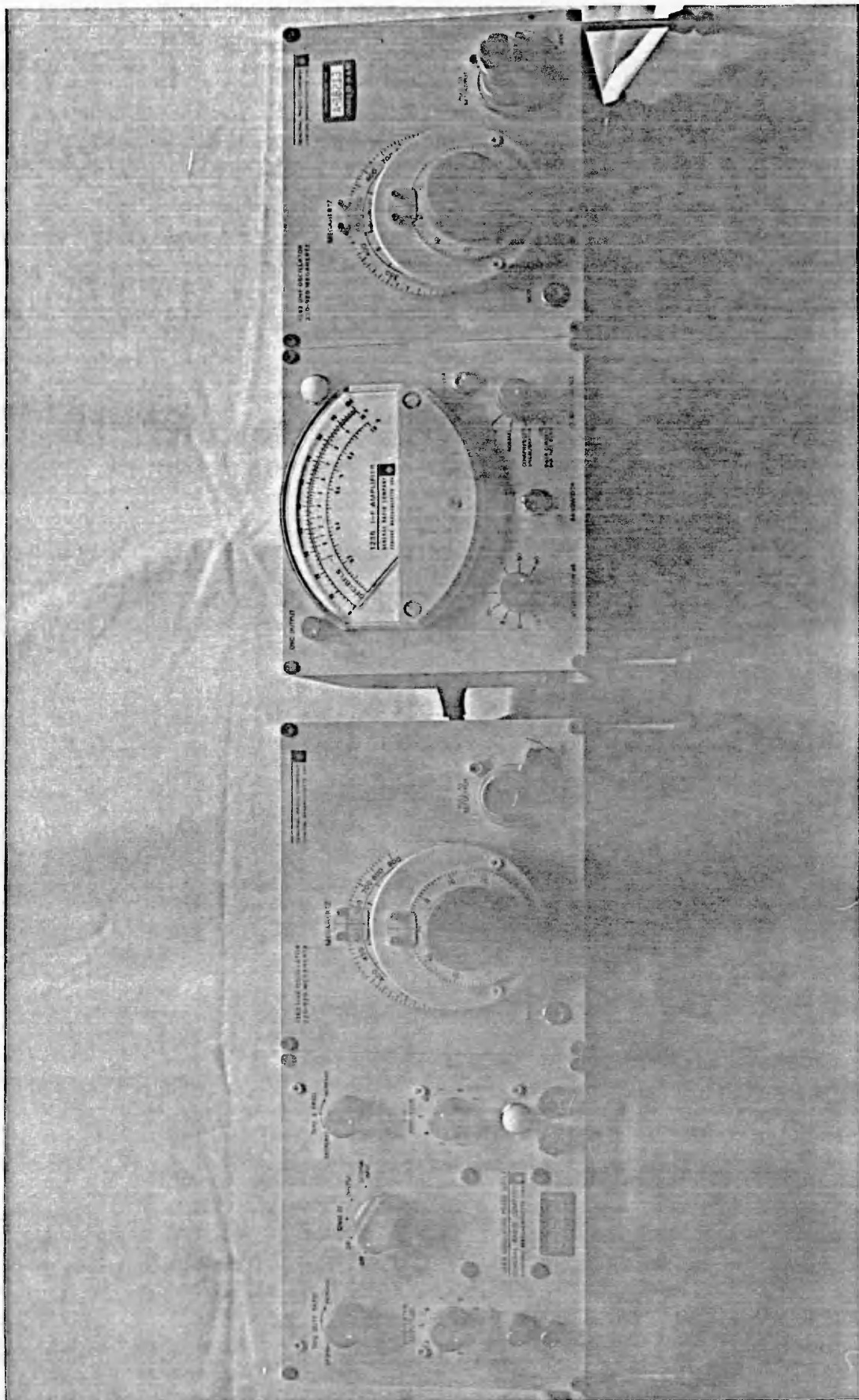


PLATE 6
UHF Signal Generator and IF Amplifier

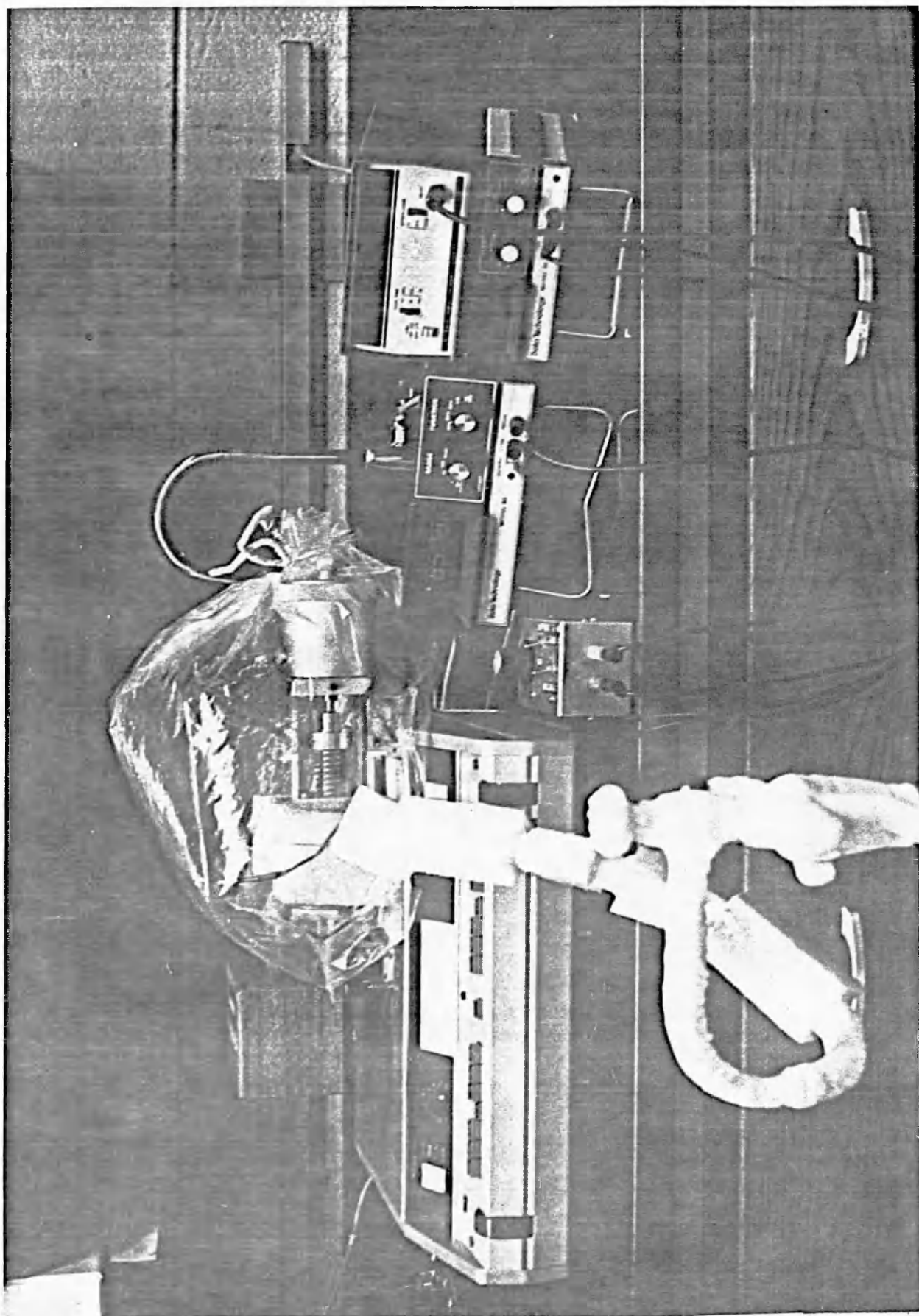


PLATE 7
Interconnection of RF Components



PLATE 8
Interconnection of RF Components - Detail

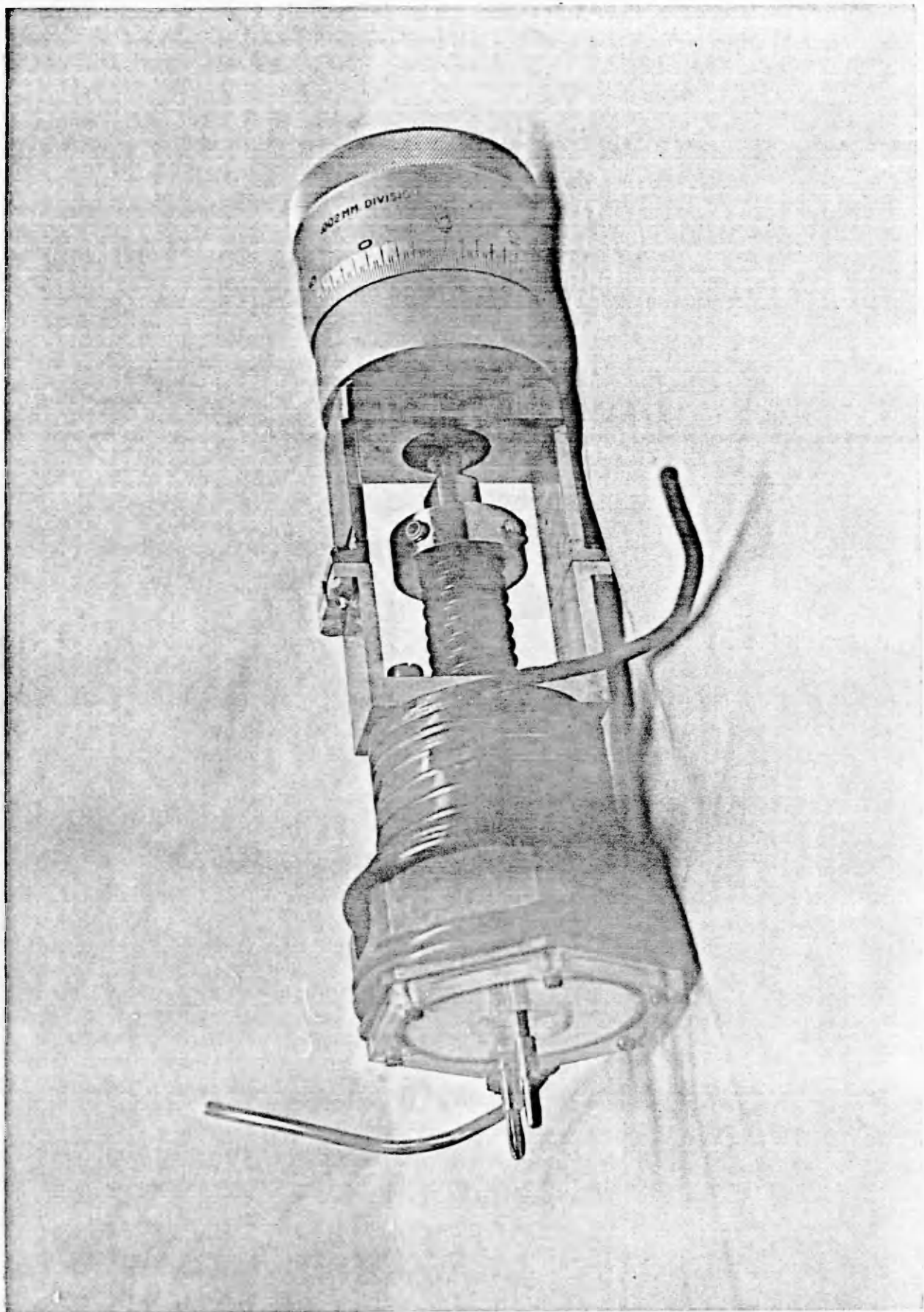


PLATE 9
RF Cell — Assembled

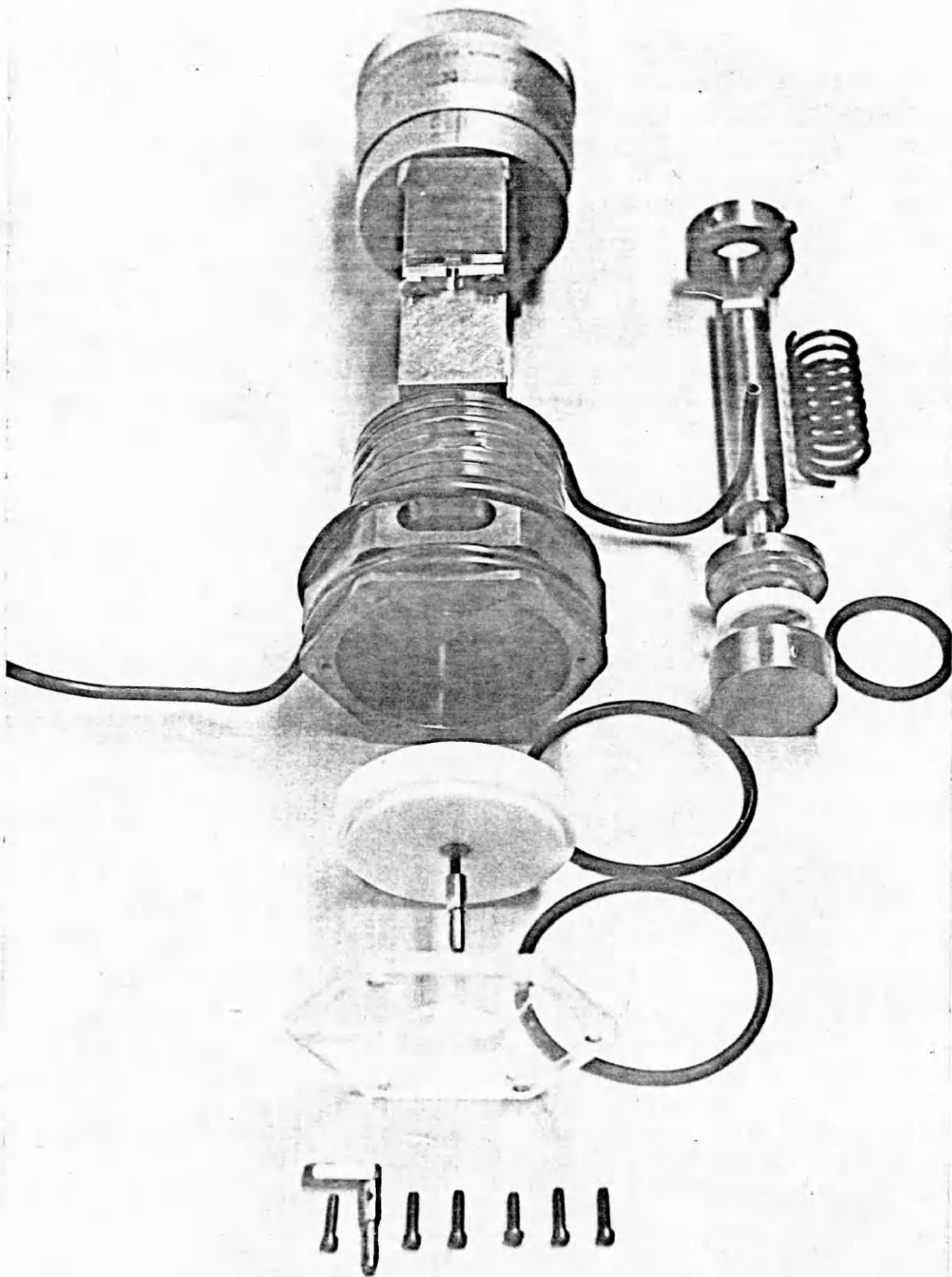


PLATE 10
RF Cell - Disassembled

APPENDIX I

COMPUTER PROGRAM TO CALCULATE

c_n , $b^2 - a^2$, $2ab$, AND $\tan \delta$

```

      ▽ PROC CO
[1]  CN← 1 3 5
[2]  K←-1
[3]  SQR← 101 3 00
[4]  AB2← 101 3 00
[5]  TAN← 101 3 00
[6]  AB← 101 2 00
[7]  CN0← 40 4 00
[8]  CN1← 101 4 00
[9]  CN2← 80 4 00
[10] CS←0.1×101
[11] LOOP:K←K+1
[12] C←CO
[13] →(K=2)/DOUBLE
[14] INC←0.1
[15] →SKIP
[16] DOUBLE:INC←0.2
[17] SKIP:J←0
[18] LI:A←0
[19] B←0CN[K]
[20] MAIN A,B
[21] AB[J;]←Y
[22] SQR[J;K]←(AB[J;1]*2)-(AB[J;0]*2)
[23] AB2[J;K]←2×(AB[J;0])×(AB[J;1])
[24] TAN[J;K]←(AB2[J;K]:SQR[J;K])
[25] C←C+INC
[26] →(100≥J+J+1)/LI
[27] →(K<2)/LOOP
[28] CN0[;0]←40+CS
[29] CN0[;1]←40+SQR[;0]
[30] CN0[;2]←40+AB2[;0]
[31] CN0[;3]←40+TAN[;0]
[32] CN1[;0]←CS
[33] CN1[;1]←SQR[;1]
[34] CN1[;2]←AB2[;1]
[35] CN1[;3]←TAN[;1]
[36] CN2[;0]←0.2×180
[37] CN2[;1]←80+SQR[;2]
[38] CN2[;2]←80+AB2[;2]
[39] CN2[;3]←80+TAN[;2]
[40] 'TYPE 'PRINT' TO PRINT OUT TABLES.'
      ▽

```

```

      ▽ MAIN X
[ 1]  I←0
[ 2]  Y←X
[ 3]  L1:Z←-(FN Y)FFP Y
[ 4]  →L2×1(50≤I+I+1)
[ 5]  →0×1((I/Z)≤0.00001)
[ 6]  Y←Y+Z
[ 7]  →L1
[ 8]  L2:→0,ρI← 'DID NOT CONVERGE'
      ▽

```

```

      ▽ R←FN X;A;B
[ 1]  A←X[0]
[ 2]  B←X[1]
[ 3]  R←(A×50A)+(P×10B)
[ 4]  R←P,(((B×50A)-(A×10B))÷((60A)-20B))-C
      ▽

```

```

      ▽ R←FP X;A;P;NUM1;NUM2;NUM3;NUM4
[ 1]  A←X[0]
[ 2]  P←X[1]
[ 3]  R← 2 2 ρ0
[ 4]  R[0;0]←(A×60A)+50A
[ 5]  R[0;1]←(P×20B)+10B
[ 6]  NUM1←(((60A)-20B)×((P×60A)-10B))
[ 7]  NUM2←((B×50A)-A×10B)×50A
[ 8]  NUM3←(((60A)-20B)×((50A)-A×20B))
[ 9]  NUM4←((B×50A)-A×10B)×10B
[10]  DEN←((60A)-20B)*2
[11]  R[1;0]←(NUM1-NUM2)÷DEN
[12]  R[1;1]←(NUM3-NUM4)÷DEN
      ▽

```

```

      ▽ PRINT;K
[ 1]  'WHICH C[N] DO YOU WANT?  1, 3, OF 5?'
[ 2]  K←□
[ 3]  →(K=1)/K0
[ 4]  →(K=3)/K1
[ 5]  K←2
[ 6]  OUTPUT←CN2
[ 7]  →TYPEF
[ 8]  K0:K←0
[ 9]  OUTPUT←CN0
[10]  →TYPEF
[11]  K1:K←1
[12]  OUTPUT←CN1
[13]  TYPEF:SHAPE← 11 2 15 5 15 3 15 5
[14]  ''
[15]  ''
[16]  ''
[17]  SHAPE DFT OUTPUT
      ▽

```

APPENDIX II

TABLE OF C_n ($n=1,2,3$), b^2-a^2 , $2ab$, AND $\tan \delta$

<u>c₁</u>	<u>b² - a²</u>	<u>2ab</u>	<u>tan δ</u>
.00	9.86960	.000	.00000
.10	9.87366	.400	.04051
.20	9.88587	.800	.08090
.30	9.90607	1.199	.12106
.40	9.93442	1.598	.16087
.50	9.97086	1.996	.20022
.60	10.01537	2.394	.23900
.70	10.06793	2.790	.27712
.80	10.12854	3.185	.31446
.90	10.19717	3.579	.35095
1.00	10.27381	3.971	.38650
1.10	10.35841	4.361	.42102
1.20	10.45096	4.749	.45445
1.30	10.55141	5.136	.48673
1.40	10.65974	5.520	.51781
1.50	10.77591	5.901	.54763
1.60	10.89988	6.280	.57610
1.70	11.03161	6.656	.60337
1.80	11.17100	7.029	.62922
1.90	11.31807	7.399	.65372

<u>c_1</u>	<u>$b^2 - a^2$</u>	<u>$2ab$</u>	<u>$\tan \delta$</u>
2.00	11.47274	7.765	.67684
2.10	11.63495	8.128	.69859
2.20	11.80463	8.487	.71897
2.30	11.98171	8.842	.73798
2.40	12.16612	9.193	.75565
2.50	12.35779	9.540	.77198
2.60	12.55662	9.882	.78701
2.70	12.76254	10.220	.80076
2.80	12.97545	10.552	.81325
2.90	13.19523	10.880	.82453
3.00	13.42184	11.202	.83462
3.10	13.65511	11.519	.84356
3.20	13.89493	11.830	.85140
3.30	14.14120	12.136	.85817
3.40	14.39377	12.435	.86390
3.50	14.65251	12.728	.86865
3.60	14.91728	13.015	.87246
3.70	15.18792	13.295	.87535
3.80	15.46427	13.568	.87739
3.90	15.74615	13.835	.87860

<u>C_3</u>	<u>$b^2 - a^2$</u>	<u>$2ab$</u>	<u>$\tan \delta$</u>
.00	88.82644	.000	.00000
.10	88.82689	.400	.00450
.20	88.82824	.800	.00901
.30	88.83050	1.200	.01351
.40	88.83367	1.601	.01802
.50	88.83776	2.002	.02253
.60	88.84277	2.403	.02705
.70	88.84873	2.804	.03156
.80	88.85565	3.207	.03609
.90	88.86354	3.610	.04062
1.00	88.87243	4.013	.04516
1.10	88.88233	4.417	.04970
1.20	88.89328	4.823	.05425
1.30	88.90529	5.229	.05881
1.40	88.91841	5.636	.06338
1.50	88.93242	6.044	.06796
1.60	88.94777	6.454	.07255
1.70	88.96432	6.864	.07716
1.80	88.98210	7.276	.08177
1.90	89.00116	7.690	.08640

$\underline{c_3}$	$\underline{b^2 - a^2}$	$\underline{2ab}$	$\underline{\tan \delta}$
2.00	89.02156	8.105	.09104
2.10	89.04332	8.521	.09570
2.20	89.06652	8.940	.10037
2.30	89.09122	9.360	.10506
2.40	89.11746	9.782	.10976
2.50	89.14532	10.206	.11448
2.60	89.17487	10.632	.11922
2.70	89.20618	11.060	.12398
2.80	89.23934	11.490	.12875
2.90	89.27442	11.922	.13355
3.00	89.31152	12.357	.13836
3.10	89.35073	12.795	.14320
3.20	89.39215	13.235	.14805
3.30	89.43588	13.677	.15293
3.40	89.48205	14.122	.15782
3.50	89.53076	14.570	.16274
3.60	89.58215	15.021	.16768
3.70	89.63635	15.475	.17264
3.80	89.69349	15.932	.17763
3.90	89.75372	16.392	.18263

$\underline{C_3}$	$\underline{b^2 - a^2}$	$\underline{2ab}$	$\underline{\tan \delta}$
4.00	89.81719	16.855	.18766
4.10	89.88408	17.321	.19271
4.20	89.95454	17.791	.19778
4.30	90.02876	18.264	.20287
4.40	90.10692	18.741	.20798
4.50	90.18922	19.221	.21312
4.60	90.27587	19.704	.21827
4.70	90.36707	20.191	.22344
4.80	90.46305	20.682	.22862
4.90	90.56403	21.176	.23383
5.00	90.67049	21.674	.23904
5.10	90.78229	22.176	.24427
5.20	90.89985	22.681	.24951
5.30	91.02345	23.190	.25476
5.40	91.15336	23.702	.26002
5.50	91.28985	24.218	.26528
5.60	91.43323	24.737	.27055
5.70	91.58378	25.259	.27581
5.80	91.74181	25.785	.28106
5.90	91.90761	26.314	.28631

<u>C₃</u>	<u>b² - a²</u>	<u>2ab</u>	<u>tan δ</u>
6.00	92.08149	26.846	.29155
6.10	92.26377	27.381	.29677
6.20	92.45474	27.919	.30197
6.30	92.65472	28.459	.30715
6.40	92.86401	29.001	.31229
6.50	93.08290	29.545	.31741
6.60	93.31168	30.091	.32248
6.70	93.55064	30.639	.32751
6.80	93.80005	31.187	.33248
6.90	94.06017	31.736	.33741
7.00	94.33123	32.286	.34226
7.10	94.61348	32.836	.34706
7.20	94.90711	33.386	.35177
7.30	95.21232	33.935	.35641
7.40	95.52927	34.482	.36096
7.50	95.85811	35.028	.36542
7.60	96.19896	35.573	.36978
7.70	96.55191	36.114	.37404
7.80	96.91703	36.653	.37819
7.90	97.29437	37.188	.38222

$\underline{c_3}$	$\underline{b^2 - a^2}$	$\underline{2ab}$	$\underline{\tan \delta}$
8.00	97.68394	37.719	.38613
8.10	98.08573	38.245	.38992
8.20	98.49970	38.767	.39358
8.30	98.92580	39.283	.39710
8.40	99.36393	39.794	.40049
8.50	99.81397	40.298	.40373
8.60	100.27579	40.795	.40683
8.70	100.74922	41.285	.40978
8.80	101.23408	41.767	.41258
8.90	101.73016	42.241	.41522
9.00	102.23723	42.706	.41771
9.10	102.75505	43.162	.42005
9.20	103.28335	43.609	.42222
9.30	103.82185	44.045	.42424
9.40	104.37025	44.472	.42609
9.50	104.92823	44.887	.42779
9.60	105.49546	45.292	.42933
9.70	106.07160	45.686	.43071
9.80	106.65628	46.067	.43192
9.90	107.24944	46.437	.43298
10.00	107.85022	46.795	.43389

$\underline{C_5}$	$\underline{b^2 - a^2}$	$\underline{2ab}$	$\underline{\tan \delta}$
.00	246.74011	.000	.00000
.20	246.74076	.800	.00324
.40	246.74271	1.600	.00649
.60	246.74596	2.401	.00973
.80	246.75054	3.203	.01298
1.00	246.75645	4.005	.01623
1.20	246.76372	4.809	.01949
1.40	246.77238	5.614	.02275
1.60	246.78246	6.421	.02602
1.80	246.79400	7.230	.02930
2.00	246.80704	8.041	.03258
2.20	246.82164	8.855	.03588
2.40	246.83785	9.672	.03918
2.60	246.85573	10.492	.04250
2.80	246.87536	11.315	.04583
3.00	246.89666	12.141	.04918
3.20	246.91999	12.972	.05253
3.40	246.94530	13.807	.05591
3.60	246.97272	14.646	.05930
3.80	247.00234	15.490	.06271

$\underline{C_5}$	$\underline{b^2 - a^2}$	$\underline{2ab}$	$\underline{\tan \delta}$
4.00	247.03430	16.339	.06614
4.20	247.06873	17.194	.06959
4.40	247.10577	18.054	.07306
4.60	247.14558	18.921	.07656
4.80	247.18833	19.794	.08008
5.00	247.23421	20.674	.08362
5.20	247.28343	21.561	.08719
5.40	247.33620	22.456	.09079
5.60	247.39277	23.358	.09442
5.80	247.45340	24.269	.09808
6.00	247.51838	25.189	.10177
6.20	247.58800	26.118	.10549
6.40	247.66262	27.057	.10925
6.60	247.74260	28.006	.11304
6.80	247.82834	28.965	.11687
7.00	247.92027	29.935	.12075
7.20	248.01888	30.917	.12466
7.40	248.12467	31.911	.12861
7.60	248.23820	32.917	.13260
7.80	248.36011	33.937	.13664

$\underline{C_5}$	$\underline{b^2 - a^2}$	$\underline{2ab}$	$\underline{\tan \delta}$
8.00	248.49104	34.970	.14073
8.20	248.63175	36.017	.14486
8.40	248.78301	37.079	.14904
8.60	248.94570	38.156	.15327
8.80	249.12076	39.249	.15755
9.00	249.30923	40.358	.16188
9.20	249.51222	41.483	.16626
9.40	249.73095	42.626	.17069
9.60	249.96674	43.787	.17517
9.80	250.22103	44.965	.17970
10.00	250.49536	46.162	.18428
10.20	250.79141	47.378	.18891
10.40	251.11098	48.613	.19359
10.60	251.45599	49.866	.19831
10.80	251.82895	51.139	.20307
11.00	252.23132	52.430	.20786
11.20	252.66576	53.740	.21269
11.40	253.13470	55.067	.21754
11.60	253.64070	56.412	.22241
11.80	254.18638	57.772	.22728

C_5	$b^2 - a^2$	$2ab$	$\tan \delta$
12.00	254.77444	59.147	.23216
12.20	255.40759	60.536	.23702
12.40	256.08855	61.935	.24185
12.60	256.81996	63.342	.24664
12.80	257.60436	64.756	.25138
13.00	258.44415	66.173	.25604
13.20	259.34147	67.589	.26062
13.40	260.29821	69.000	.26508
13.60	261.31592	70.403	.26942
13.80	262.39576	71.794	.27361
14.00	263.53845	73.167	.27763
14.20	264.74456	74.517	.28147
14.40	266.01348	75.841	.28510
14.60	267.34468	77.133	.28851
14.80	268.73700	78.388	.29169
15.00	270.18879	79.602	.29462
15.20	271.69795	80.770	.29728
15.40	273.26194	81.887	.29967
15.60	274.87786	82.950	.30177
15.80	276.54243	83.955	.30359

TABLE OF CONTENTS

<u>Solute</u>	<u>Freq(MHz)</u>	<u>T (K)</u>	<u>Plot</u>	<u>Page</u>
Nitrobenzene	500. . 25. . . .	ϵ'	vs Conc. . . .	116
	500. . 25. . . .	ϵ''	vs Conc. . . .	117
	700. . 25. . . .	ϵ'	vs Conc. . . .	118
	700. . 25. . . .	ϵ''	vs Conc. . . .	119
	500. . 60. . . .	ϵ'	vs Conc. . . .	120
	500. . 60. . . .	ϵ''	vs Conc. . . .	121
	700. . 60. . . .	ϵ'	vs Conc. . . .	122
	700. . 60. . . .	ϵ''	vs Conc. . . .	123
o-Nitrobiphenyl	500. . 25. . . .	ϵ'	vs Conc. . . .	124
	500. . 25. . . .	ϵ''	vs Conc. . . .	125
	700. . 25. . . .	ϵ'	vs Conc. . . .	126
	700. . 25. . . .	ϵ''	vs Conc. . . .	127
	500. . 60. . . .	ϵ'	vs Conc. . . .	128
	500. . 60. . . .	ϵ''	vs Conc. . . .	129
	700. . 60. . . .	ϵ'	vs Conc. . . .	130
	700. . 60. . . .	ϵ''	vs Conc. . . .	131
p-Nitrobiphenyl	500. . 25. . . .	ϵ'	vs Conc. . . .	132
	500. . 25. . . .	ϵ''	vs Conc. . . .	133
	700. . 25. . . .	ϵ'	vs Conc. . . .	134
	700. . 25. . . .	ϵ''	vs Conc. . . .	135
	500. . 60. . . .	ϵ'	vs Conc. . . .	136
	500. . 60. . . .	ϵ''	vs Conc. . . .	137
	700. . 60. . . .	ϵ'	vs Conc. . . .	138
	700. . 60. . . .	ϵ''	vs Conc. . . .	139
2,2'-Dinitrobiphenyl	500. . 25. . . .	ϵ'	vs Conc. . . .	140
	500. . 25. . . .	ϵ''	vs Conc. . . .	141
	700. . 25. . . .	ϵ'	vs Conc. . . .	142
	700. . 25. . . .	ϵ''	vs Conc. . . .	143
	500. . 60. . . .	ϵ'	vs Conc. . . .	144
	500. . 60. . . .	ϵ''	vs Conc. . . .	145
	700. . 60. . . .	ϵ'	vs Conc. . . .	146
	700. . 60. . . .	ϵ''	vs Conc. . . .	147

C_5	$b^2 - a^2$	$2ab$	$\tan \delta$
.00	246.74011	.000	.00000
.20	246.74070	.000	.00024
.40	246.74271	1.000	.00043
.60	246.74630	2.401	.00073
.80	246.75064	3.200	.01200
1.00	246.75340	4.000	.01020
1.20	246.75372	4.800	.01340
1.40	246.77230	5.614	.02270
1.60	246.78240	6.421	.02802
1.80	246.79400	7.200	.02900
2.00	246.80704	8.041	.03250
2.20	246.82104	8.855	.03500
2.40	246.83700	9.672	.03610
2.60	246.85573	10.402	.04280
2.80	246.87530	11.015	.04600
3.00	246.89600	12.141	.04910
3.20	246.91830	12.672	.05200
3.40	246.94330	13.307	.05601
3.60	246.97272	14.040	.06000
3.80	247.00264	14.700	.06271

<u>C₅</u>	<u>b² - a²</u>	<u>2ab</u>	<u>tan δ</u>
4.00	247.03430	16.339	.06614
4.20	247.06673	17.194	.06359
4.40	247.10377	18.054	.07306
4.60	247.14553	18.921	.07656
4.80	247.18833	19.794	.08006
5.00	247.23421	20.674	.08352
5.20	247.28343	21.561	.08710
5.40	247.33620	22.456	.09073
5.60	247.39277	23.358	.09442
5.80	247.45340	24.269	.09808
6.00	247.51833	25.189	.10177
6.20	247.58600	26.116	.10549
6.40	247.65262	27.057	.10925
6.60	247.74260	28.006	.11304
6.80	247.82634	28.965	.11687
7.00	247.92027	29.935	.12075
7.20	248.01868	30.917	.12466
7.40	248.12467	31.911	.12861
7.60	248.23820	32.917	.13260
7.80	248.36011	33.937	.13664

C_5	$b^2 - a^2$	$2ab$	$\tan \delta$
8.00	248.43104	34.373	.14373
8.20	248.53173	36.317	.14453
8.40	248.73301	37.373	.14534
8.60	248.94570	38.433	.14627
8.80	249.12370	39.243	.14755
9.00	249.33323	40.333	.14833
9.20	249.51222	41.433	.14923
9.40	249.73333	42.323	.15033
9.60	249.93374	43.737	.15117
9.80	250.22133	44.333	.15373
10.00	250.43336	45.132	.15423
10.20	250.73141	47.373	.15531
10.40	251.11333	48.313	.15533
10.60	251.43333	49.333	.15631
10.80	251.82333	51.133	.15837
11.00	252.23132	52.433	.15933
11.20	252.63373	53.743	.16123
11.40	253.13473	55.337	.16173
11.60	253.64073	56.412	.16241
11.80	254.13333	57.772	.16273

C_5	$b^2 - a^2$	$2ab$	$\tan \delta$
12.00	254.77444	59.147	.23215
12.20	255.40759	60.536	.23702
12.40	256.06855	61.935	.24185
12.60	256.81936	63.342	.24664
12.80	257.60456	64.756	.25138
13.00	258.44415	66.178	.25604
13.20	259.34147	67.589	.26062
13.40	260.29821	69.000	.26508
13.60	261.31592	70.403	.26942
13.80	262.39576	71.794	.27361
14.00	263.53845	73.167	.27763
14.20	264.74456	74.517	.28147
14.40	266.01348	75.841	.28510
14.60	267.34466	77.133	.28851
14.80	268.73700	78.386	.29169
15.00	270.18879	79.602	.29462
15.20	271.69795	80.770	.29728
15.40	273.26194	81.887	.29967
15.60	274.87766	82.959	.30177
15.80	276.54243	83.985	.30359

APPENDIX III

COMPONENTS OF UHF MEASUREMENT SYSTEM

Signal Generator:

General Radio Type 1264-B Modulating Power Supply
and Type 1362 UHF Oscillator (220-920MHz)

Detector:

General Radio Type 1362 UHF Oscillator
General Radio Type 1236 IF Amplifier
General Radio Type 874-MRAL Mixer

Measuring Equipment:

General Radio Type 1602-B UHF Admittance Meter
General Radio Type 1602-P4 50 Ohm Termination
Gaertner Scientific 0.001 cm. Cathetometer

Connecting Equipment:

General Radio Type 874-R22LA Patch Cords (2 ea.)
General Radio Type 874-F1000L Low Pass Filter
General Radio Type 874-G10L 10db Attenuator Pad
General Radio Type 874-WOL Open Circuit Termination
General Radio Type 874-ELL 90° Elbow
General Radio Type 874-LK20L 20 cm. Constant Impedance
Line

UHF Cell:

*General Radio Type 874-D50L 50 cm. Adjustable Stub
*General Radio Type 874-QBPAL BNC Jack to Type 874
Adapter

*These parts were used in the construction of the cell as
described on pages 47 and 48.

APPENDIX IV

COMPUTER PROGRAM TO FIND BEST FIT FOR
ALL UHF DATA


```

      ▽ TAUFIT
[1]  'ENTER HEADING.'
[2]  HEAD2←□
[3]  'FREQ?'
[4]  FR←□
[5]  →(FR=0)/0
[6]  OM←(ρFR)ρ0
[7]  APCAL←(ρFR)ρ0
[8]  ADPCAL←(ρFR)ρ0
[9]  'TAU START?'
[10] TAU←□
[11] →(TAU=0)/0
[12] 'INCR?'
[13] IN←□
[14] →(IN=0)/0
[15] 'AP EXP?'
[16] APEX←□
[17] →(APEX=0)/0
[18] 'ADP EXP?'
[19] ADPEX←□
[20] →(ADPEX=0)/0
[21] 'A0 ?'
[22] A0←□
[23] →(A0=0)/0
[24] 'AINF ?'
[25] AINF←□
[26] →(AINF=0)/0
[27] OM←2×(OFR)
[28] C←0
[29] 'TAU(PICOSECONDS)    SUM OF THE SQUARES OF THE RESIDUALS'
[30] ''
[31] ''
[32] LOOP:TAU←TAU+IN
[33]  C←C+1
[34]  J←0
[35]  LOOP2:J←J+1
[36]  APCAL[J]←((A0-AINF)÷(1+(OM[J]*2)×(TAU*2)))+AINF
[37]  ADPCAL[J]←((A0-AINF)×OM[J]×TAU)÷(1+(OM[J]*2)×TAU*2)
[38]  →(J<(ρFR))/LOOP2
[39]  SUMSQ←((+/(APCAL-APEX)*2)+(+/ (ADPCAL-ADPEX)*2))
[40]  FORM← 16 2 45 4
[41]  TAU←TAU×1000000000000
[42]  FORM DFT TAU AND SUMSQ
[43]  TAU←TAU×1E-12
[44]  →(C=1)/GIVE
[45]  →(SAVE≤SUMSQ)/STORE
[46]  SAVE←SUMSQ
[47]  →LOOP
[48]  GIVE:SAVE←SUMSQ
[49]  →LOOP

```


APPENDIX V

LEAST SQUARES PLOTS OF ϵ' AND ϵ''
VS CONCENTRATION

TABLE OF CONTENTS

<u>Solute</u>	<u>Freq (MHz)</u>	<u>T (K)</u>	<u>Plot</u>	<u>Page</u>
Nitrobenzene	500.	25.	ϵ' vs Conc.	116
	500.	25.	ϵ'' vs Conc.	117
	700.	25.	ϵ' vs Conc.	118
	700.	25.	ϵ'' vs Conc.	119
	500.	60.	ϵ' vs Conc.	120
	500.	60.	ϵ'' vs Conc.	121
	700.	60.	ϵ' vs Conc.	122
	700.	60.	ϵ'' vs Conc.	123
o-Nitrobiphenyl	500.	25.	ϵ' vs Conc.	124
	500.	25.	ϵ'' vs Conc.	125
	700.	25.	ϵ' vs Conc.	126
	700.	25.	ϵ'' vs Conc.	127
	500.	60.	ϵ' vs Conc.	128
	500.	60.	ϵ'' vs Conc.	129
	700.	60.	ϵ' vs Conc.	130
	700.	60.	ϵ'' vs Conc.	131
p-Nitrobiphenyl	500.	25.	ϵ' vs Conc.	132
	500.	25.	ϵ'' vs Conc.	133
	700.	25.	ϵ' vs Conc.	134
	700.	25.	ϵ'' vs Conc.	135
	500.	60.	ϵ' vs Conc.	136
	500.	60.	ϵ'' vs Conc.	137
	700.	60.	ϵ' vs Conc.	138
	700.	60.	ϵ'' vs Conc.	139
2,2'-Dinitrobiphenyl	500.	25.	ϵ' vs Conc.	140
	500.	25.	ϵ'' vs Conc.	141
	700.	25.	ϵ' vs Conc.	142
	700.	25.	ϵ'' vs Conc.	143
	500.	60.	ϵ' vs Conc.	144
	500.	60.	ϵ'' vs Conc.	145
	700.	60.	ϵ' vs Conc.	146
	700.	60.	ϵ'' vs Conc.	147

NITROBENZENE / BENZENE 500MHZ 25C

0.0250
0.0225
0.0200
0.0175
ε"
0.0150
0.0125
0.0100
0.0075
0.0050
0.000

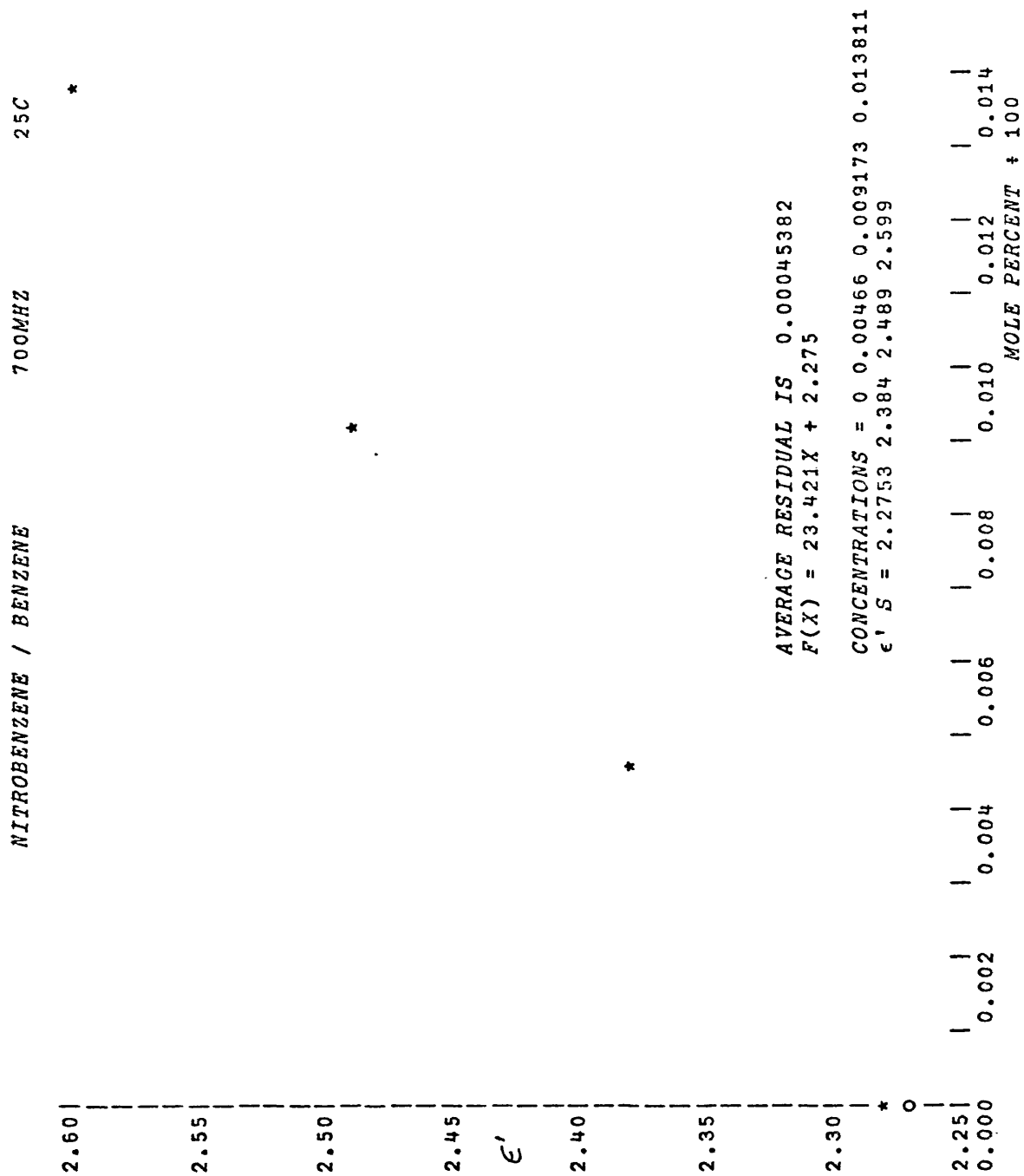
*

*

*

AVERAGE RESIDUAL IS 0.00020367
F(X) = 1.2599X + 0.0057177
CONCENTRATIONS = 0 0.00466 0.009173 0.013811
ε'' S = 0.0058 0.0113 0.0176 0.023

0.002 0.004 0.006 0.008 0.010 0.012 0.014
MOLE PERCENT * 100



NITROBENZENE / BENZENE

700MHZ

25C

0.040 |
 0.035 |
 0.030 |
 ε'' |
 0.025 |
 0.020 |
 0.015 |
 0.010 |
 0.000 |

*

*

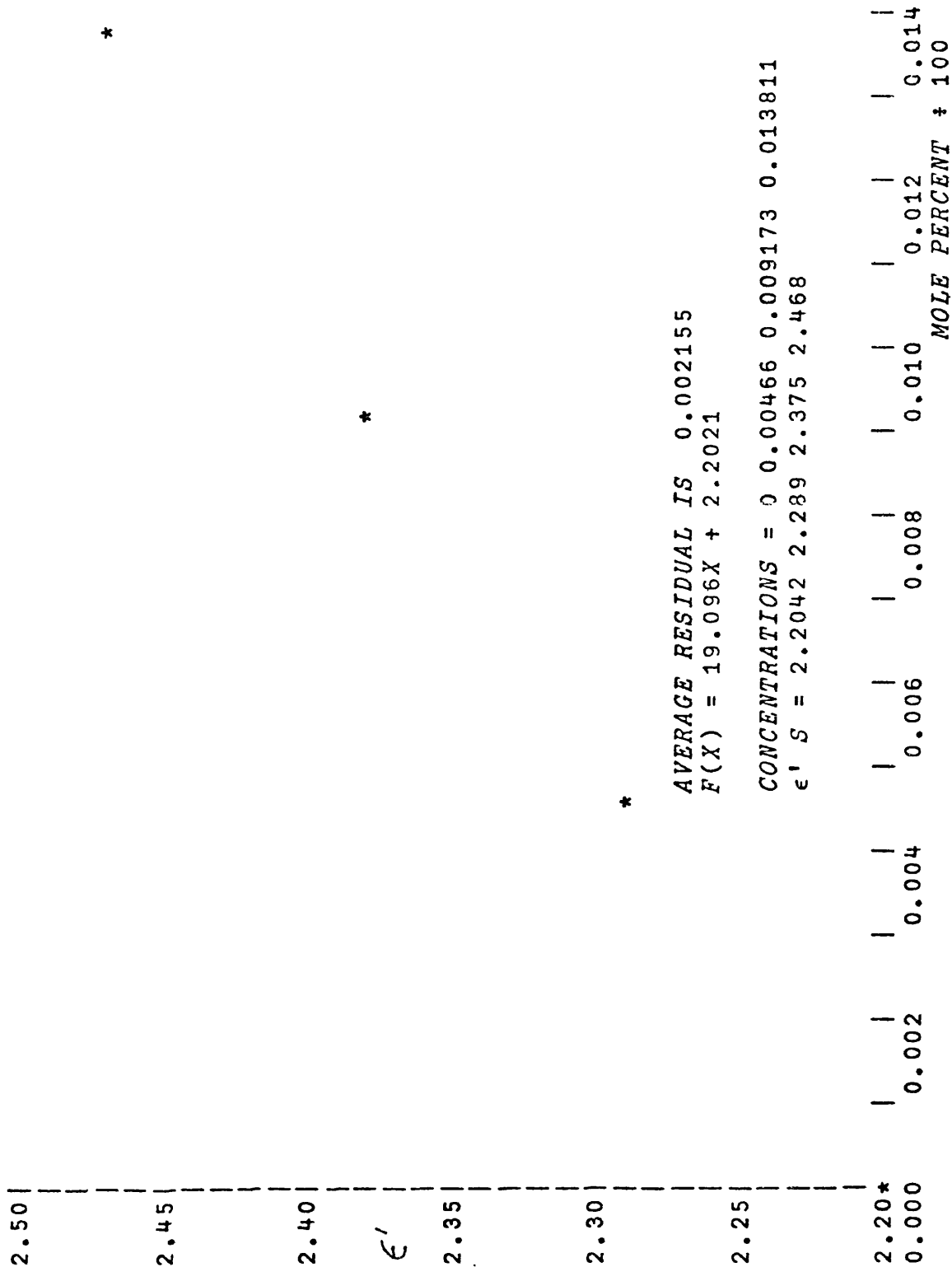
*

AVERAGE RESIDUAL IS 0.00013285
 $F(X) = 1.8305X + 0.010574$

CONCENTRATIONS = 0 0.00466 0.009173 0.013811
 ϵ'' S = 0.0106 0.0192 0.0271 0.036

0.002 | 0.004 | 0.006 | 0.008 | 0.010 | 0.012 | 0.014 |
 * | | | | | | |
 MOLE PERCENT ÷ 100

NITROBENZENE / BENZENE 500MHZ 60C



NITROBENZENE / BENZENE

500MHZ

60C

0.017
0.016
0.015
0.014
0.013
0.012
€"
0.011
0.010
0.009
0.008
0.007
0.006
0.000

•
•

•
•

•

AVERAGE RESIDUAL IS 0.00007186
P(X) = 0.74877X + 0.0060752

CONCENTRATIONS = 0 0.00456 0.009173 0.013811
€" S = 0.0061 0.0096 0.0128 0.0165

0.002 0.004 0.006 0.008 0.010 0.012 0.014
MOLE PERCENT + 100

NITROBENZENE / BENZENE 700MHZ 60C

2.475
2.450
2.425
2.400
2.375
2.350
2.325
2.300
2.275
2.250
2.225
2.200
0.000

ε'

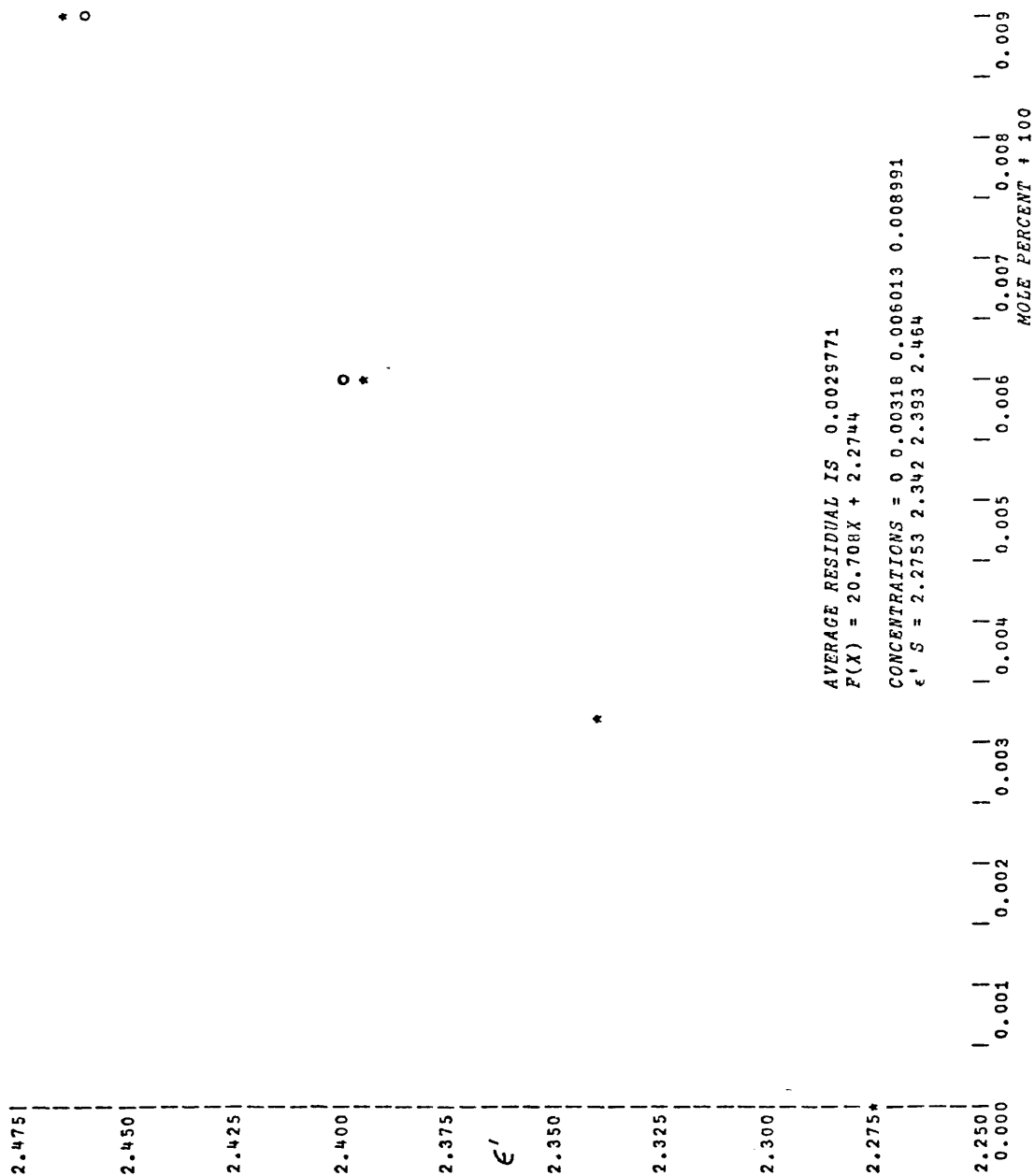
AVERAGE RESIDUAL IS 0.00059269
F(X) = 19.51X + 2.205
CONCENTRATIONS = 0 0.00466 0.009173 0.013811
ε' S = 2.2042 2.297 2.384 2.474

0.002 0.004 0.006 0.008 0.010 0.012 0.014
HOLE PERCENT + 100

O-NITROBIPHENYL / BENZENE

500MHZ

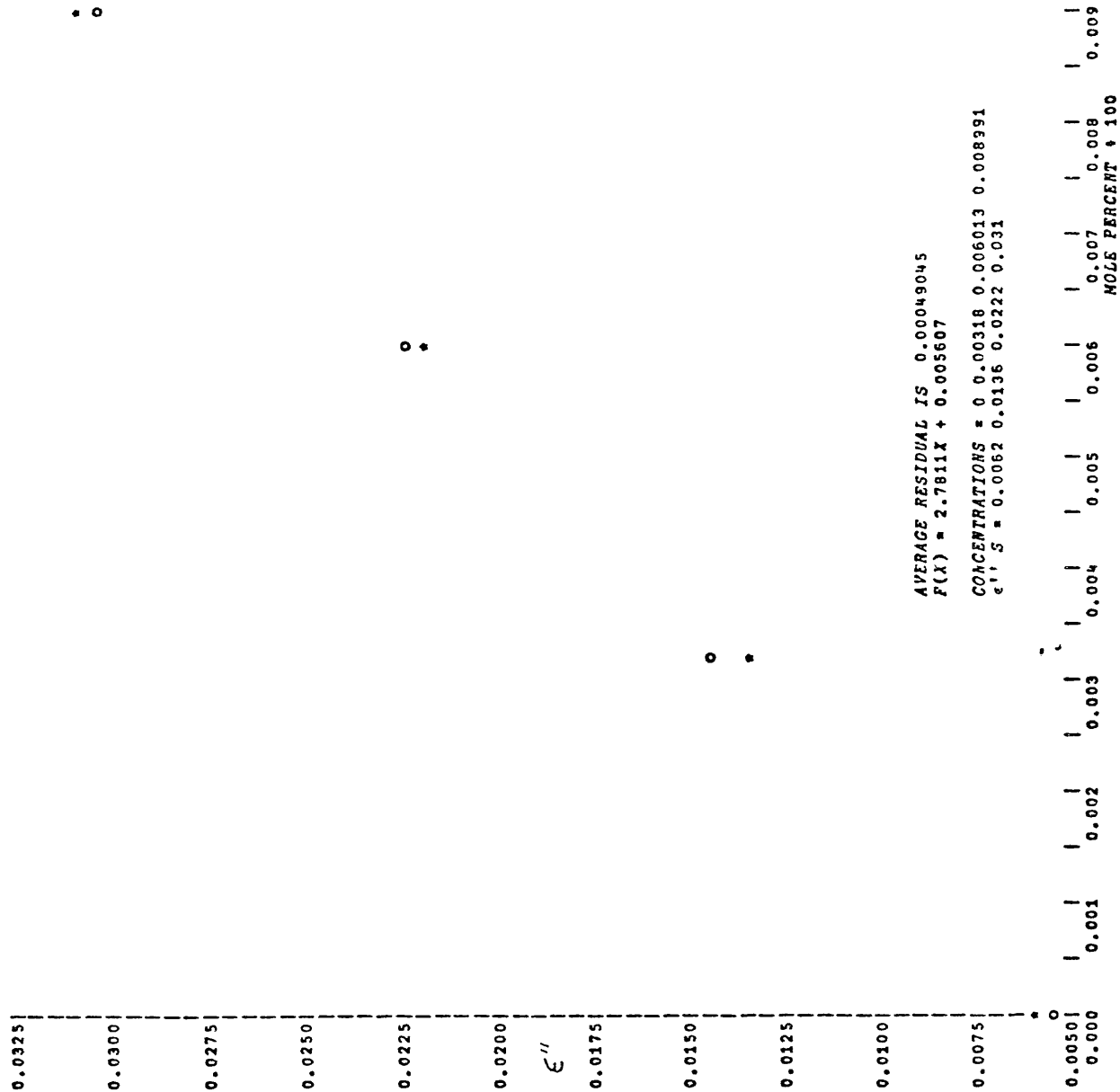
25C



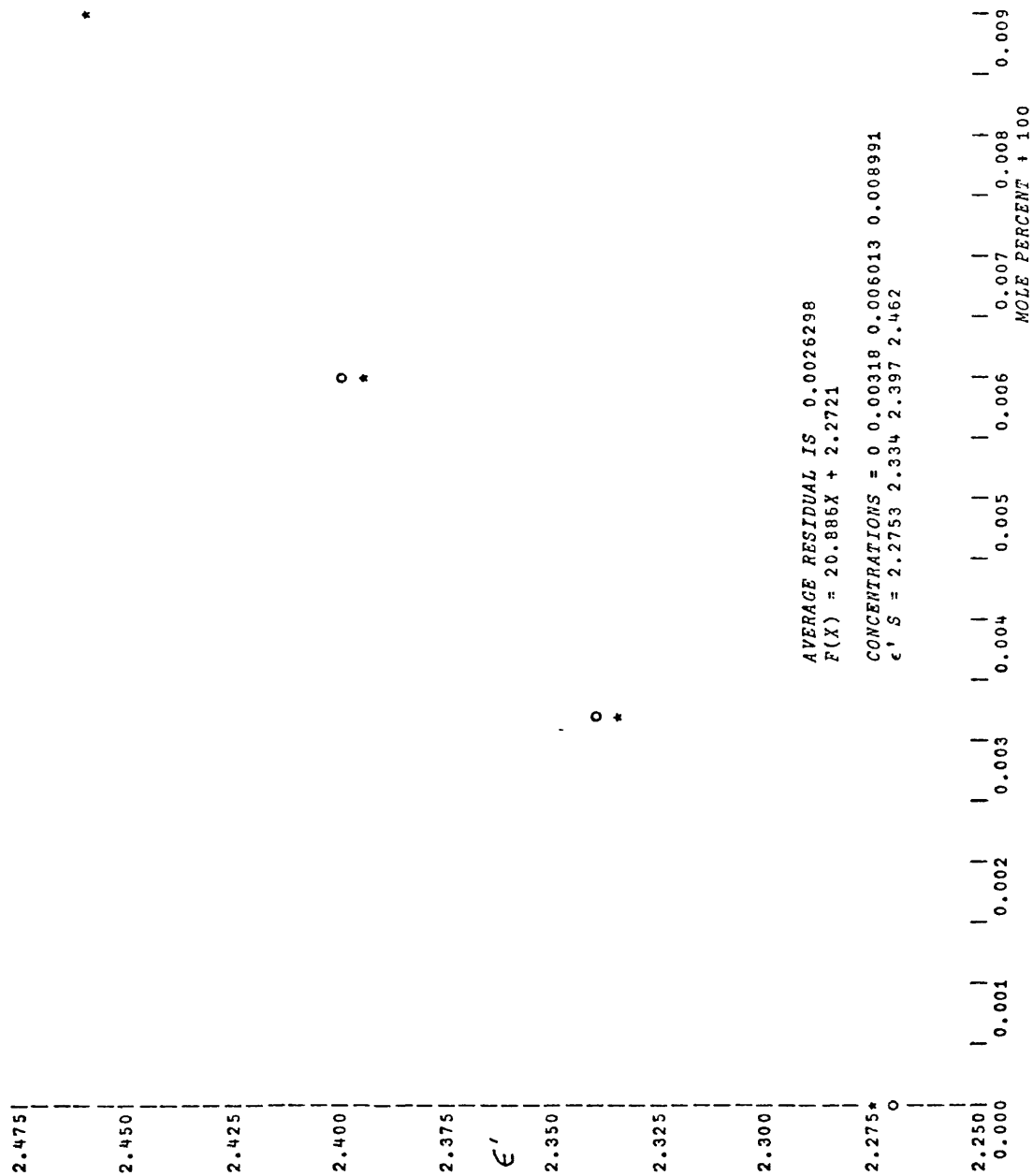
o-NITROBIPHENYL / BENZENE

500MHZ

25C



O-NITROBIPHENYL / BENZENE 700MHZ 25C



O-NITROBIPHENYL / BENZENE

700MHZ

25C

0.045
0.040
0.035
0.030
 ϵ''
0.025
0.020
0.015
0
0.010
0.000

*

*

o *

AVERAGE RESIDUAL IS 0.00069092
 $F(X) = 3.7806X + 0.010763$

CONCENTRATIONS = 0 0.00318 0.006013 0.008991
 ϵ'' S = 0.0115 0.0219 0.033 0.0454

* o

0.001 0.002 0.003 0.004 0.005 0.006 0.007 0.008 0.009
MOLE PERCENT + 100

O-NITROBIPHENYL / BENZENE

500MHZ

60C

2.350 |
 2.325 |
 2.300 |
 2.275 |
 2.250 |
 2.225 |
 2.200 |
 0.000 |

ε'

*

*
 o

AVERAGE RESIDUAL IS 0.002073
 F(X) = 15.997X + 2.2056

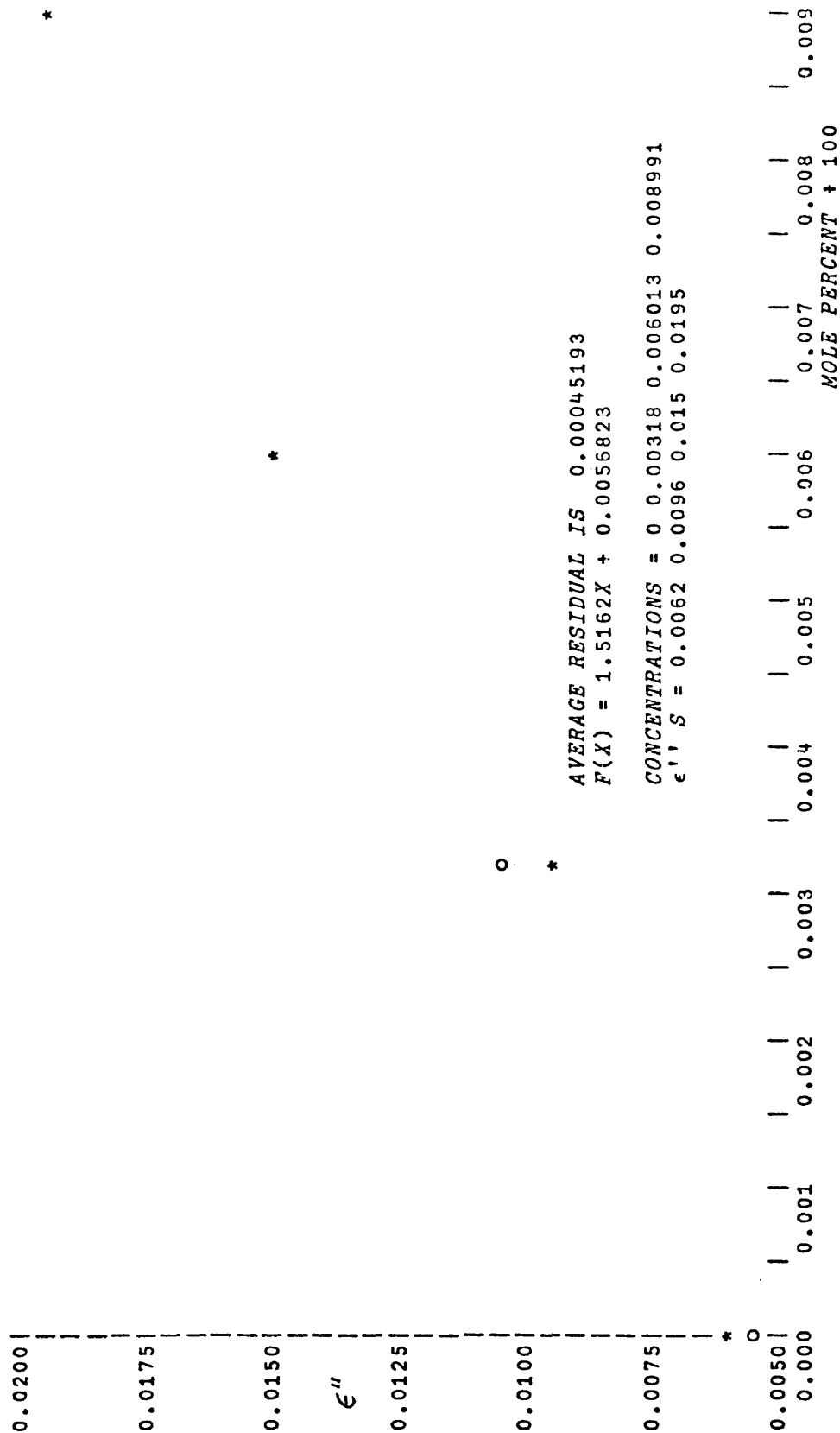
CONCENTRATIONS = 0 0.00318 0.006013 0.008991
 ε' S = 2.2042 2.26 2.299 2.35

MOLE PERCENT + 100	0.000	0.001	0.002	0.003	0.004	0.005	0.006	0.007	0.008	0.009

O-NITROBIPHENYL / BENZENE

500MHZ

60C



O-NITROBIPHENYL / BENZENE 700MHZ 60C

0.0300|
 |
 |
 0.0275|
 |
 |
 0.0250|
 |
 |
 0.0225|
 |
 |
 €"
 |
 0.0200|
 |
 |
 0.0175|
 |
 |
 0.0150|
 |
 |
 0.0125|
 |
 |
 *
 0
 |
 0.0100|
 0.000

* O

O *

*

AVERAGE RESIDUAL IS 0.00049208
 $F(X) = 1.8234X + 0.010861$

CONCENTRATIONS = 0 0.00318 0.006013 0.008991
 $\epsilon'' S = 0.0113 0.0163 0.0212 0.0278$

0.001	0.002	0.003	0.004	0.005	0.006	0.007	0.008	0.009
MOLE PERCENT ÷ 100								

p-NITROBIPHENYL / BENZENE

500MR2

25C

O *

2.37

2.36

2.35

2.34

2.33

ϵ'

2.32

2.31

2.30

,

2.29

2.28

*

2.27

0.0000

* O

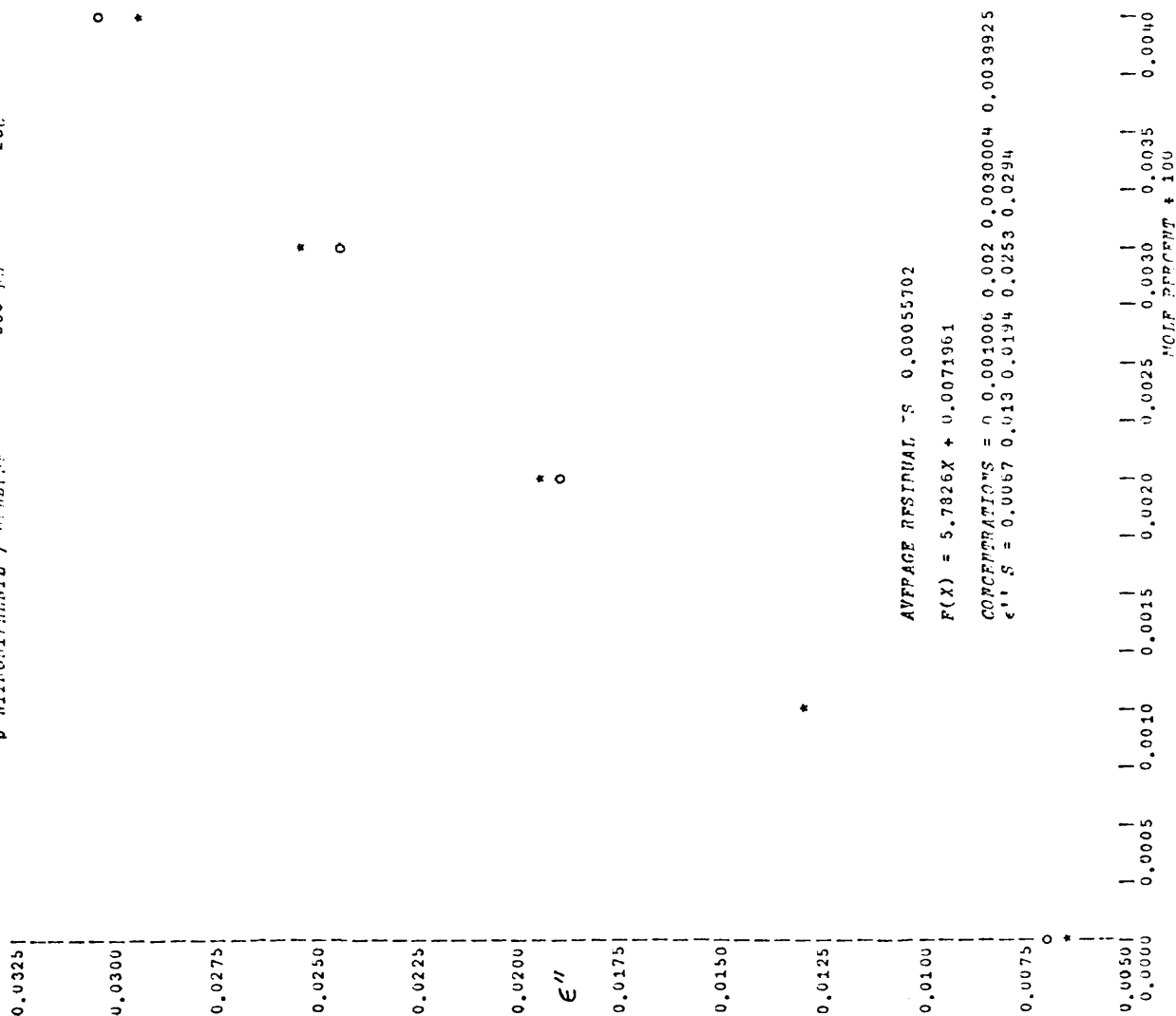
O *

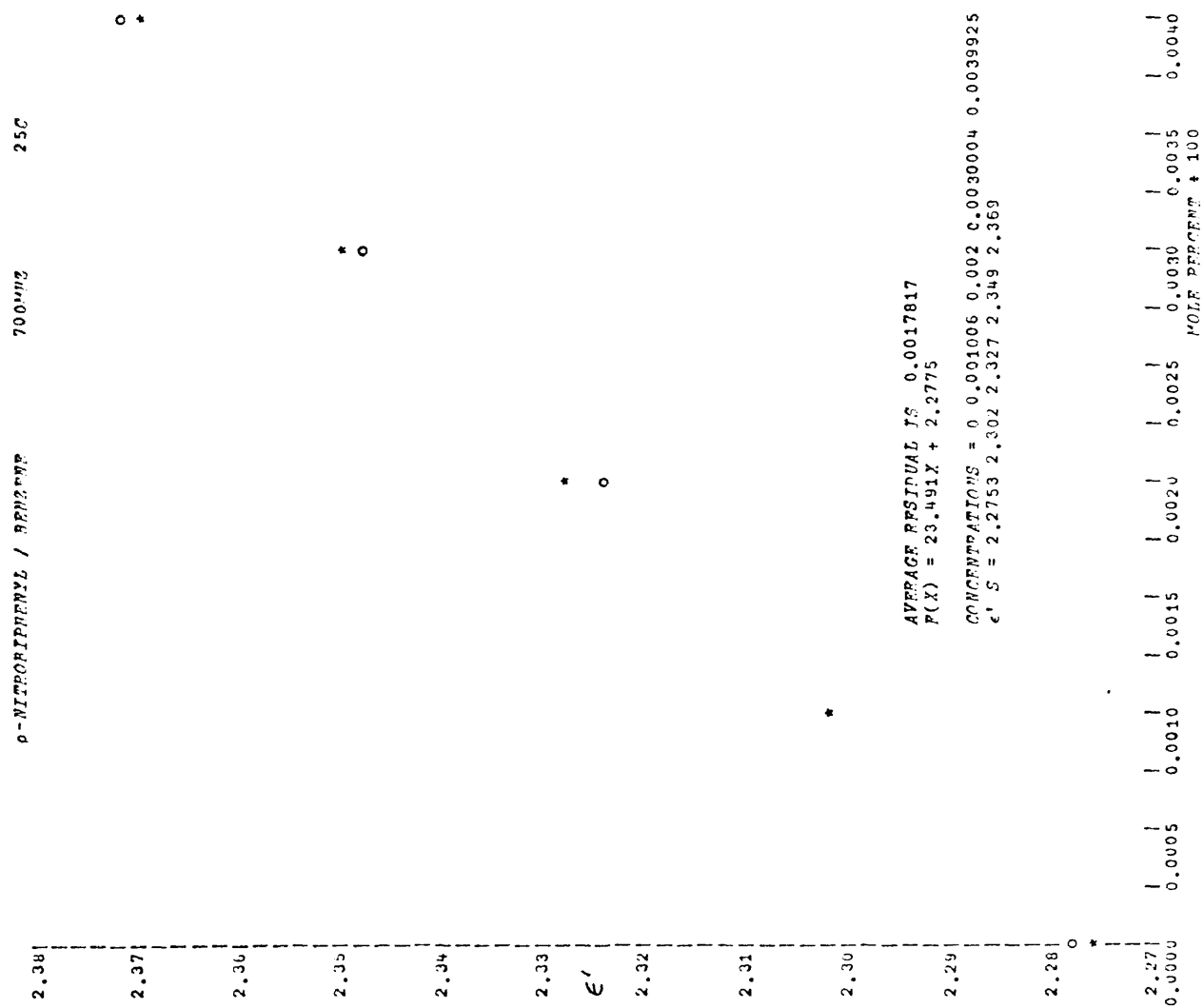
AVERAGE RESIDUAL IS 0.0017937
 $F(X) = 23.539X + 2.2753$

CONCENTRATIONS = 0 0.001006 0.002 0.0030004 0.0039925
 ϵ' S = 2.2733 2.297 2.324 2.349 2.367

	0.0005	0.0010	0.0015	0.0020	0.0025	0.0030	0.0035	0.0040

MOLE PERCENT * 100





p-NITROBIPHENYL / BENZENE

700MHZ

25C

o *

0.045 |
 0.040 |
 0.035 |
 0.030 |
 ε" |
 0.025 |
 0.020 |
 0.015 |
 0.010 |
 0.000 |

*

* o

*

AVERAGE RESIDUAL IS 0.00082527
 F(X) = 8.0475X + 0.011567

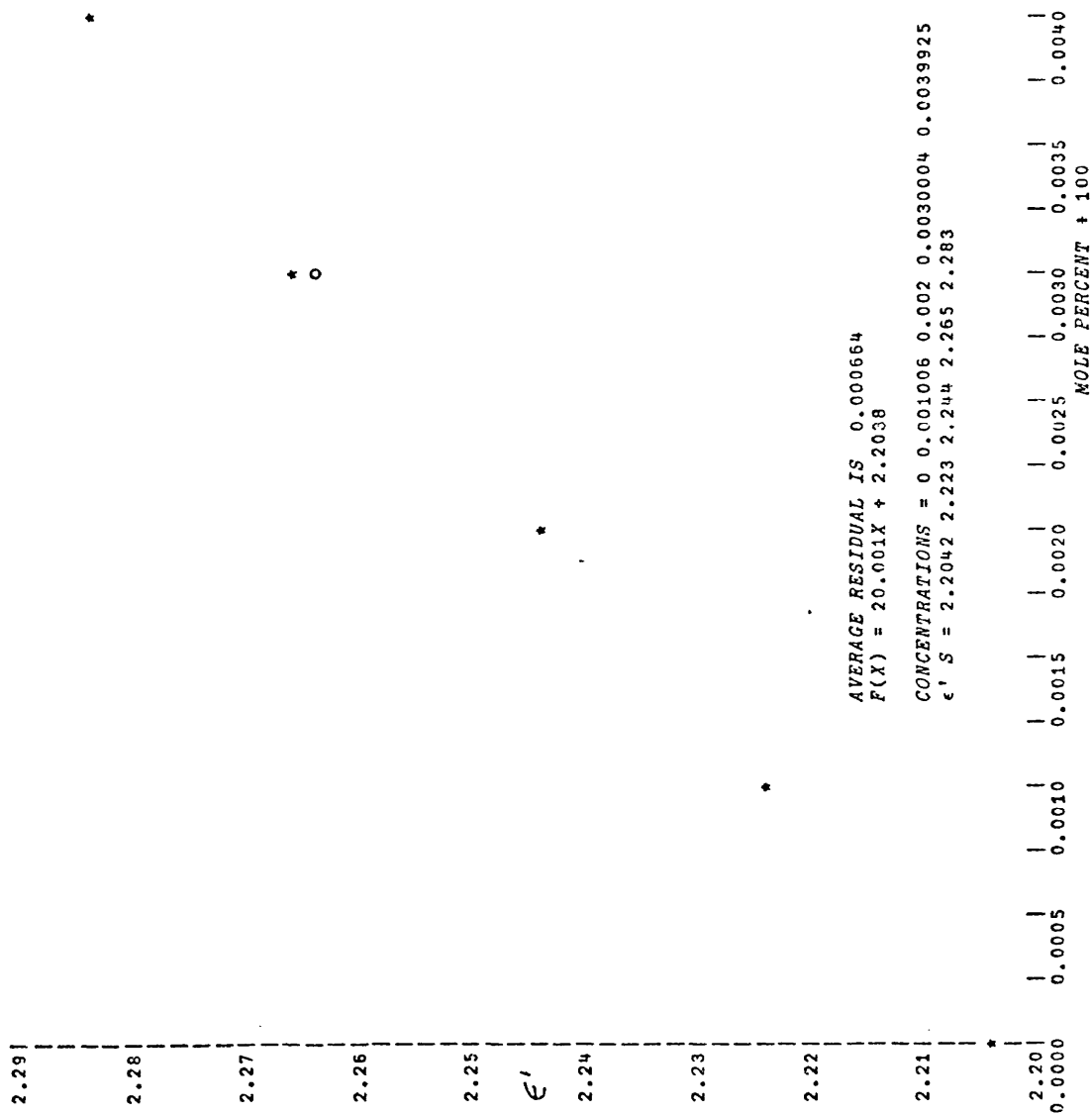
CONCENTRATIONS = 0 0.001006 0.002 0.0030004 0.0039925
 ε'' S = 0.0106 0.0198 0.0292 0.0361 0.0426

0.0005 | 0.0010 | 0.0015 | 0.0020 | 0.0025 | 0.0030 | 0.0035 | 0.0040 |
 MOLE PERCENT * 100

p-NITROBIPHENYL / BENZENE

500MHZ

60C



p-NITROBIPHENYL / BENZENE

500MHZ

60C

0.0250

0.0225

0.0200

0.0175

ϵ''

0.0150

0.0125

0.0100

0.0075

0.0050

0.0000

*

O

O

*

*

*

O

AVERAGE RESIDUAL IS 0.00056651
 $F(X) = 4.1081X + 0.0062247$

CONCENTRATIONS = 0 0.001006 0.002 0.0030004 0.0039925
 ϵ'' S = 0.0062 0.0109 0.0143 0.0173 0.0235

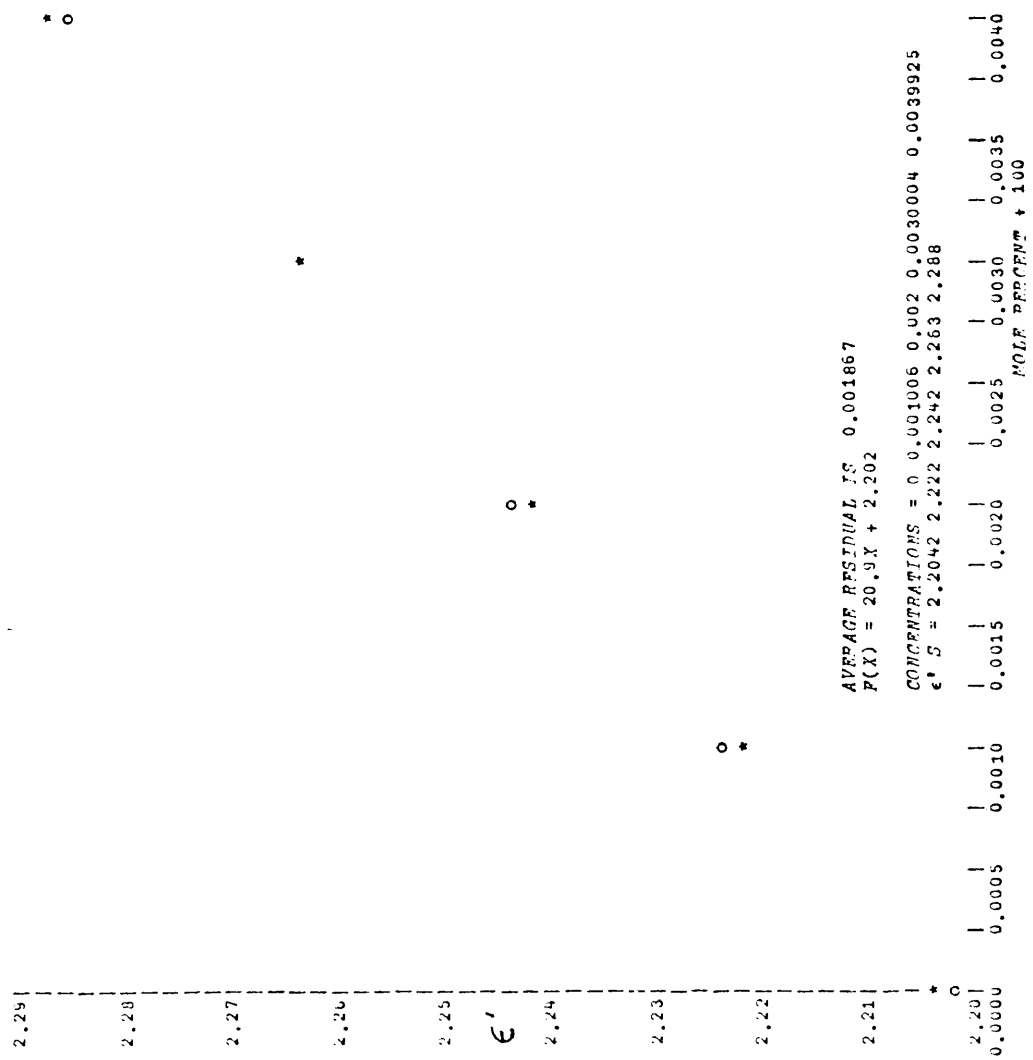
0.0005	0.0010	0.0015	0.0020	0.0025	0.0030	0.0035	0.0040

HOLE PERCENT * 100

p-NITROBIPHENYL / BENZENE

700MHz

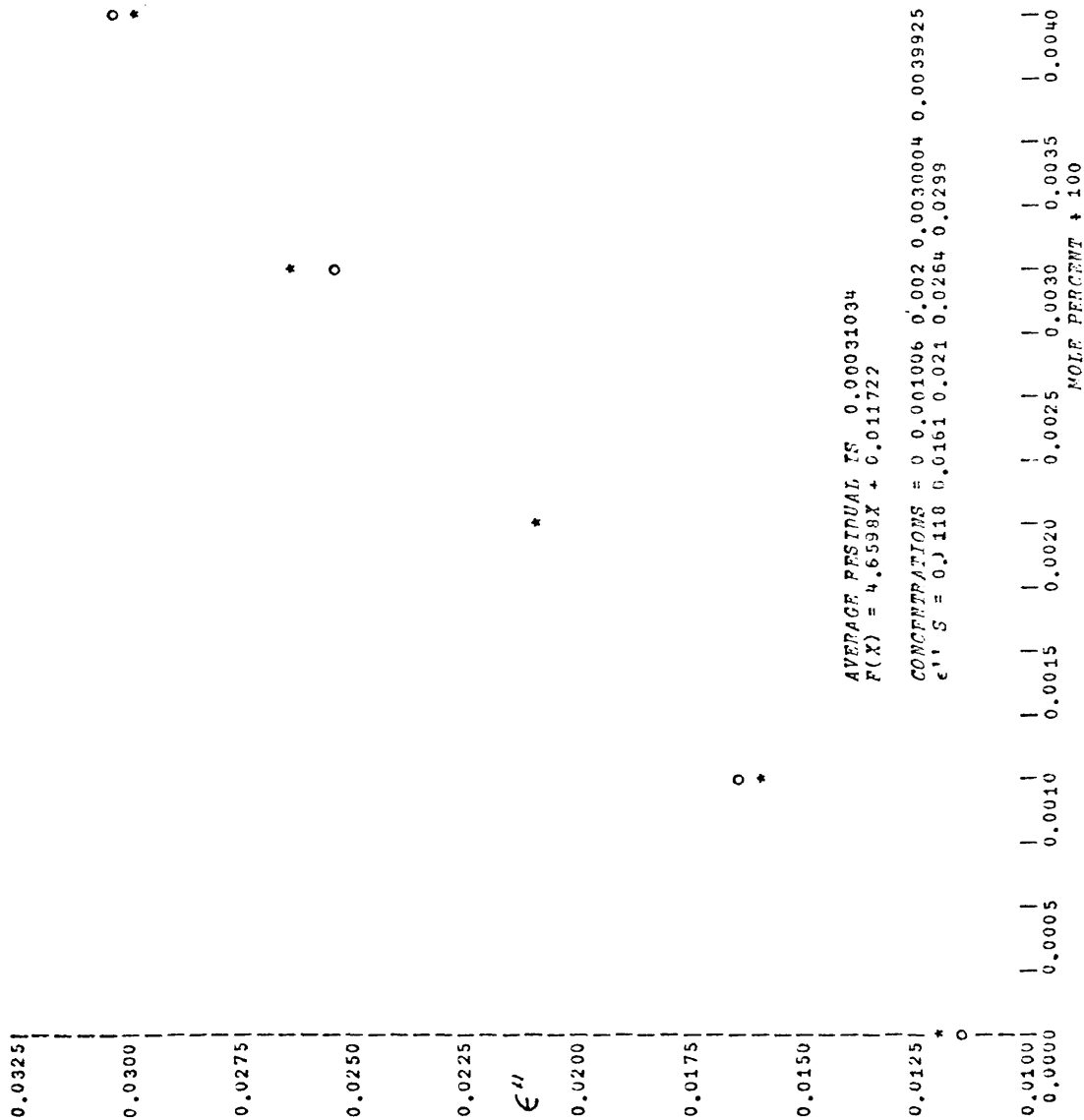
60C



p-NITROBIPHENYL / BENZENE

700MHZ

60C



2,2'-DINITROBIPHENYL / BENZENE

500MHz

25C

o *

2.450 |
|
|
2.425 |
|
|
2.400 |
|
|
2.375 |
|
|
2.350 |
|
|
2.325 |
|
|
2.300 |
|
|
2.275* |
0.0000 |

ϵ'

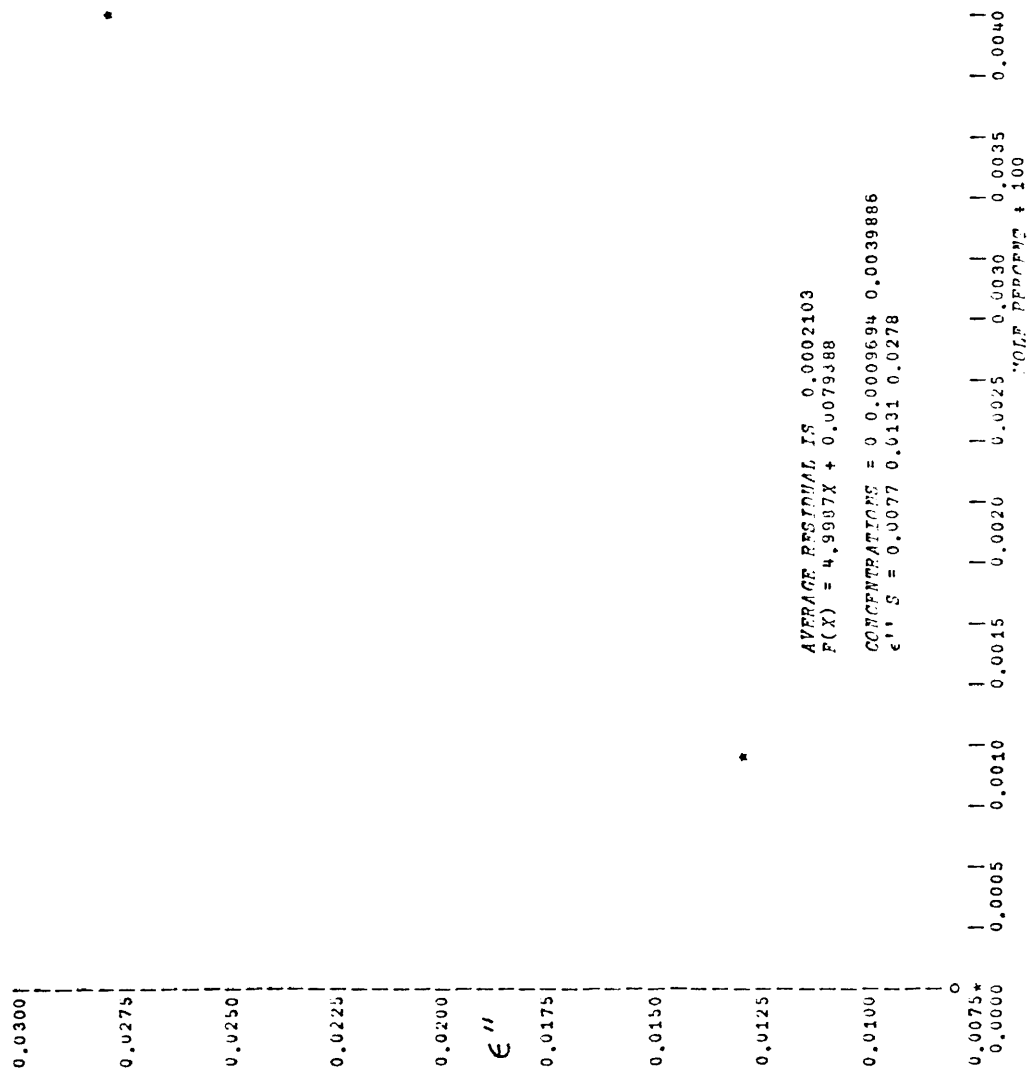
*

*
o

AVERAGE RESIDUAL IS 0.0020127,
 $P(X) = 40.269X + 2.2782$

CONCENTRATIONS = 0 0.0009694 0.001998 0.0039886
 $\epsilon' S = 2.276 \ 2.318 \ 2.362 \ 2.437$
| | | | | | | | | | | | | | | |
0.0015 0.0020 0.0025 0.0030 0.0035 0.0040
MOLT PERCENT + 100

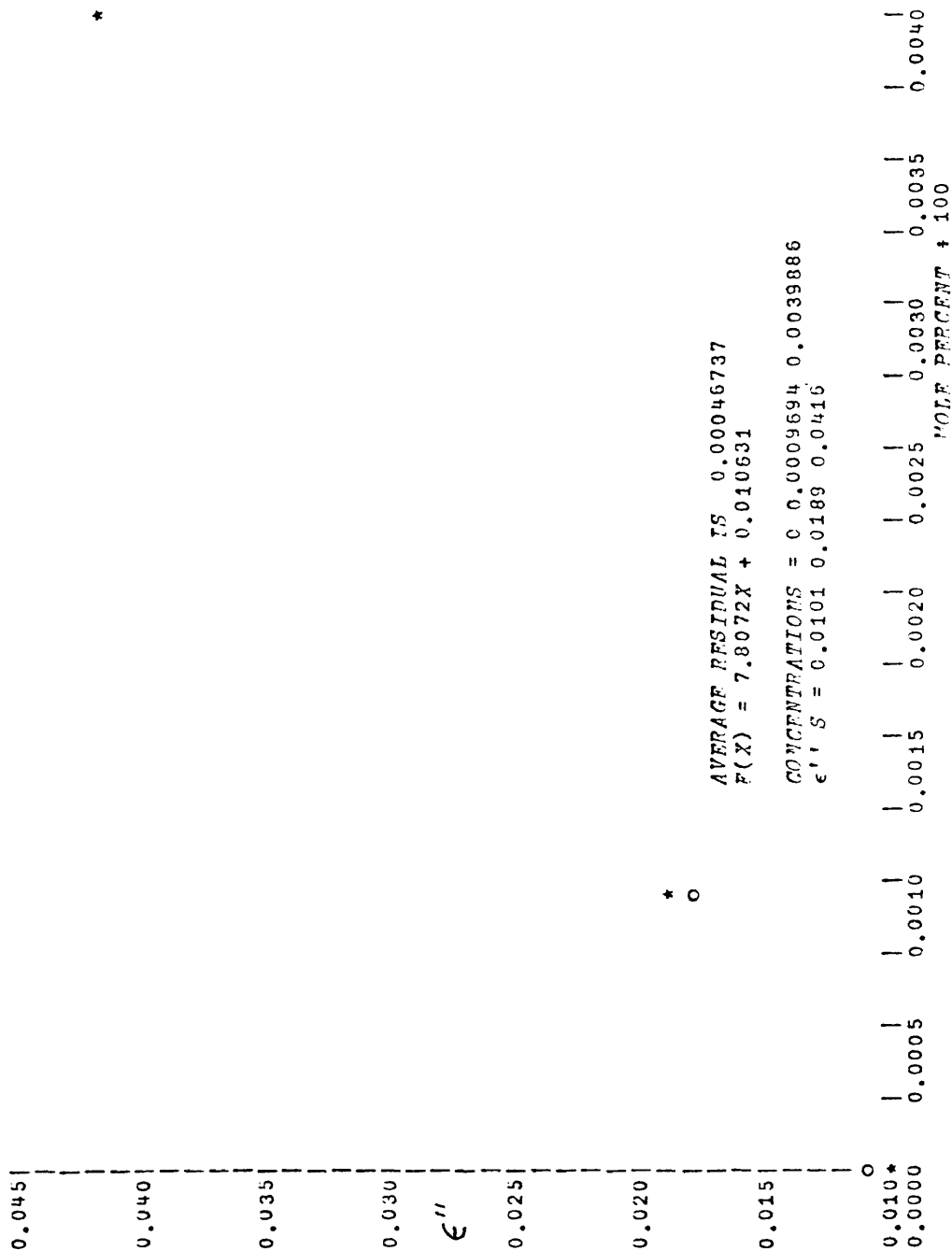
2,2'-DINITROBIPHENYL / BENZENE 500MHZ 25C



2,2'-DINITROBIPHENYL / BENZENE

700MHz

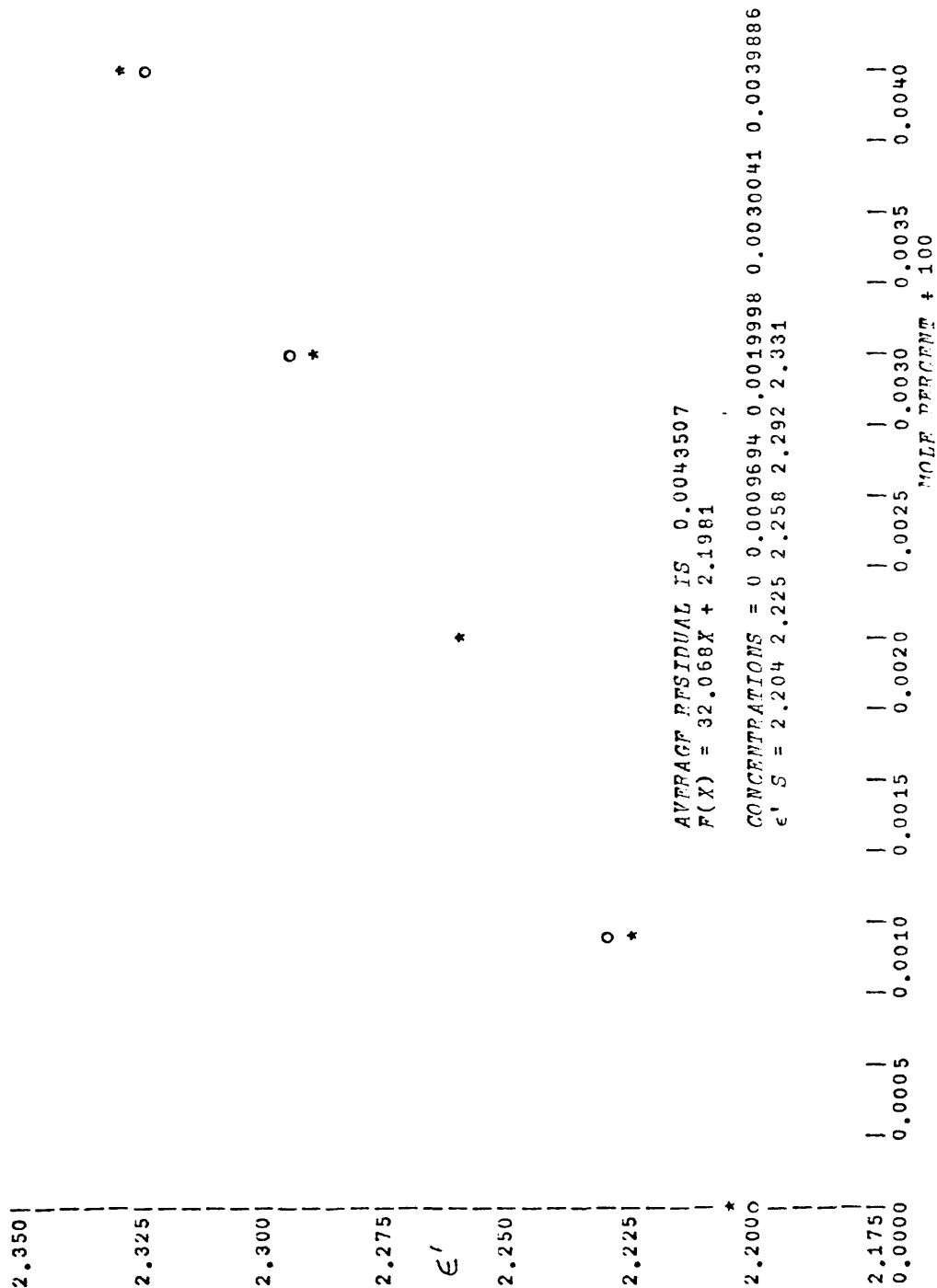
25C



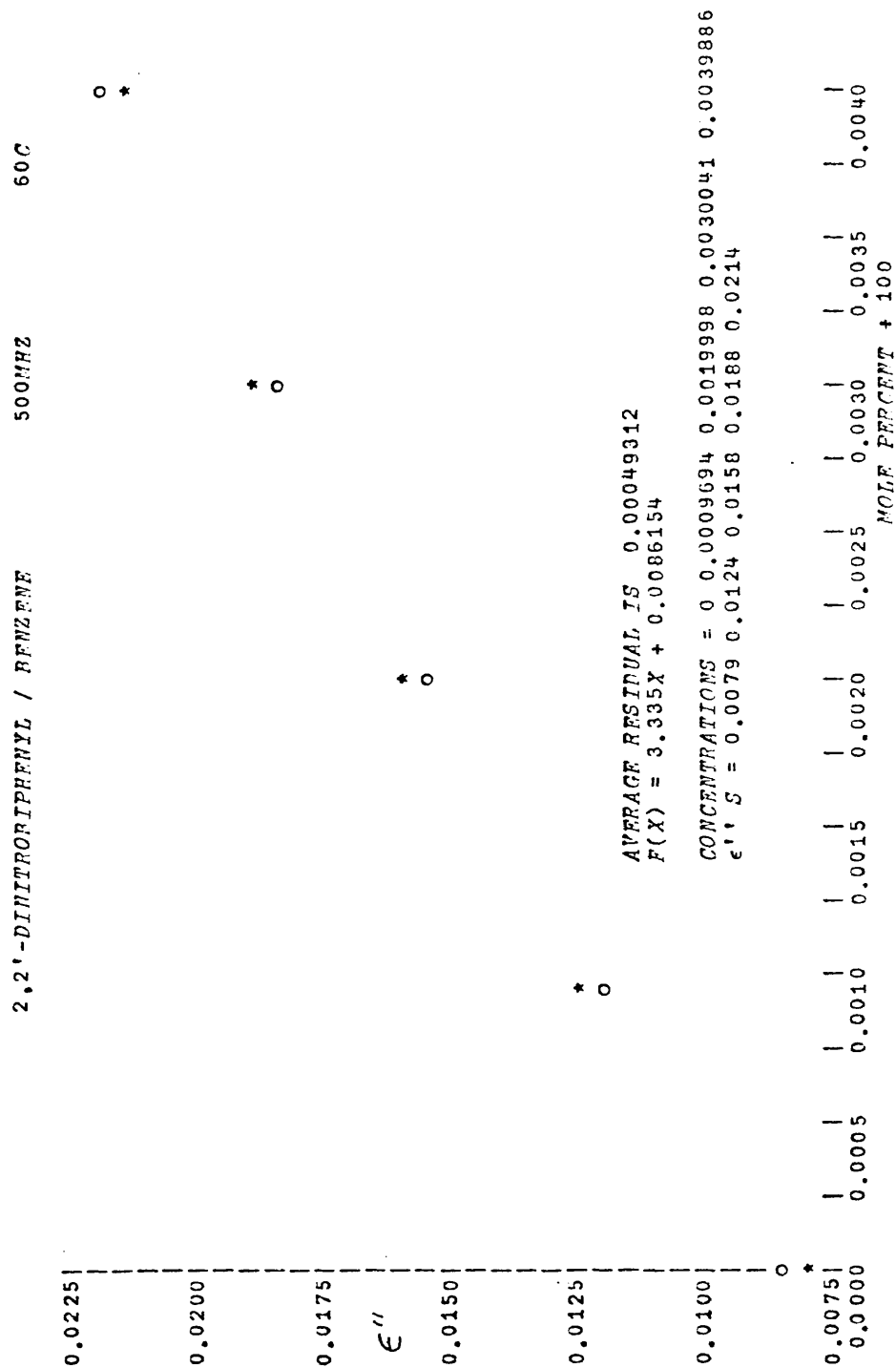
2,2'-DINITROBIPHENYL / BENZENE

500482

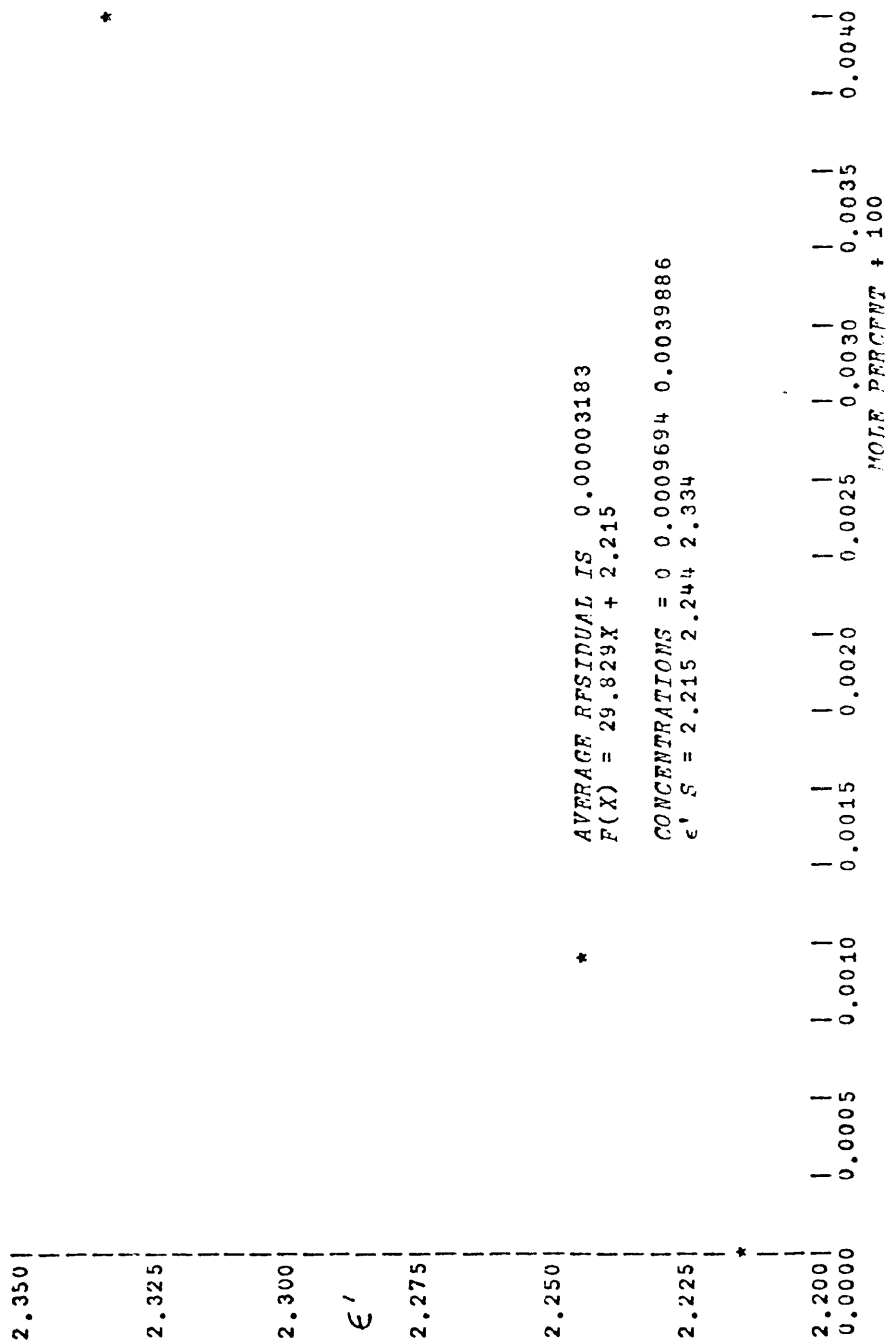
209



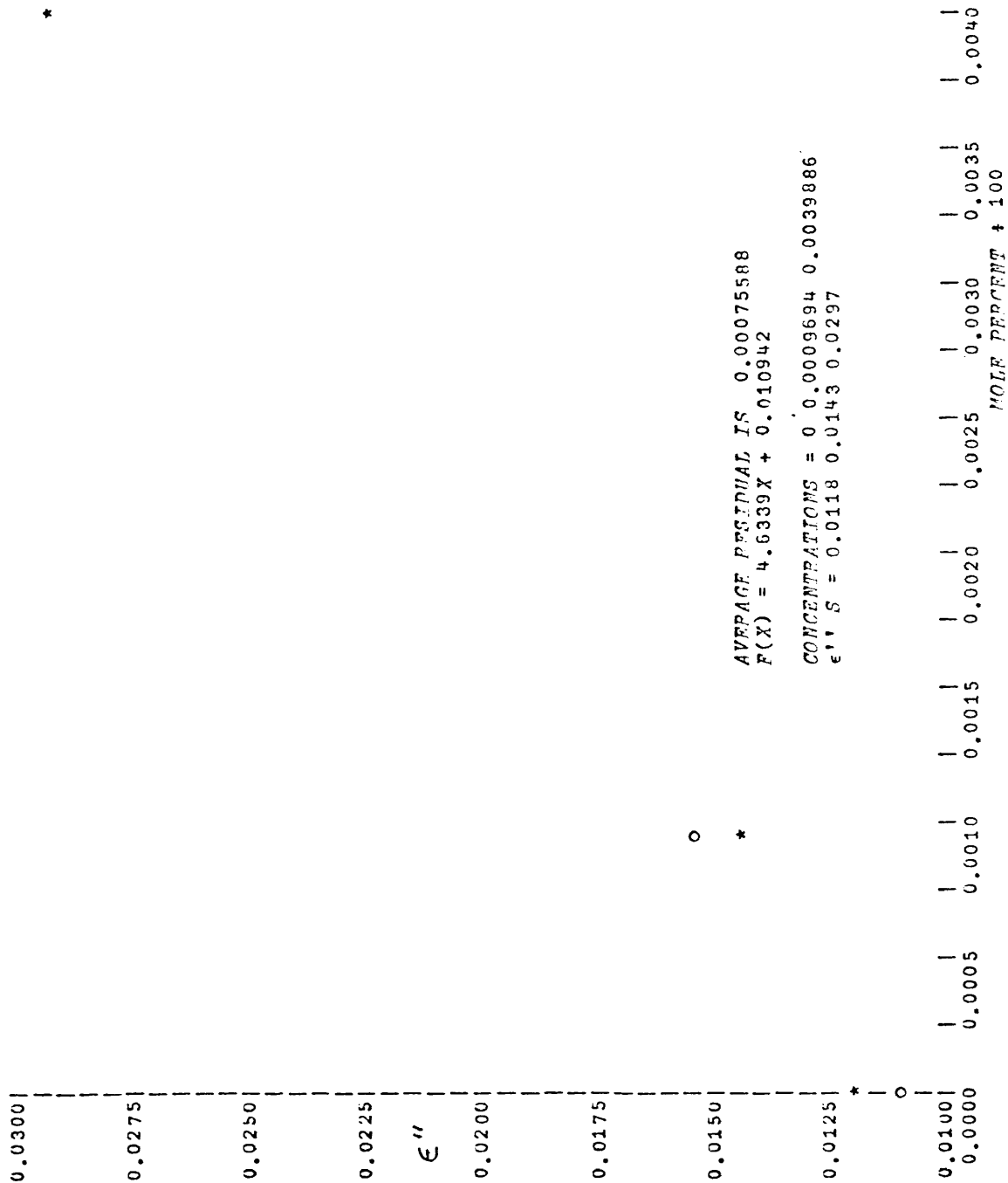
244.



2,2'-DINITROTRIPHENYL / BENZENE 700MPZ 60C



2,2'-DINITROBIPHENYL / REFERENCE 700MHZ 60C



APPENDIX VI

RELAXATION TIMES AND SMYTH PARAMETERS FOR UHF DATA

TABLE OF CONTENTS

	Page
Nitrobenzene at 25°C	150
Nitrobenzene at 60°C	151
o-Nitrobiphenyl at 25°C.	152
o-Nitrobiphenyl at 60°C.	153
p-Nitrobiphenyl at 25°C.	154
p-Nitrobiphenyl at 60°C.	155
2,2'-Dinitrobiphenyl at 25°C	156
2,2'-Dinitrobiphenyl at 60°C	157

Tau (picoseconds)	Sum of the Squares of the Residuals
9.65	4.5268
9.66	4.5185
9.67	4.5112
9.68	4.5047
9.69	4.4992
9.70	4.4945
9.71	4.4908
9.72	4.4880
9.73	4.4860
9.74	4.4850
9.75	4.4849
9.76	4.4856

$$a_o = 22.183 \qquad a_{\infty} = 0.19032$$

Low Loss Permittivity Slopes for Nitrobenzene in Benzene at 25 C

<u>Freq(MHz)</u>	<u>α' (Exp)</u>	<u>α' (Cal)</u>	<u>$\Delta\alpha'$</u>	<u>α'' (Exp)</u>	<u>α'' (Cal)</u>	<u>$\Delta\alpha''$</u>
500	22.70	22.16	.54	1.26	.67	.59
700	23.42	22.14	1.28	1.83	.94	.89
10260	16.39	15.95	.45	10.49	9.91	.58
10480	15.90	15.75	.15	9.52	10.00	-.48
11810	13.99	14.62	-.63	10.53	10.45	.08
12190	14.71	14.30	.41	10.82	10.55	.28

Tau (picoseconds)	Sum of the Squares of the Residuals
6.65	11.7437
6.66	11.7349
6.67	11.7272
6.68	11.7206
6.69	11.7150
6.70	11.7105
6.71	11.7071
6.72	11.7047
6.73	11.7034
6.74	11.7031
6.75	11.7039

$$a_o = 19.254 \qquad a_\infty = 0.36046$$

Low Loss Permittivity Slopes for Nitrobenzene in Benzene at 60 C

<u>Freq(MHz)</u>	<u>a' (Exp)</u>	<u>a' (Cal)</u>	<u>Δa'</u>	<u>a'' (Exp)</u>	<u>a'' (Cal)</u>	<u>Δa''</u>
500	19.10	19.25	-.15	.75	.40	.35
700	19.51	19.24	.27	1.07	.56	.51
10260	17.91	16.25	1.66	8.47	6.91	1.55
10480	18.07	16.14	1.93	7.93	7.01	.92
11810	14.89	15.46	-.58	8.59	9.57	1.02
12190	15.57	15.27	.30	7.64	7.71	-.06

Tau (picoseconds)	Sum of the Squares of the Residuals
30.30	7.1412
30.31	7.1410
30.32	7.1409
30.33	7.1409
30.34	7.1409
<u>30.35</u>	<u>7.1409</u>

$$a_o = 20.268 \qquad a_\infty = 0.66204$$

Low Loss Permittivity Slopes for o-Nitrobiphenyl in Benzene at 25 C

<u>Freq(MHz)</u>	<u>α' (Exp)</u>	<u>α' (Cal)</u>	<u>$\Delta\alpha'$</u>	<u>α'' (Exp)</u>	<u>α'' (Cal)</u>	<u>$\Delta\alpha''$</u>
500	20.71	20.45	.26	2.78	1.89	.89
700	20.89	20.28	.61	3.78	2.62	1.16
10260	5.43	4.80	.63	7.32	8.09	-.77
10480	4.98	4.66	.32	7.08	7.99	-.91
11810	4.70	3.95	.75	6.71	7.41	-.70
12190	5.02	3.78	1.24	7.02	7.25	-.23

Tau (picoseconds)	Sum of the Squares of the Residuals
18.15	6.2050
18.16	6.2037
18.17	6.2026
18.18	6.2017
18.19	6.2009
18.20	6.2002
18.21	6.1997
18.22	6.1994
18.23	6.1991
<u>18.24</u>	<u>6.1991</u>
18.25	6.1991

$$a_o = 17.069 \qquad a_{\infty} = 0.86045$$

Low Loss Permittivity Slopes for o-Nitrobiphenyl in Benzene at 60 C

<u>Freq(MHz)</u>	<u>α' (Exp)</u>	<u>α' (Cal)</u>	<u>$\Delta \alpha'$</u>	<u>α'' (Exp)</u>	<u>α'' (Cal)</u>	<u>$\Delta \alpha''$</u>
500	16.00	17.02	-1.02	1.52	.93	.59
700	15.31	16.97	-1.66	1.82	1.29	.53
10260	7.23	7.66	-.43	7.82	8.00	-.18
10480	8.22	7.49	.73	7.55	7.97	-.42
11810	7.23	6.58	.65	7.50	7.75	-.24
12190	5.75	6.35	-.59	7.84	7.67	.17
						153.

Tau (picoseconds)	Sum of the Squares of the Residuals
62.95	29.3893
62.96	29.3892
62.97	29.3892
62.98	29.3892
62.99	29.3891
63.00	29.3891
63.01	29.3891
63.02	29.3891
63.03	29.3891

$$a_o = 25.763 \qquad a_\infty = 0.50822$$

Low Loss Permittivity Slopes for ρ -Nitrobiphenyl in Benzene at 25 C

<u>Freq(MHz)</u>	<u>α' (Exp)</u>	<u>α' (Cal)</u>	<u>$\Delta\alpha'$</u>	<u>α'' (Exp)</u>	<u>α'' (Cal)</u>	<u>$\Delta\alpha''$</u>
500	23.59	24.81	-1.22	5.78	4.81	.97
700	23.49	23.96	-.47	8.05	6.50	1.55
10260	2.54	1.95	.59	5.26	5.86	-.60
10480	2.91	1.89	1.02	5.36	5.75	-.40
11810	4.43	1.61	2.82	5.56	5.16	.40
12190	5.30	1.55	3.75	5.52	5.02	.51

Tau (picoseconds)	Sum of the Squares of the Residuals
41.95	20.6621
41.96	20.6620
41.97	20.6619
41.98	20.6618
41.99	20.6617
42.00	20.6616
42.01	20.6616
42.02	20.6616
42.03	20.6616
42.04	20.6616

$$a_o = 20.465 \qquad a_{\infty} = 2.1091$$

Low Loss Permittivity Slopes for ρ -Nitrobiphenyl in Benzene at 60 C

<u>Freq(MHz)</u>	<u>α' (Exp)</u>	<u>α' (Cal)</u>	<u>$\Delta\alpha'$</u>	<u>α'' (Exp)</u>	<u>α'' (Cal)</u>	<u>$\Delta\alpha''$</u>
500	20.00	20.15	-.15	4.11	2.38	1.73
700	20.90	19.86	1.04	4.66	3.28	1.38
10260	3.38	4.31	-.93	6.90	5.96	.94
10480	4.72	4.23	.49	6.56	5.87	.70
11810	1.62	3.82	-2.20	7.18	5.34	1.85
12190	2.12	3.72	-1.61	6.37	5.20	1.17

Tau (picoseconds)	Sum of the Squares of the Residuals
37.80	48.0641
37.81	48.0637
37.82	48.0633
37.83	48.0630
37.84	48.0628
37.85	48.0626
37.86	48.0624
37.87	48.0624
37.88	48.0624
37.89	48.0624

$$a_o = 38.3 \quad a_\infty = 0.87$$

Low Loss Permittivity Slopes for 2,2'-Dinitrobiphenyl in Benzene at 25 C

<u>Freq(MHz)</u>	<u>α' (Exp)</u>	<u>α' (Cal)</u>	<u>$\Delta\alpha'$</u>	<u>α'' (Exp)</u>	<u>α'' (Cal)</u>	<u>$\Delta\alpha''$</u>
500	40.27	37.78	2.49	5.00	4.39	.61
700	37.86	37.29	.57	7.81	6.06	1.74
10260	8.37	6.27	2.10	10.45	13.11	-2.66
10480	8.25	6.08	2.17	10.56	12.92	-2.35
12190	8.75	4.87	3.88	10.38	11.52	-1.14

Tau (picoseconds)	Sum of the Squares of the Residuals
24.99	21.0040
25.00	21.0033
25.01	21.0026
25.02	21.0021
25.03	21.0016
25.04	21.0013
25.05	21.0011
25.06	21.0009
25.07	21.0009
25.08	21.0010

$$a_o = 31.83 \quad a_\infty = 1.02$$

Low Loss Permittivity Slopes for 2,2'-Dinitrobiphenyl in Benzene at 60 C

<u>Freq(MHz)</u>	<u>α' (Exp)</u>	<u>α' (Cal)</u>	<u>$\Delta \alpha'$</u>	<u>α'' (Exp)</u>	<u>α'' (Cal)</u>	<u>$\Delta \alpha''$</u>
500	32.07	32.80	-.73	3.33	2.51	.83
700	29.83	32.62	-2.79	4.63	3.49	1.15
10260	11.71	9.85	1.86	11.83	14.32	-2.48
12190	8.46	7.82	.63	12.28	13.11	-.82

APPENDIX VII

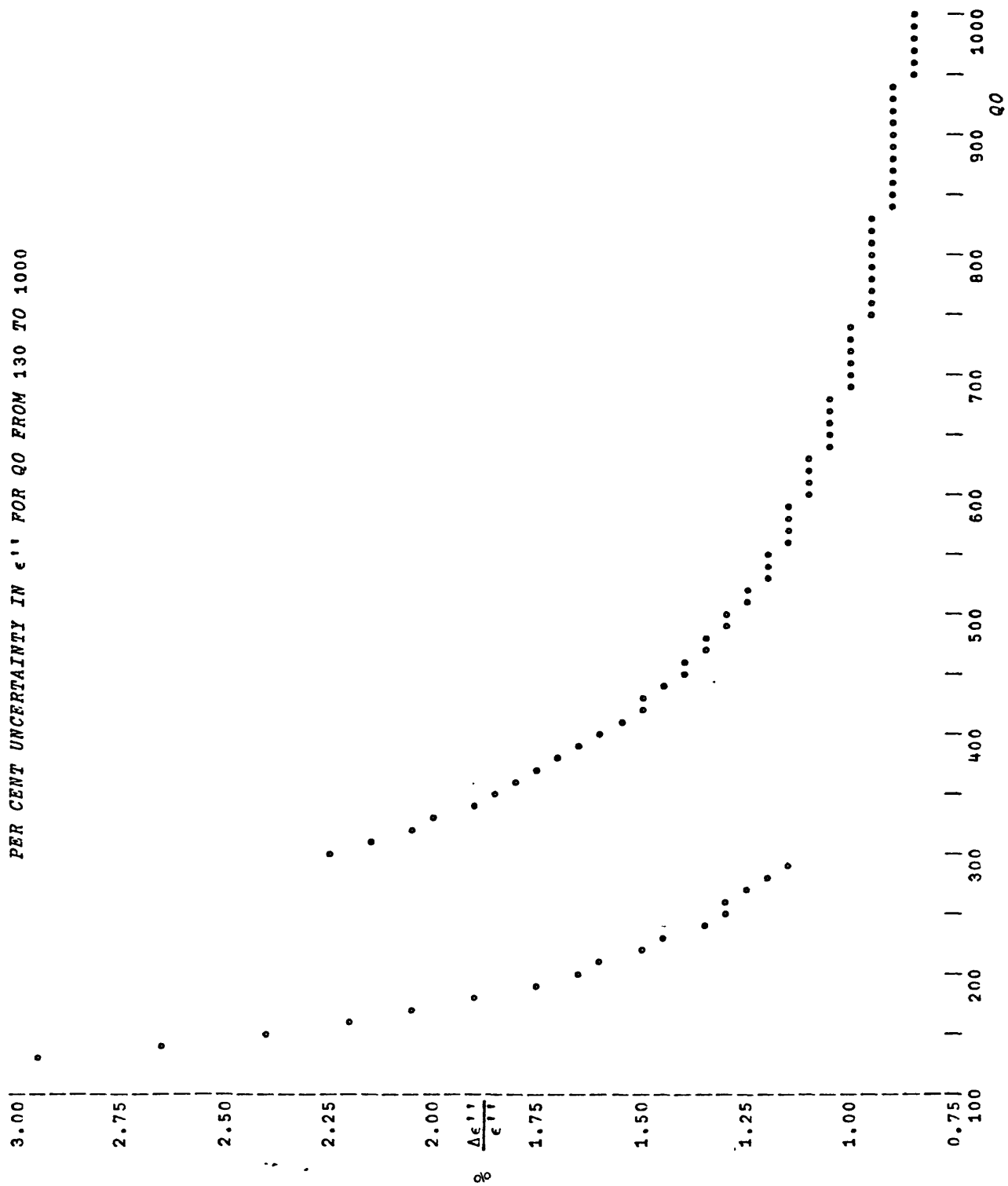
COMPUTER PROGRAM, TABLE OF VALUES AND
PLOT OF UNCERTAINTY IN ϵ " VS. Q

```

V QPRE;QO;QI;I;DEPP
DEPP←88ρ0
QO←88ρ(120+10×188)
I←0
QI←88ρ÷(0.0002363459008+(÷QO))
LOOP:I←I+1
→(QO[I]<300)/LOW,DQ←0.06
DQ←0.2
LOW:DEPP[I]←0.0066452+(((2×DQ*2)*0.5)÷(QO[I]-QI[I]))+(DQ÷QO[I])+(DQ÷QI[I])
→(I<88)/LOOP
QO←Q( 2 44 ρQO)
QI←Q( 2 44 ρQI)
DEPP←Q( 2 44 ρDEPP)×100
SHP← 8 2 10 0 10 1 14 2 10 0 10 1
PG1← 44 6 ρ(DEPP[;1]AND QO[;1]AND QI[;1]AND DEPP[;2]AND QO[;2]AND QI[;2])
'Δε''''/ε'''' QO QI Δε''''/ε'''' QI
''
SHP DFT PG1
V

```


$\Delta\epsilon''/\epsilon''$ (%)	<i>QO</i>	<i>QI</i>	$\Delta\epsilon''/\epsilon''$ (%)	<i>QO</i>	<i>QI</i>
2.95	130	126.1	1.16	570	502.3
2.64	140	135.5	1.14	580	510.1
2.40	150	144.9	1.13	590	517.8
2.20	160	154.2	1.12	600	525.5
2.03	170	163.4	1.10	610	533.1
1.89	180	172.7	1.09	620	540.8
1.77	190	181.8	1.08	630	548.4
1.67	200	191.0	1.07	640	555.9
1.58	210	200.1	1.06	650	563.4
1.50	220	209.1	1.05	660	570.9
1.43	230	218.1	1.04	670	578.4
1.37	240	227.1	1.03	680	585.8
1.32	250	236.1	1.02	690	593.3
1.28	260	244.9	1.01	700	600.6
1.23	270	253.8	1.00	710	608.0
1.20	280	262.6	.99	720	615.3
1.16	290	271.4	.99	730	622.6
2.23	300	280.1	.98	740	629.8
2.13	310	288.8	.97	750	637.1
2.05	320	297.5	.97	760	644.3
1.98	330	306.1	.96	770	651.4
1.91	340	314.7	.95	780	658.6
1.84	350	323.3	.95	790	665.7
1.78	360	331.8	.94	800	672.8
1.73	370	340.2	.94	810	679.8
1.68	380	348.7	.93	820	686.9
1.63	390	357.1	.93	830	693.9
1.59	400	365.5	.92	840	700.9
1.55	410	373.8	.92	850	707.8
1.51	420	382.1	.91	860	714.7
1.48	430	390.3	.91	870	721.6
1.44	440	398.6	.90	880	728.5
1.41	450	406.7	.90	890	735.3
1.38	460	414.9	.89	900	742.1
1.36	470	423.0	.89	910	748.9
1.33	480	431.1	.88	920	755.7
1.31	490	439.1	.88	930	762.4
1.28	500	447.2	.88	940	769.1
1.26	510	455.1	.87	950	775.8
1.24	520	463.1	.87	960	782.5
1.22	530	471.0	.87	970	789.1
1.21	540	478.9	.86	980	795.7
1.19	550	486.7	.86	990	802.3
1.17	560	494.5	.86	1000	808.8



APPENDIX VIII

COMPUTER PROGRAMS FOR Q-METER DATA CALCULATIONS

```

      ▽ QCALC
[1]  'RUN NUMBER? LAST RUN WAS ' , (▽(ρOTT[;1]))
[2]  LC←□
[3]  →(LC≤(ρOTT[;1]))/OLD
[4]  OTT←OTT,[1] 1 8 ρ0
[5]  OTQ←OTQ,[1] 1 8 ρ0
[6]  OTSP←OTSP,1ρ0
[7]  OTDC←OTDC,[1] 1 8 ρ0
[8]  REFSP←REFSP,[1] 1 4 8 ρ0
[9]  REFSPC←REFSPC,[1] 1 4 8 ρ0
[10] REFT←REFT,[1] 1 4 8 ρ0
[11] REFQ←REFQ,[1] 1 4 8 ρ0
[12] RDC←RDC,[1] 1 4 8 ρ0
[13] RDCC←RDCC,[1] 1 4 8 ρ0
[14] EPP←EPP,[1] 1 8 ρ0
[15] FRSAVE←FRSAVE,[1] 1 8 ρ0
[16] UNKINPUT
[17] OLD:FR←8ρFRSAVE[LC;]
[18] REFINPUT
[19] TEMP
[20] TOLS
[21] OTEP
[22] EDP
[23] 'CALC COMPLETE.'
      ▽
      ▽ UNKINPUT
[1]  NR←1
[2]  FRSAVE[LC;]←FR←□,0ρ□← 'FREQUENCIES?'
[3]  OTSP[LC;]←□,0ρ□← 'O-TERPHENYL SPACING?'
[4]  OTT[LC;]←□,0ρ□←(▽ 'UNK TEMPS, RUN ' ),▽LC
[5]  →((ρOTT[LC;])≠(ρFR))/4
[6]  OTQ[LC;]←□,0ρ□←(▽ 'UNK Q''S, RUN ' ),▽LC
[7]  →((ρOTQ[LC;])≠(ρFR))/6
      ▽
      ▽ REFINPUT;I
[1]  NREF←□,0ρ□← 'NUMBER OF REFERENCE LIQUIDS?'
[2]  →('N'=(1+□))/OLD,0ρ□← 'NEW REFERENCE DATA?'
[3]  I←0
[4]  'GIVE A COEFF''S, THEN α''S.'
[5]  REFLOOP:I←I+1
[6]  REFSP[LC;I;]←□,0ρ□←(▽ 'REF ' ),(▽I),(▽ ' SPACING' )
[7]  →((ρREFSP[LC;I;])≠(ρFR))/6
[8]  REFT[LC;I;]←□,0ρ□←(▽ 'REF ' ),(▽I),(▽ ' TEMP' )
[9]  →((ρREFT[LC;I;])≠(ρFR))/8
[10] REFQ[LC;I;]←□,0ρ□←(▽ 'REF ' ),(▽I),(▽ ' Q''S' )
[11] →((ρREFQ[LC;I;])≠(ρFR))/10
[12] →(I<NREF)/REFLOOP
[13] OLD: 'REFERENCE NUMBER FOR RUN ' ,▽LC
[14] OLDREF←□
[15] REFSP[LC;;]←REFSP[OLDREF;;]
[16] REFT[LC;;]←REFT[OLDREF;;]
[17] REFQ[LC;;]←REFQ[OLDREF;;]
      ▽

```

```

V TEMP;I;J
FR←8ρFRSAVE[LC;]
I←0
R←[],0ρ[]← 'WHICH LIQUID IS THE Q REFERENCE, 1, 2, 3, OR 4?'
→('N'=(1+[]))/LOOP1,0ρ[]← 'MORE INPUT FOR TEMP?'
→('Y'=(1+[]))/FLAG,0ρ[]← 'MIXTURE INCLUDED?'
FL←0
DCM←0ρ0
INP:DCA←[],0ρ[]← 'ε'S FOR LIQUIDS WITH A COEFF'S.'
DCAT←[],0ρ[]← 'TEMPS FOR DCA?'
DCAC←[],0ρ[]← 'COEFF'S FOR DCA?'
→((ρ(DCA,DCM))=NREF)/LOOP1
DCB←[],0ρ[]← 'ε'S FOR LIQUIDS WITH α'S.'
DCBT←[],0ρ[]← 'TEMPS FOR DCα?'
DCBC←[],0ρ[]← 'COEFF'S FOR DCα?'
LOOP1:I←I+1
→(FL=I)/MIXCALC
RDCC[LC;I;]←((A←(ρFR)ρDCAT[I])-OTT[LC;])×DCAC[I])+DCA[I]
RDC[LC;I;]←((A←(ρFR)ρDCAT[I])-REFT[LC;I;])×DCAC[I])+DCA[I]
CK:→(I<(ρ(DCA,DCM)))/LOOP1
→(I=NREF)/0
LOOP2:I←I+1
HALF←((C←(ρFR)ρDCBT[I]-(ρ(DCA,DCM)))]-REFT[LC;I;])×DCBC[I]-(ρ(DCA,DCM)))]
HALFC←((C←(ρFR)ρDCBT[I]-(ρ(DCA,DCM)))]-OTT[LC;])×DCBC[I]-(ρ(DCA,DCM)))]
RDC[LC;I;]←10*((10*(B←(ρFR)ρDCB[I]-(ρ(DCA,DCM)))]))+HALF)
RDCC[LC;I;]←10*((10*(B←(ρFR)ρDCB[I]-(ρ(DCA,DCM)))]))+HALFC)
→(I<(ρ(DCA,DCB,DCM)))/LOOP2
→0

```

```

[28] FLAG:FL←[],OP← 'WHICH LIQUID IS MIXTURE? 1, 2, 3, OR 4'
[29] →('N'=(1+[]))/INP,OP← 'NEW DATA FOR MIXTURE?'
[30] DCM←[],OP← 'MIXTURE ε'?'
[31] DCMT←[],OP← 'MIXTURE TEMP?'
[32] DCM1←[],OP← 'COMPONENT 1 ε'?'
[33] CT1←[],OP← 'COMPONENT 1 TEMP?'
[34] DCM2←[],OP← 'COMPONENT 2 ε'?'
[35] CT2←[],OP← 'COMPONENT 2 TEMP?'
[36] DCMC←[],OP← 'COMPONENT COEFF'?'S?'
[37] →INP
[38] MIXCALC:P11←(PS11+1)÷(2+PS11←((CT1-DCMT)×DCMC[1])+DCM1)
[39] P21←(PS21+1)÷(2+PS21←(10*(((CT2-DCMT)×DCMC[2])+(10⊗DCM2))))
[40] X2←(((DCM+1)÷(DCM+2))-P11)÷(P21-P11)
[41] X1←1-X2
[42] P1←(PS1+1)÷(2+PS1←((72.77+CT1-REFT[LC;I;])×DCMC[1])+DCM1)
[43] P1C←(PS1+1)÷(2+PS1←((72.77+CT1-OTT[LC;])×DCMC[1])+DCM1)
[44] P2←(PS2+1)÷(2+PS2←(10*(((72.77+CT2-REFT[LC;I;])×DCMC[2])+(10⊗DCM2))))
[45] P2C←(PS2+1)÷(2+PS2←(10*(((72.77+CT2-OTT[LC;])×DCMC[2])+(10⊗DCM2))))
[46] RDC[LC;I;]←((2×((X1×P1)+X2×P2))-1)÷(1-((X1×P1)+X2×P2))
[47] RDC[LC;I;]←((2×((X1×P1C)+X2×P2C))-1)÷(1-((X1×P1C)+X2×P2C))
[48] →CK

```

```

[1]  V TOLS; I; J
[2]  I ← 0
[3]  LOOP6: I ← I + 1
[4]  J ← 0
[5]  LOOP6A: J ← J + 1
[6]  REFSPC[LC; I; J] ← (RDCC[LC; I; J] × 0.12) + ((NREF + REFSP[LC; I]) × (NREF + RDC[LC; I]) × 0.12)
[7]  → (J < (ρFR)) / LOOP6A
[8]  → (I < NREF) / LOOP6
[9]  V
[10] V OTEP; I
[11] I ← 0
[12] LOOP5: I ← I + 1
[13] OTDC[LC; I] ← (OTSP[LC] × 0.12) + ((NREF + RDC[LC; I]) × (NREF + REFSP[LC; I]) × 0.12)
[14] → (I < (ρFR)) / LOOP5
[15] V
[16] V FDP
[17] TOLDC ← 8ρRDCC[LC; R; ]
[18] TOLSP ← 8ρREFSPC[LC; R; ]
[19] EFP[LC; ] ← (OTSP[LC] × (19.8146 + (TOLDC ÷ TOLSP)) × (÷ OTQ[LC; ] - (÷ FQ + 8ρREFQ[LC; R; ])))
[20] V

```

APPENDIX IX

TABLES AND GRAPHS OF
RF Q-METER DATA

TABLE OF CONTENTS

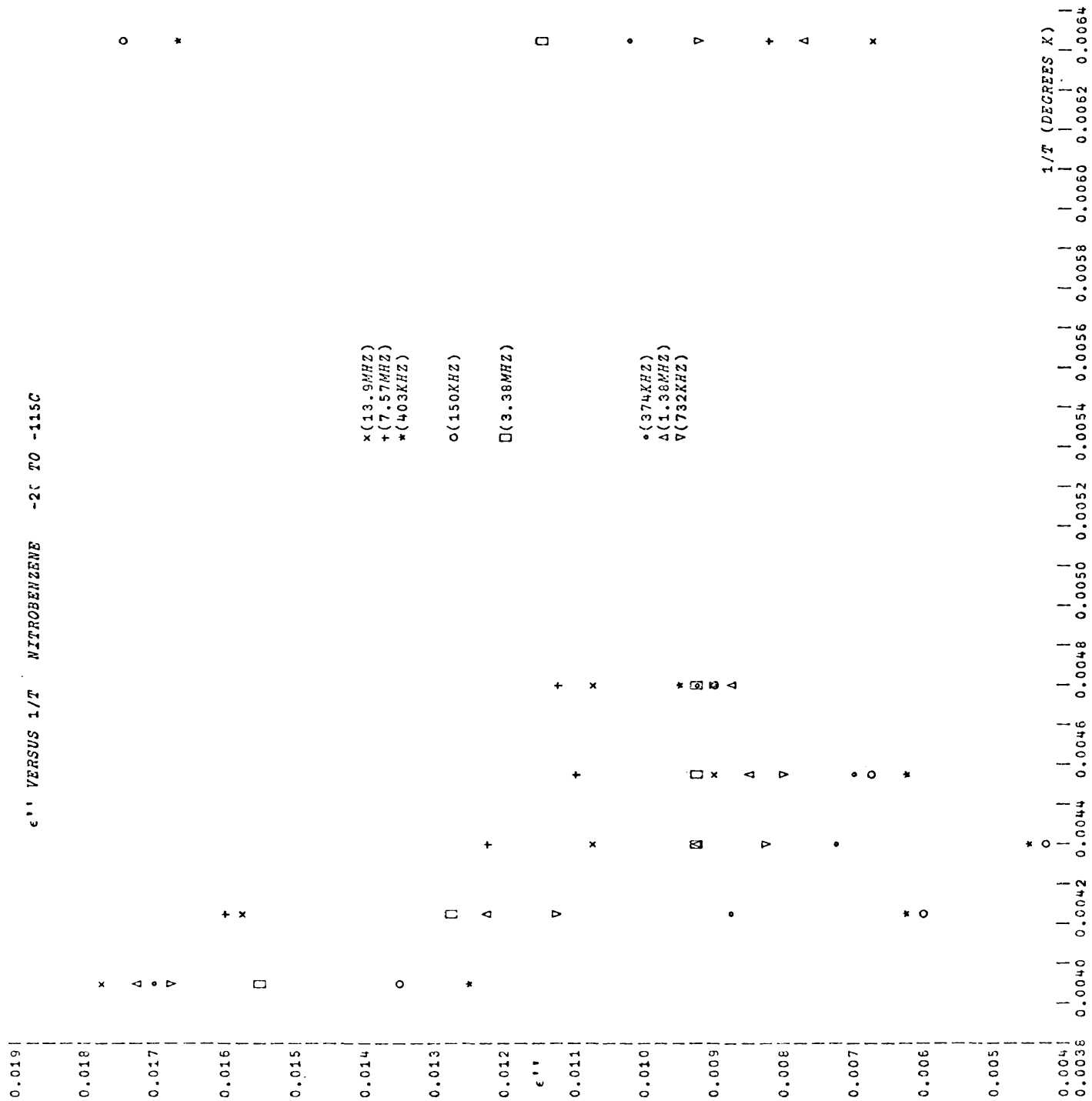
FIRST NITROBENZENE	TABLE OF ϵ''	169
SECOND NITROBENZENE	TABLE OF ϵ''	170
SECOND NITROBENZENE	ϵ'' VS $1/T$	171
SECOND NITROBENZENE	ϵ'' VS LOG FREQUENCY	172
FIRST 2,2'-DINITROBIPHENYL	TABLE OF ϵ''	173
SECOND 2,2'-DINITROBIPHENYL	TABLE OF ϵ''	174
SECOND 2,2'-DINITROBIPHENYL	ϵ'' VS $1/T$	175
SECOND 2,2'-DINITROBIPHENYL	ϵ'' VS LOG FREQUENCY	176
FIRST T-BUTYL BROMIDE	TABLE OF ϵ''	177
SECOND T-BUTYL BROMIDE	TABLE OF ϵ''	178
SECOND T-BUTYL BROMIDE	ϵ'' VS $1/T$	179
SECOND T-BUTYL BROMIDE	ϵ'' VS LOG FREQUENCY	180

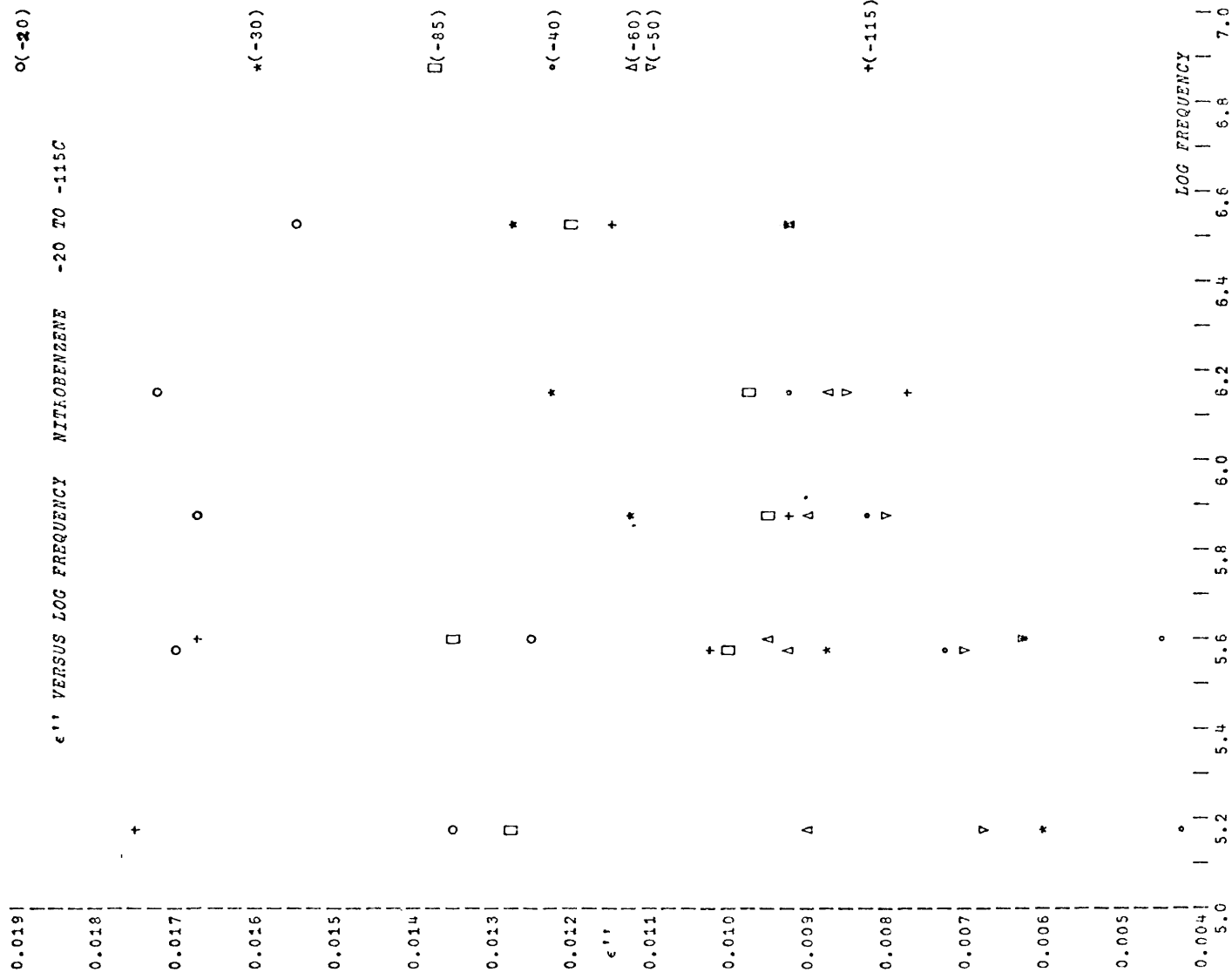
ϵ'' FOR 4 PER CENT NITROBENZENE FREQUENCIES AVERAGED

FREQ(HZ)	-20C	-30C	-40C	-50C	-60C	-85C	-115C
150279	.0135	.0060	.0043	.0068	.0090	.0128	.0175
403243	.0126	.0062	.0044	.0064	.0096	.0136	.0167
373691	.0170	.0089	.0071	.0071	.0093	.0100	.0103
732013	.0166	.0112	.0081	.0079	.0090	.0095	.0091
1379615	.0173	.0122	.0093	.0086	.0089	.0099	.0077
3376353	.0156	.0128	.0094	.0093	.0093	.0119	.0115
7574052	.0189	.0160	.0124	.0109	.0113	.0137	.0082
13911089	.0177	.0158	.0107	.0091	.0106	.0140	.0068

ϵ'' FOR 4 PER CENT NITROBENZENE FREQUENCIES AVERAGED

FREQ(HZ)	-10C	-20C	-30C	-40C	-50C	-60C	-85C
150333	.0421	.0117	.0127	.0130	.0131	.0104	.0109
403303	.0302	.0118	.0140	.0134	.0117	.0101	.0091
373783	.0337	.0130	.0104	.0102	.0088	.0081	.0093
732222	.0271	.0119	.0117	.0108	.0087	.0084	.0090
1379793	.0232	.0135	.0140	.0124	.0097	.0091	.0092
3377873	.0224	.0141	.0187	.0168	.0137	.0122	.0093
7577036	.0222	.0156	.0219	.0190	.0154	.0127	.0100
13917147	.0214	.0138	.0243	.0194	.0162	.0125	.0110



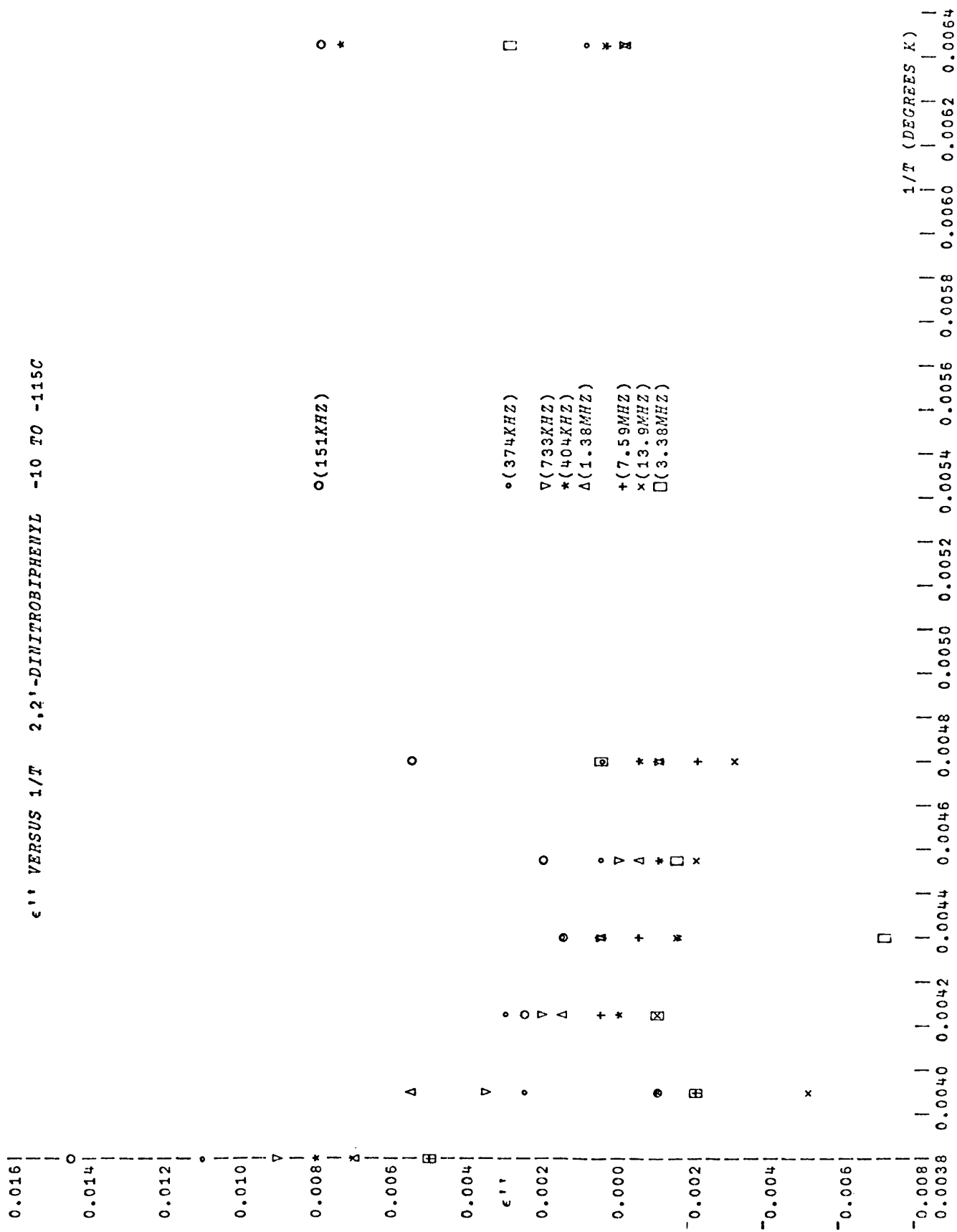


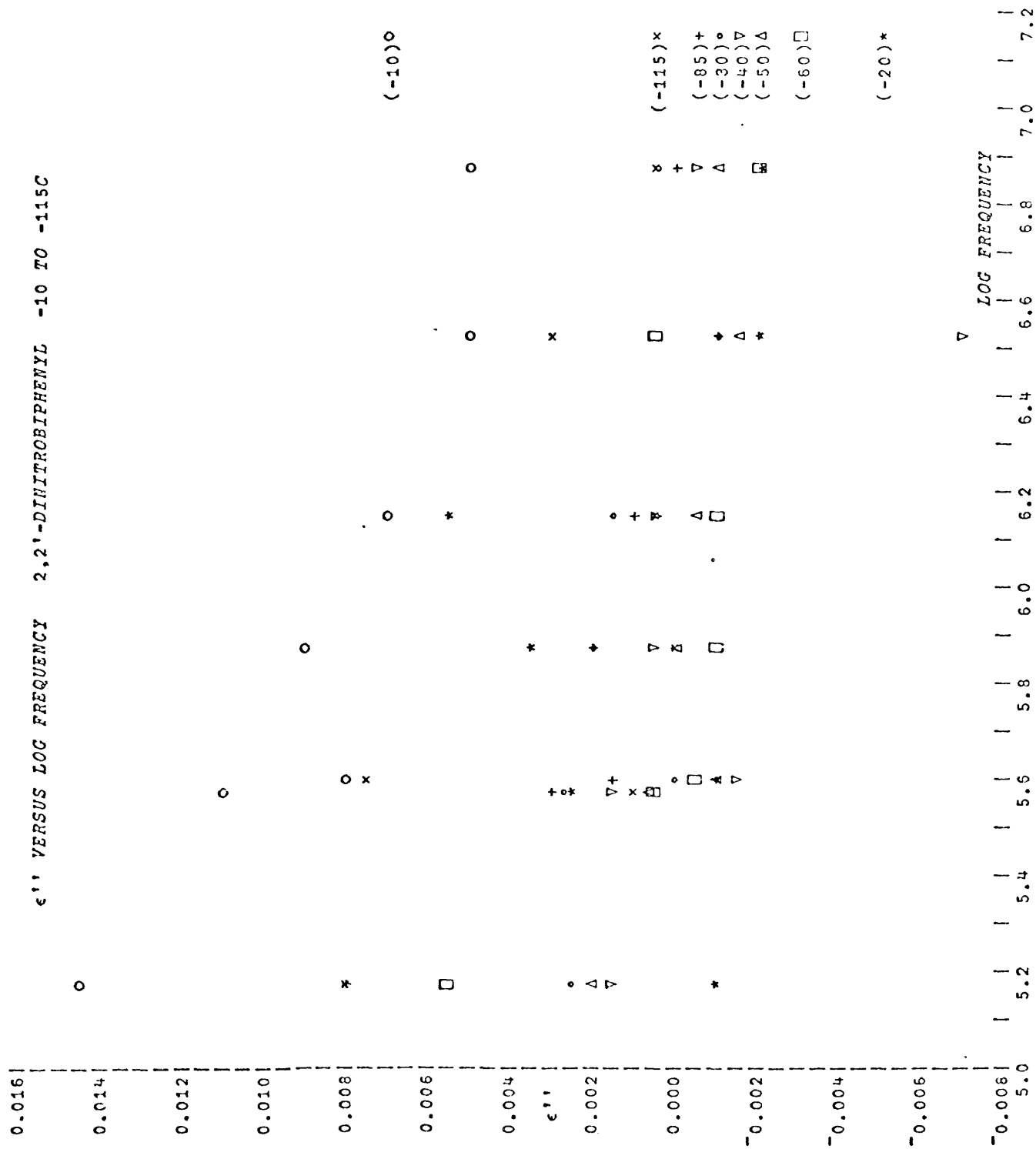
ϵ'' FOR 2.3 PER CENT 2,2'-DINITROBIPHENYL FREQUENCIES AVERAGED

FREQ(HZ)	-10C	-20C	-30C	-40C	-50C	-60C	-85C
150525	.0111	-.0027	.0011	.0015	.0044	.0055	.0086
403764	.0057	-.0030	-.0015	-.0012	.0014	.0036	.0071
374141	.0067	-.0005	-.0001	-.0001	.0002	.0006	.0032
732934	.0063	-.0006	.0005	.0006	.0003	.0008	.0034
1381159	.0046	-.0002	.0001	.0001	.0002	.0006	.0028
3381905	.0058	-.0023	.0008	.0013	.0027	.0040	.0064
7586457	.0043	-.0030	.0005	.0011	.0019	.0046	.0065
13934275	.0046	-.0054	-.0011	-.0011	-.0001	.0020	.0067

ϵ'' FOR 3.3 PER CENT 2,2'-DINITROBIPHENYL FREQUENCIES AVERAGED

FREQ(HZ)	-10C	-20C	-30C	-40C	-50C	-60C	-85C	-115C
150564	.0143	-.0010	.0026	.0015	.0018	.0057	.0079	.0078
403845	.0080	-.0012	.0002	-.0015	-.0012	-.0005	.0014	.0077
374410	.0110	.0027	.0028	.0015	.0007	.0004	.0029	.0012
733350	.0090	.0033	.0022	.0006	-.0001	-.0009	.0022	.0002
1382000	.0072	.0054	.0013	.0003	-.0005	-.0011	.0011	.0003
3382140	.0051	-.0020	-.0010	-.0069	-.0016	.0007	-.0009	.0030
7587055	.0051	-.0022	.0003	-.0005	-.0010	-.0022	-.0001	.0005
13932665	.0069	-.0048	-.0008	-.0016	-.0021	-.0028	-.0007	.0007



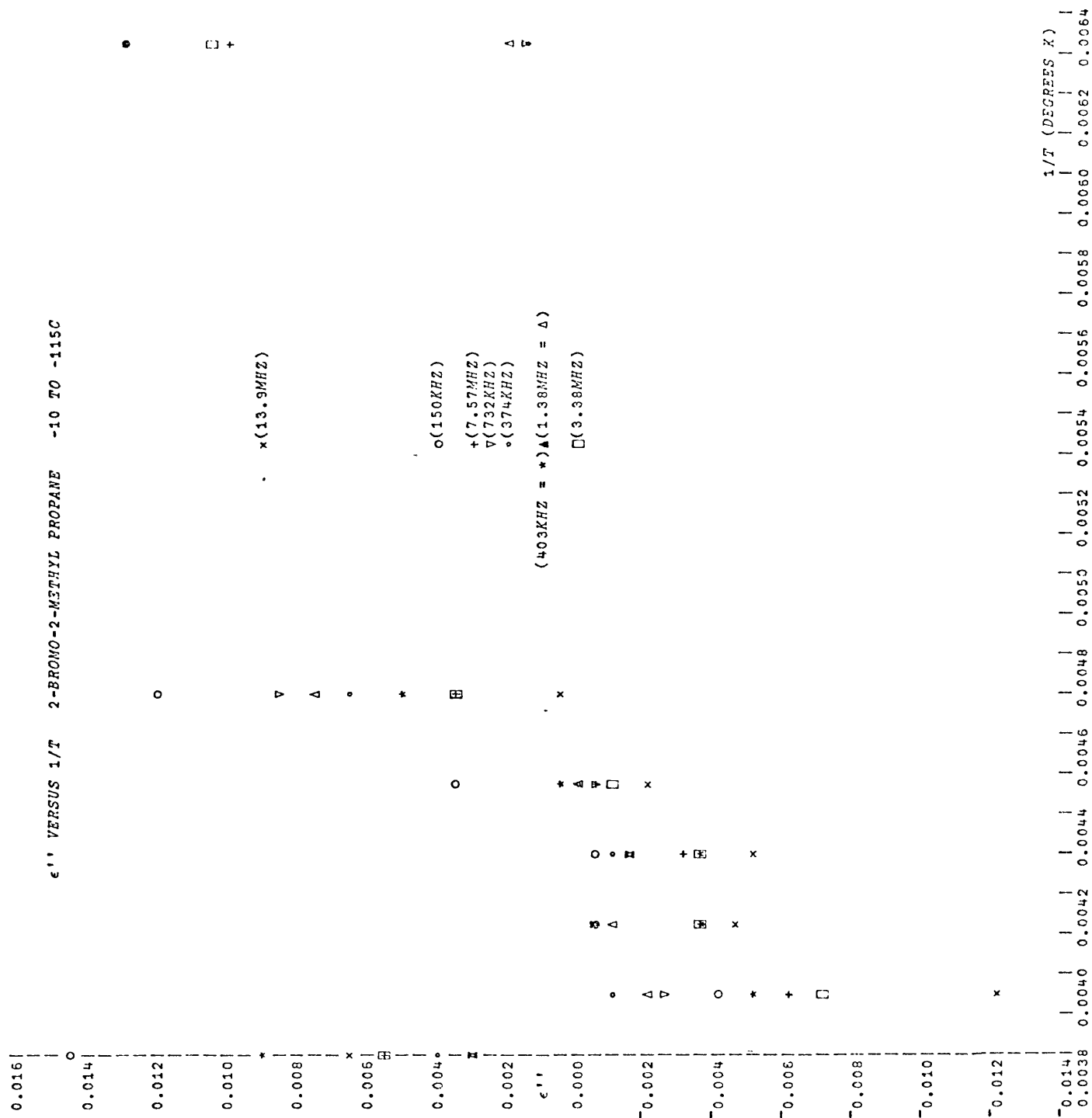


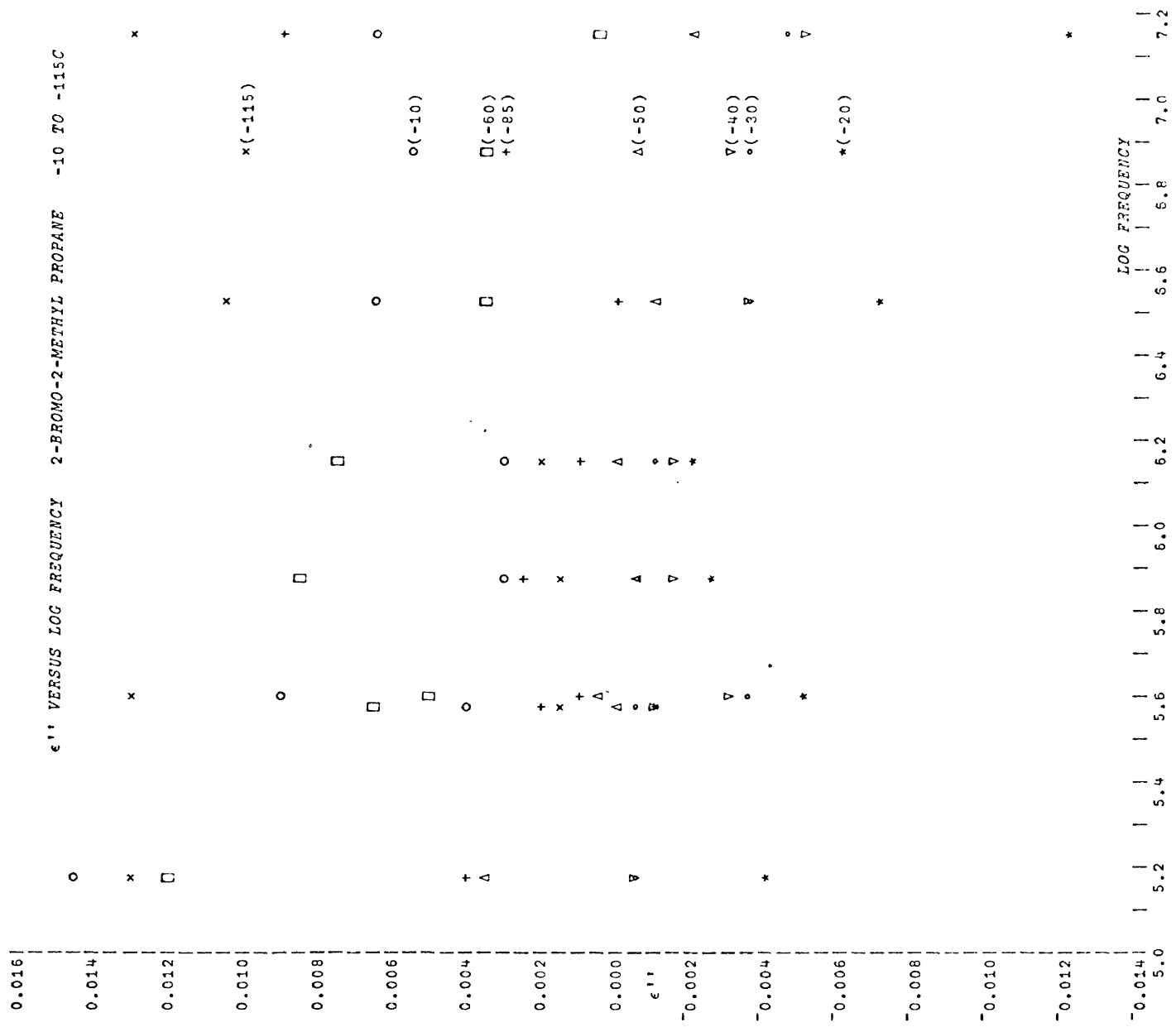
ε'' FOR 4 PER CENT 2-BROMO-2-METHYL PROPANE FREQUENCIES AVERAGED

FREQ(HZ)	-10C	-20C	-30C	-40C	-50C	-60C	-85C
150304	.0093	-.0021	-.0017	-.0024	-.0014	-.0014	.0009
403166	.0022	-.0042	-.0039	-.0043	-.0026	-.0017	.0022
373842	.0056	.0003	-.0005	-.0012	-.0018	-.0017	.0009
732191	.0029	-.0021	-.0013	-.0017	-.0021	-.0018	.0009
1379911	.0016	-.0014	-.0009	-.0014	-.0014	-.0009	.0011
3376499	-.0016	-.0071	-.0041	-.0032	-.0013	-.0013	.0016
7574177	-.0013	-.0074	-.0035	-.0027	-.0014	.0003	.0027
13911762	-.0028	-.0148	-.0064	-.0059	-.0018	.0012	.0032

ϵ'' FOR 4 PER CENT 2-BROMO-2-METHYL PROPANE FREQUENCIES AVERAGED

FREQ(HZ)	-10C	-20C	-30C	-40C	-50C	-60C	-85C	-115C
150528	.0145	-.0042	-.0007	-.0005	.0035	.0121	.0038	.0130
403728	.0090	-.0049	-.0034	-.0031	.0007	.0051	.0012	.0132
374320	.0039	-.0012	-.0007	-.0008	.0000	.0066	.0019	.0015
733241	.0032	-.0027	-.0006	-.0015	-.0004	.0084	.0024	.0016
1381862	.0031	-.0021	-.0012	-.0014	-.0002	.0073	.0009	.0022
3380736	.0067	-.0069	-.0034	-.0033	-.0012	.0033	-.0001	.0104
7583986	.0055	-.0062	-.0033	-.0029	-.0007	.0034	.0028	.0100
13929667	.0065	-.0122	-.0047	-.0049	-.0022	.0007	.0089	.0130





BIBLIOGRAPHY

- J.E. Anderson and R. Ullman, J. Chem. Phys., 47, 2178(1967).
- E. Bauer, Cah. Phys., 20, 1(1944).
- Arnold A. Bondi, "Physical Properties of Molecular Crystals, Liquids, and Glasses," John Wiley & Sons, Inc., New York, N.Y., 1968.
- Martin G. Broadhurst and Anthony J. Bur, J. Res. NBS 69C (Eng. and Instr.), No. 3, 165(1965).
- A. Budo, E. Fischer, and S. Miyanoto, Phys. Z., 40, 337(1939).
- M.H. Cohen and D. Turnbull, J. Chem. Phys., 31, 1164(1959).
- K.S. Cole and R.H. Cole, J. Chem. Phys., 9, 341(1949).
- R.H. Cole, J. Chem. Phys., 42, 637(1965).
- D.W. Davidson and R.H. Cole, J. Chem. Phys., 18, 1417(1951).
- D.W. Davidson and R.H. Cole, J. Chem. Phys., 19, 1484(1951).
- Peter Debye, "Polar Molecules," The Chemical Catalogue Company, Inc., New York, N.Y., 1929.
- E. Fatuzzo and P.R. Mason, Proc. Phys. Soc., 90, 741(1967).
- E. Fischer, Phys. Z., 60, 645(1939).
- H. Frohlich, "Theory of Dielectrics," Oxford University Press, London, 1949.
- General Radio Company, Instruction Manual, Type 1602-B Admittance Meter, General Radio Company, West Concord, Massachusetts, 1968.
- A. Gierer and K. Wirtz, Z. Naturf., 8a, 532(1953).
- S.H. Glarum, Doctoral Thesis, Brown University, 1960; University Microfilms, 62-5745, Ann Arbor, Michigan, 1975.

- S.H. Glarum, J. Chem. Phys., 33, 369 (1960).
- S.H. Glarum, J. Chem. Phys., 33, 1371 (1960).
- S. Glasstone, K.I. Laidler, and H. Eyring, "The Theory of Rate Processes," McGraw-Hill, New York, N.Y., 1941.
- M. Goldstein, Am. Chem. Soc., 30, 117 (1970).
- Gilroy Harrison, "The Dynamic Properties of Supercooled Liquids," Academic Press, New York, N.Y., 1976.
- Hewlett Packard, Operating and Service Manual - Model 4342A Q Meter, Yokogawa-Hewlett-Packard, Ltd., Tokyo, 1973.
- Nora E. Hill, et.al., "Dielectric Properties and Molecular Behavior," Van Nostrand Reinhold Co., New York, N.Y., 1969.
- Allen K. Howe, Jr., Honors Thesis in Chemistry, The College of William and Mary in Virginia, 1974.
- G.P. Johari, J. Chem. Phys., 4, 1766 (1973).
- G.P. Johari, J. Chem. Ed., 51, 23 (1974).
- Akira Kakimoto, Rev. Sci. Instr., 43, 763 (1972).
- J.G. Kirkwood, J. Chem. Phys., 7, 911 (1939).
- Dennis D. Klug, David E. Kranbuehl, and Worth E. Vaughan, J. Chem. Phys., 50(9), 3904 (1969).
- F.I. Mopsik, Doctoral Thesis, Brown University, 1964; University Microfilms, 65-2229, Ann Arbor, Michigan, 1975.
- O.F. Mosotti, Mem. Soc. Ital., 14, 49 (1850).
- L. Onsager, J. Am. Chem. Soc., 58, 1486 (1939).
- F. Perrin, J. Phys. Radium, Paris, 5, 497 (1934).
- M.Y. Rocard, J. Phys. Radium, Paris, 4, 247 (1933).
- W.T. Scott, "The Physics of Electricity and Magnetism," John Wiley & Sons, Inc., New York, N.Y., 1966.
- S.P. Tay and S. Walker, J. Chem. Phys., 63, 1634 (1975).
- Karen Rae Trimmer, Honors Thesis in Chemistry, The College of William and Mary in Virginia, 1975.

Worth E. Vaughan, Chapter II: Experimental Methods, in
"Dielectric Properties and Molecular Behavior," Nora
E. Hill, Ed., Van Nostrand Reinhold, Co., New York,
N.Y., 1969.

Arthur R. Von Hippel, "Dielectrics and Waves," The M.I.T.
Press, Cambridge, Massachusetts, 1966.

Robert C. Weast, Ed., "Handbook of Chemistry and Physics,
54th Edition" CRC Press, Cleveland, Ohio, 1973.

Charles A. Wilkes, Honors Thesis in Chemistry, The College
of William and Mary in Virginia, 1976.

G. Williams, M. Cook, and P.J. Hains, Faraday Transactions
II, 68, 1045 (1972).

G. Williams and P.J. Hains, Faraday Society of the Chemical
Symposium, 6, 14 (1972).

VITA

Theodore Bryant Kingsbury IV

Born in Richmond, Virginia, October 28, 1947.
Graduated as valedictorian of Franklin High School, Franklin, Virginia, in June, 1965. Attended Dartmouth College in Hanover, New Hampshire, and St. Andrews College in Laurinburg, North Carolina from 1965 to 1969. Served from 1969 to 1973 in the United States Air Force, attaining the rank of Staff Sergeant in the field of airborne electronics. B.S., Morris-Harvey College, Charleston, West Virginia, 1974.

The author entered the graduate program of the Department of Chemistry of the College of William and Mary in January, 1975.